UC Berkeley
UC Berkeley Electronic Theses and Dissertations

Title

Transitions in Plant Community Composition in North American Desert and Coastal Ecosystems Sustained by Climate Drivers and Microclimate Feedbacks

Permalink

https://escholarship.org/uc/item/7m52n102

Author

Huang, Heng

Publication Date

2020

Peer reviewed|Thesis/dissertation

Transitions in Plant Community Composition in North American Desert and Coastal Ecosystems
Sustained by Climate Drivers and Microclimate Feedbacks

By

Heng Huang

A dissertation submitted in partial satisfaction of the

requirements for the degree of

Doctor of Philosophy

in

Environmental Science, Policy, and Management

in the

Graduate Division

of the

University of California, Berkeley

Committee in charge:

Professor Paolo D'Odorico, Chair
Professor Dennis Baldocchi
Professor Todd E. Dawson
Professor Iryna Dronova

Fall 2020

Transitions in Plant Community Composition in North American Desert and Coastal Ecosystems
Sustained by Climate Drivers and Microclimate Feedbacks

by

Heng Huang

Abstract

Transitions in Plant Community Composition in North American Desert and Coastal Ecosystems Sustained by Climate Drivers and Microclimate Feedbacks

by

Heng Huang

Doctor of Philosophy in Environmental Science, Policy, and Management

University of California, Berkeley

Professor Paolo D'Odorico, Chair

The ongoing climate change is driving significant changes in vegetation composition and species range shifts in many ecosystems worldwide. For example, climate warming has reduced the frequency of extreme low temperature events, which may facilitate woody plant encroachment in woodland-grassland ecotones worldwide where freezing stress inhibits the growth of cold-sensitive woody plants. In addition, global warming and increasing rainfall variability can significantly affect community dynamics and ecosystem functioning especially in drylands where plant growth is primarily constrained by water availability. Both CAM plant expansion in desert ecosystems and woody plant encroachment in cold ecotones have been empirically observed, the underlying mechanisms, however, still remain unclear. A more mechanistic understanding of how global climate change and local positive microclimate feedbacks will affect plant community composition, species range expansion and resilience of these ecosystems is still lacking.

In this dissertation work, I first conducted greenhouse and growth chamber experiments to investigate the responses of two CAM-grass communities in arid ecosystems across the southwestern United States and Chihuahuan desert to asymmetric warming and increasing rainfall variability. In addition, I integrated lab experiments and field observations with process-based modelling frameworks to examine the microclimate warming effects of woody canopies, investigate the physiological cold intolerance of woody species, and quantitatively evaluate to what extent climate warming may trigger critical transitions from grassland to woodland in Northern American coastal ecosystems. Furthermore, I used high-resolution imagery data and stochastic cellular automata models to investigate the spatial patterning of woody patches on Hog Island (Virginia) and its associations with critical transitions in vegetation dynamics.

I found that increasing rainfall variability can enable deep-rooted grasses to gain competitive advantages over shallow-rooted CAM plants through increasing deep soil water availability under current temperature scenario. However, the competitive advantage is likely to shift from grasses to CAM plants due to drought-induced grass mortality under asymmetric warming.

1

I also found that abrupt transitions from grassland to woodland may occur in coastal woodland-grassland ecotones including mangrove-salt marsh ecotones along the Atlantic coast of Florida when the minimum nocturnal temperature exceeds a critical threshold. Such critical transitions may be induced by positive vegetation-microclimate feedbacks whereby woody plants create a local warming effect through modifying the surface energy balance. Furthermore, the spatial patterns of woody vegetation on Hog Island exhibit signs of critical phenomena as evidenced by the emergence of power law distribution of woody patch size in some specific years.

These findings suggest that the ongoing climate change may facilitate CAM plant expansion in Northern American desert ecosystems and woody plant encroachment in Northern American coastal ecosystems where the latitudinal limits of woody plants are majorly constrained by freezing stress. The results also provide novel empirical and theoretical evidence of whether the observed scale-invariant vegetation patterning may be considered as a general early warning signal of critical transitions from grassland to woodland in coastal and potentially other ecosystems. Overall, this dissertation highlights the important role of environmental drivers and microclimate feedbacks in driving transitions in plant community composition, species range shifts, and ecosystem structure and functioning in desert and coastal ecosystems.

Table of Contents

INTRODUCTION

Climate models and empirical studies indicate that the variability of weather variables is changing at multiple scales (IPCC 2013). For example, in many regions of the world the minimum nighttime temperature is increasing more rapidly than the maximum daytime temperature (Vose et al. 2005, Peng et al. 2013, Davy et al. 2016), and the intensity of extreme rainfall events is increasing even where the mean total rainfall remains relatively unchanged (Huntington 2006, Durack et al. 2012). These climatic changes can affect ecological processes across different scales and drive significant shifts in community structure and dynamics including plant community composition, and further influence ecosystem functioning and services (D'Odorico and Bhattachan 2012, Maestre et al. 2012, Gherardi and Sala 2015). While previous studies have primarily focused on the ecological effects of changes in the mean of climate variables (Parmesan and Yohe 2003, D'Odorico and Bhattachan 2012, Rudgers et al. 2018), the effects of changes in climate variability on plant communities remain relatively poorly understood.

CAM plants are increasing their abundance in many dryland ecosystems worldwide (Drennan and Nobel 2000, Borland et al. 2009, Yu et al. 2017). For example, empirical observations show that CAM species including *Cylindropuntia imbricata* and *Opuntia phaeacantha* have been expanding their geographical ranges in desert ecosystems of the southwestern United States and northern Mexico (Benson and Walkington 1965, Yu et al. 2019). However, the underlying mechanisms driving CAM plant expansion remain unclear. Global warming may favor CAM plant growth by enhancing nighttime carbon assimilation (Reyes-García and Andrade 2009), while increasing rainfall intensity may benefit deep-rooted grasses due to increased deep soil water availability. Therefore, climate change associated with warming trends and changes in rainfall regimes may alter the competitive interactions between CAM plants and coexisting grass species and therefore contribute to species range shifts. To date, however, experimental evidence demonstrating this direct effect of climate change on CAM–grass communities is lacking.

Another major shift in plant distribution and abundance that is occurring around the globe is associated with the relatively rapid encroachment of woody plants into adjacent grasslands, a phenomenon that has been observed worldwide, from arctic tundras to alpine and desert ecosystems (Archer et al. 1995, Chapin et al. 2000, Maher et al. 2005, Bader et al. 2007, Knapp et al. 2008, McKee and Rooth 2008, Ravi et al. 2009). This abrupt change in plant community composition has important impacts on ecosystem structure, function, and services such as livestock grazing, regulation of surface soil moisture and carbon sequestration (Schlesinger et al. 1999, Huenneke et al. 2002, Li et al. 2007). Woody plant encroachment has been attributed to many exogenic and endogenic factors such as overgrazing, fire suppression, increased atmospheric CO_2 concentrations, nitrogen deposition, and climate change (Van Auken 2000, Sankaran et al. 2005, Ward 2005, Gehrig-Fasel et al. 2007, D'Odorico et al. 2012). Climate warming has been suggested to facilitate woody plant encroachment in ecotones worldwide where extreme low temperatures inhibit the growth of cold-sensitive woody plants (D'Odorico et al. 2010, 2013, Cavanaugh et al. 2014, Devaney et al. 2017). The cold sensitivity of woody plants has been ascribed to many different physiological mechanisms, including freezing-induced xylem embolisms, growth and reproduction limitation, frost damage, and winter frost desiccation (Pockman and Sperry 1997, Tranquillini 1979, D'Odorico et al. 2013). In addition to

1

global or regional climate warming, woody expansion can be enhanced by vegetation–microclimate feedbacks, whereby woody plants modify the surface energy balance with the effect of increasing the minimum temperatures thereby reducing the mortality of cold-intolerant woody seedlings (D'Odorico et al. 2010, 2013). However, the positive effects of vegetation–microclimate feedbacks may be counteracted by biotic drivers such as browsing (Devaney et al. 2017). Currently, field measurements documenting the occurrence of this feedback and explaining the underlying mechanisms are still lacking. It is still unknown under what conditions woody plants can modify their microclimate and whether this effect can accelerate the rate of woody plant encroachment, particularly in coastal ecosystems.

In many cases woody plant encroachment has resulted in an abrupt and highly irreversible land cover change, suggesting that the underlying dynamics are those of a bi-stable system with alternative stable states of grass and woody plant dominance and prone to critical transitions between such states (Van Auken 2000, D'Odorico et al. 2012). Research on leading indicators of state shifts in ecology has shown that in many ecosystems vegetation cover exhibits self-organized patterns (Scanlon et al. 2007, Berdugo et al. 2017, Staver et al. 2019). The observed characteristic vegetation patterns may indicate important underlying processes, including the susceptibility of the system to abrupt shifts to an alternative stable state as a result of climate change or environmental disturbances (Scheffer et al. 2009, Majumder et al. 2019). For example, vegetation patterns in some arid ecosystems including savannas may exhibit patches of all sizes distributed according to a power law (Staver et al. 2019). Notably, this scale-invariant power law property of vegetation patterning may be considered as an early warning signal of critical transitions, which allows for a better prediction of ecosystem-level vegetation dynamics in response to external drivers such as climate change (Scheffer et al. 2009). While previous work has primarily focused on arid ecosystems where water is the major limiting factor (e.g., Scanlon et al. 2007), the spatial distribution and patterning of vegetation patches in ecosystems controlled by temperature remains poorly understood. It is unknown whether in these woodland-grassland ecotones woody vegetation shows the emergence of self-organized patters, whether such patterns exhibit scaling properties, and to what extent they are induced by local positive feedbacks.

In this dissertation work, I use a combination of experimental and modelling approaches to address the following questions:

(1) Can asymmetric climate warming and changes in rainfall variability increase the competitive advantage of CAM plants over co-existing grasses and contribute to CAM plant expansion in North American desert ecosystems?
(2) Can woody vegetation create significantly warmer microclimatic conditions compared to grassland in coastal woodland-grassland ecotones?
(3) Will the ecological responses of woody plants to cold microclimate conditions differ in microsites located under the woody canopy and in adjacent grassland?
(4) Can microclimate feedbacks induce bistability in woody vegetation dynamics under climate warming? To what extent can climate warming lead to a critical transition to the woodland state?
(5) How does the spatial patterning of woody plants change over time as they encroach into grasslands?
(6) Can such a spatial patterning serve as an early warning signal of critical transitions to

2

woody plant dominance in coastal ecosystems?

References

Archer, S., D. S. Schimel, and E. A. Holland. 1995. Mechanisms of shrubland expansion: land use, climate, or carbon dioxide. Climate Change 29:91–99.

Bader, M., M. Rietkerk, and A. Bregt. 2007. Vegetation structure and temperature regimes of tropical alpine treelines. Arctic, Antarctic, and Alpine Research 39:353–364.

Benson, L., and D. L. Walkington. 1965. The southern Californian prickly pears–invasion, adulteration, and trail-by-fire. Annals of the Missouri Botanical Garden 52:262–273.

Berdugo, M., S. Kéfi, S. Soliveres, and F. T. Maestre. 2017. Plant spatial patterns identify alternative ecosystem multifunctionality states in global drylands. Nature Ecology and Evolution 1:3.

Borland, A. M., H. Griffiths, J. Hartwell, and J. A. C. Smith. 2009. Exploiting the potential of plants with crassulacean acid metabolism for bioenergy production on marginal lands. Journal of Experimental Botany 60:2879–2896.

Cavanaugh, K. C., J. R. Kellner, A. J. Forde, D. S. Gruner, J. D. Parker, W. Rodriguez, and I. C. Feller. 2014. Poleward expansion of mangroves is a threshold response to decreased frequency of extreme cold events. Proceedings of the National Academy of Sciences 111:723–727.

Chapin, F. S., A. D. McGuire, J. Randerson, R. Pielke, D. Baldocchi, S. E. Hobbie, N. Roulet, W. Eugster, E. Kasischke, E. B. Rastetter, S. A. Zimov, and S. W. Running. 2000. Arctic and boreal ecosystems of western North America as components of the climate system. Global Change Biology 6:211–223.

Davy, R., I. Esau, A. Chernokulsky, S. Outten, and S. Zilitinkevich. 2016 Diurnal asymmetry to the observed global warming. International Journal of Climatology 37:79–93.

Devaney, J. L., M. Lehmann, I. C. Feller, and J. D. Parker. 2017. Mangrove microclimates alter seedling dynamics at the range edge. Ecology 98:2513–2520.

D'Odorico, P., J. D. Fuentes, W. T. Pockman, S. L. Collins, Y. He, J. S. Medeiros, S. De Wekker, and M. E. Litvak. 2010. Positive feedback between microclimate and shrub encroachment in the northern Chihuahuan desert. Ecosphere 1:1–11.

D'Odorico, P., and A. Bhattachan. 2012. Hydrologic variability in dryland regions: impacts on ecosystem dynamics and food security. Philosophical Transactions of the Royal Society B: Biological Sciences 367:3145–3157.

D'Odorico, P., G. S. Okin, and B. T. Bestelmeyer. 2012. A synthetic review of feedbacks and drivers of shrub encroachment in arid grasslands. Ecohydrology 5:520–530.

D'Odorico, P., Y. He, S. Collins, S. F. De Wekker, V. Engel, and J. D. Fuentes. 2013. Vegetation–microclimate feedbacks in woodland–grassland ecotones. Global Ecology and Biogeography 22:364–379.

Drennan, P. M., and P. S. Nobel. 2000. Responses of CAM species to increasing atmospheric CO_2 concentrations. Plant, Cell & Environment 23:767–781.

Durack, P. J., S. E. Wijffels, and R. J. Matear. 2012. Ocean salinities reveal strong global water cycle intensification during 1950 to 2000. Science 336:455–458.

Gehrig-Fasel, J., A. Guisan, and N. E. Zimmermann. 2007. Tree line shifts in the Swiss Alps: Climate change or land abandonment? Journal of Vegetation Science 18:571–582.

Gherardi, L. A., and O. E. Sala. 2015. Enhanced precipitation variability decreases grass- and increases shrub- productivity. Proceedings of the National Academy of Sciences

112:12735–12740.

Huenneke, L. F., J. P. Anderson, M. Remmenga, and W. H. Schlesinger. 2002. Desertification alters patterns of aboveground net primary production in Chihuahuan ecosystems. Global Change Biology 8:247–264.

Huntington, T. G. 2006. Evidence for intensification of the global water cycle: review and synthesis. Journal of Hydrology 319:83–95.

Intergovermental Panel on Climate Change (IPCC). 2013. Climate change 2013: the physical science basis. Contribution of working group I to the fifth assessment report of the Intergovermental Panel on Climate Change. IPCC, Cambridge University Press, Cambridge, United Kingdom and New York, New York, USA.

Knapp, A. K., J. M. Briggs, S. L. Collins, S. R. Archer, M. S. Bret-Harte, B. E. Ewers, D. P. Peters, D. R. Young, G. R. Shaver, E. Pendall, and M. B. Cleary. 2008. Shrub encroachment in North American grasslands: shifts in growth form dominance rapidly alters control of ecosystem carbon inputs. Global Change Biology 14:615–623.

Li, J., G. S. Okin, L. J. Hartman, and H. E. Epstein. 2007. Quantitative assessment of wind erosion and soil nutrient loss in desert grasslands of southern New Mexico, USA. Biogeochemistry 85:317–332.

Maestre, F. T., R. Salguero-Gomez, and J. L. Quero. 2012. It's getting hotter in here: determining and projecting the impacts of global change on drylands. Philosophical Transactions of the Royal Society B: Biological Sciences 367:3062–3075.

Maher, E. L., M. J. Germino, and N. J. Hasselquist. 2005. Interactive effects of tree and herb cover on survivorship, physiology, and microclimate of conifer seedlings at the alpine tree-line ecotone. Canadian Journal of Forest Research 35:567–574.

Majumder, S., K. Tamma, S. Ramaswamy, and V. Guttal. 2019. Inferring critical thresholds of ecosystem transitions from spatial data. Ecology 100:e02722.

McKee, K. L., and J. E. Rooth. 2008. Where temperate meets tropical: multi-factorial effects of elevated CO2, nitrogen enrichment, and competition on a mangrove-salt marsh community. Global Change Biology 14:971–984.

Parmesan, C., and G. Yohe. 2003. A globally coherent fingerprint of climate change impacts across natural systems. Nature 421:37–42.

Peng, S., S. Piao, P. Ciais, R. B. Myneni, A. Chen, F. Chevallier, and S. Vicca. 2013. Asymmetric effects of daytime and night-time warming on Northern Hemisphere vegetation. Nature 501:88–92.

Pockman, W. T., and J. S. Sperry. 1997. Freezing-induced xylem cavitation and the northern limit of *Larrea tridentata*. Oecologia 109:19–27.

Ravi, S., P. D'Odorico, L. Wang, C. S. White, G. S. Okin, S. A. Macko, and S. L. Collins. 2009. Post-fire resource redistribution in desert grasslands: a possible negative feedback on land degradation. Ecosystems 12:434–444.

Reyes-García, C., and J. L. Andrade. 2009. Crassulacean acid metabolism under global climate change. New Phytologist 181:754–757.

Rudgers, J. A., A. Y. Chung, G. E. Maurer, D. I. Moore, E. H. Muldavin, M. E. Litvak, and S. L. Collins. 2018. Climate sensitivity functions and net primary production: A framework for incorporating climate mean and variability. Ecology 99:576–582.

Sankaran, M., N. P. Hanan, R. J. Scholes, J. Ratnam, D. J. Augustine, B. S. Cade, J. Gignoux, S. I. Higgins, X. Le Roux, and F. Ludwig. 2005. Determinants of woody cover in African savannas. Nature 438:846–849.

Scanlon, T. M., K. K. Caylor, S. A. Levin, and I. Rodriguez-Iturbe. 2007. Positive feedbacks promote power-law clustering of Kalahari vegetation. Nature 449:209–212.

Scheffer, M., J. Bascompte, W. A. Brock, V. Brovkin, S. R.Carpenter, V. Dakos, H. Held, E. H. van Nes, M. Rietkerk,and G. Sugihara. 2009. Early-warning signals for critical transitions. Nature 461:53–59.

Schlesinger, W. H., A. D. Abrahams, A. J. Parsons, and J. Wainwright. 1999. Nutrient losses in runoff from grassland and shrubland habitats in Southern New Mexico: I. rainfall simulation experiments. Biogeochemistry 45:21–34.

Staver, A. C., G. P. Asner, I. Rodriguez-Iturbe, S. A. Levin, and I. Smit. 2019. Spatial patterning among savanna trees in high resolution, spatially extensive data. Proceedings of the National Academy of Sciences 116:10685.

Tranquillini, W. 1979. Physiological ecology of the alpine timberline: tree existence at high altitudes with special reference to the European Alps. Springer, Berlin, Germany.

Van Auken, O. 2000. Shrub invasions of North American semiarid grasslands. Annual Review of Ecology and Systematics 31:197–215.

Vose, R. S., D. R. Easterling, and B. Gleason. 2005. Maximum and minimum temperature trends for the globe: an update through 2004. Geophysical Research Letters 32:L23822.

Ward, D. 2005. Do we understand the causes of bush encroachment in African savannas? African Journal of Range and Forage Science 22:101–105.

Yu, K. L., P. D'Odorico, W. Li, and Y. L. He. 2017. Effects of competition on induction of crassulacean acid metabolism in a facultative CAM plant. Oecologia 184:351–361.

Yu, K. L., P. D'Odorico, S. L. Collins, D. Carr, A. Porporato, W. R. L. Anderegg, W. P. Gilhooly III, L. Wang, A. Bhattachan, M. Bartlett, S. Hartzell, J. Yin, Y. He, W. Li, M. Tatlhego, and J. D. Fuentes. 2019. The competitive advantage of a constitutive CAM species over a C4 grass species under drought and CO_2 enrichment. Ecosphere 10:e02721.

CHAPTER 1

The competitive advantage of C4 grasses over CAM plants under increased rainfall variability

1.1 Abstract

The intensity of extreme rainfall events is increasing in many regions of the world, with important impacts on community dynamics and ecosystem functioning especially in water-limited ecosystems. The impact of the intensification of extreme precipitation on mixed communities of CAM plants and dryland C4 grasses remains poorly understood. Through a set of greenhouse experiments we investigated the effect of increasing intraseasonal rainfall variability on two separate pairs of CAM and C4 grass species (*C. imbricata* and *B. eriopoda*; *O. phaeacantha* and *B. curtipendula*) that coexist in arid grasslands across the southwest USA. The increased rainfall variability did not significantly change the biomass of *C. imbricata* while increasing the biomass of *B. eriopoda* when these two species coexisted. More extreme rainfall regimes caused a 24.8% decrease in *B. curtipendula* (grass) biomass, compared with a 71.3% decline in the *O. phaeacantha* CAM plant. Significantly lower nocturnal carbon assimilation rates and higher stem volume-to-surface area ratios were found in CAM plants in mixture than in monoculture. Our study suggests that C4 grasses may outcompete CAM plants through greater access to deep soil water under increased rainfall variability and highlights the important role of hydrologic conditions as determinants of the competitive relations between CAM plants and grasses, their community composition, and ecological resilience in dryland ecosystems.

1.2 Introduction

Global climate models project an overall increase in extreme rainfall regimes worldwide with less frequent but more intense rainfall events (i.e., increasing rainfall variability), even in regions where the mean annual precipitation remains constant (Smith 2011; IPCC 2013; Fischer et al. 2013). This ongoing change, as confirmed by many empirical studies, has significant influences on many ecological and hydrological processes such as vegetation productivity and evapotranspiration, and further affects community dynamics, ecosystem structure, and carbon sequestration (Fay et al. 2000; Adler et al. 2006; Knapp et al. 2008; Thomey et al. 2011; D'Odorico et al. 2012; Thornton et al. 2014; Gherardi and Sala 2015; Rudgers et al. 2018). While ecosystem response to climate change has been investigated in terms of changes in precipitation means on plant growth and productivity (Wu et al. 2011), the effects of climate variability on community dynamics has remained poorly understood. Addressing this challenging question is crucial to predict vegetation dynamics and community composition under projected climatic changes although different survival capacities among plant species under resource (e.g., water) interpulse also contribute to the changes in community composition (Goldberg 1997).

Drylands cover 41% of the Earth's land surface and contribute nearly 40% to the global net primary productivity (Hillel and Rosenzweig 2002). In these ecosystems the limited water availability is a major constraint on plant growth and biomass production (Knapp et al. 2002;

Reynolds et al. 2007). Climate models predict increased extreme rainfall events and aridity in many drylands worldwide, including the southwestern USA (Seager et al. 2007). These changes in hydrologic conditions may cause dramatic shifts in species composition (Maestre et al. 2012). For example, changes in the mean and variability of precipitation and temperature can favor shrub encroachment in arid and semiarid grasslands, a phenomenon that has been widely documented in the southwestern USA and southern Africa (D'Odorico and Bhattachan 2012; Kulmatiski and Beard 2013). Changes in rainfall regimes have also been associated with drought stress and widespread mortality in tree communities (Van Mantgem et al. 2009; Anderegg et al. 2013; Allen et al. 2015), further demonstrating that changes in rainfall regimes can reshape ecosystem dynamics and their stability. Previous studies in dryland ecosystems have primarily focused on the response of woody plants and grass species to global change (Knapp et al. 2002, D'Odorico et al. 2012, Fan et al. 2019). However, little is known about the way other plant functional groups such as plants with Crassulacean Acid Metabolism (CAM) photosynthesis will respond to global changes in precipitation regimes (but see Yu et al. 2016, 2017a,b).

CAM plants have recently received increasing attention from the science community because of their potential use as biofuel and food crops in dryland regions (Borland et al. 2009; Davis et al 2014; Yu et al. 2018). CAM plants are characterized by nocturnal CO_2 fixation, high water use efficiency (WUE) and drought resistance (Lüttge 2004; Borland et al. 2009, 2011). These features enable CAM plants to outcompete many C3 or C4 species under drought stress, which may explain their increasing dominance in many drylands worldwide (Drennan and Nobel 2000; Cushaman and Borland 2002; Borland et al. 2009; Yu et al. 2017b).

Several studies suggest that changes in weather (e.g., temperature and rainfall) or increase in atmospheric CO_2 concentrations could be major drivers of CAM plant expansion in drylands (e.g., Drennan and Nobel 2000; Borland et al. 2009; Reyes-García and Andrade 2009). A recent study found the existence of competitive advantage of a constitute CAM species (*Cylindropuntia imbricata*) over C4 grass (*Bouteloua eriopoda*) under drought and CO_2 enrichment conditions (Yu et al. 2019). Likewise, drought and increased nitrogen deposition can alter the competitive relationships between a facultative CAM species (*Mesembryanthemum crystallinum*) and a C3 grass (*Bromus mollis*) (Yu et al. 2017a). However, it remains unclear how CAM plants and their competitive relationships with other functional groups may respond to increased rainfall variability.

The competition of CAM plants with other functional groups depends, among other factors, on the frequency and intensity of rainfall, soil texture, rainfall gradient, and plant traits (i.e., tolerance to drought, growth rate, root depth) (Yu et al. 2018). CAM plants are typically succulents (i.e., plants that can store substantial amounts of water) and therefore they can endure long and intense drought (Lüttge 2004). This trait would allow CAM plants to outcompete C_3 or C_4 plants in situations with long and intense drought. In other situations, other functional groups (e.g., grasses with high grow rates) can be more efficient in soil water uptake and quickly take up soil water right after rainfall pulses (Williams and Albertson 2006), thereby outcompeting CAM plants in the use of soil moisture. CAM plants typically have shallow roots (Lüttge 2004) and thus may be disfavored in the competition with other functional groups (i.e., grasses with deeper roots) in response to increased rainfall variability, which increases drainage and soil moisture into the deeper soil layer. CAM plants, however, may adapt to increased rainfall variability by

altering root morphology and physiology to increase plant water uptake (Lüttge 2004; Ogburn and Edwards 2010), thus improving their ability to compete with grasses.

In this study, we focused on two pairs CAM plants and C4 grasses (*Cylindropuntia imbricata* with *Bouteloua eriopoda*, and *Opuntia phaeacantha* with *Bouteloua curtipendula*) which are found to coexist in desert ecosystems across the southwestern United States and Chihuahuan desert (Yu et al. 2019). Both CAM species (i.e., *C. imbricata* and *O. phaeacantha*) are increasing their abundance in these regions (Benson and Walkington 1965; Yu et al. 2019). For example, Yu et al. (2019) show that *C. imbricata* has expanded its destitution in native desert grasslands from 1993 to 2015. However, it is still unknown whether this phenomenon is contributed by changes in rainfall regimes, in particular rainfall variability. Therefore, the analysis of general patterns in the physiological responses of CAM species and their competitive interactions with co-existing grasses could be crucial to explain the expansion of CAM plants in arid and semi-arid regions worldwide. In this study, we investigate the effect of increasing rainfall variability on the competitive relationships between CAM plants and grasses through measurements of biomass, morphological and physiological traits, which will provide insights into the responses of CAM-grass communities under climate change.

1.3 Materials and Methods
1.3.1 Experimental design
To increase the speed and success rate of seed germination, seeds of the two CAM plant species, *Cylindropuntia imbricata* and *Opuntia phaeacantha*, were soaked in warm water overnight and then germinated in plastic trays in a Temperature Incubator 815 (Precision Scientific, Chicago, IL, USA) at 33°C/22°C Daytime/Nighttime on June 10th, 2018. Seeds of the two C4 grass species, *Bouteloua eriopoda* and *Bouteloua curtipendula*, were germinated in plastic trays in the Oxford Tract Greenhouse facility at the University of California, Berkeley on June 15th, 2018. Seeds were watered regularly to eliminate the water stress on germination. CAM seedlings were moved to the greenhouse two weeks before transplantation. On July 31th, both CAM and grass seedlings were transplanted into plastic pots (15 cm in diameter and 13 cm in height) filled with 6:1 Metromix 200 and Turface mix. Given the relatively small pot size, plants were paired and planted in monoculture (4 individuals) or mixture (2 individuals of CAM species and 2 individuals of grass species).

To better mimic natural environments, we measured the hydraulic conductivity of soil with a variety of Metromix 200:Turface ratios using a mini disk infiltrometer (Decagon, Pullman, WA, USA). A suction of 2 cm was used, and the saturated hydraulic conductivity was determined based on the infiltration data (Zhang 1997). A mixture in a ratio of 6:1 was used in this study because the average hydraulic conductivity of this soil was 3.72×10^{-5} m/s, which was similar with the values measured in the field in Chihuahuan desert reported by Ravi et al. (2009).

To investigate the effect of future rainfall regimes on biomass production in CAM plants and grasses as well as their interactions, we conducted a greenhouse experiment with a randomized block design (Figure S1) in which pots with five replicates in both monoculture and mixture were subjected to three levels of intraseasonal rainfall variability treatments (V1, V2 and V3) over 90 days. V1 is the control treatment which reflects the current natural rainfall pattern, while V2 and V3 treatments represent the increased extreme rainfall intensities to simulate future

rainfall regimes. Watering intensity and frequency were based on the average of 30-year data of growing season precipitation in Sevilleta National Wildlife Refuge (150 ± 13 mm; mean $\pm$ SE, Petrie et al. 2014) where *C. imbricata* and *B. eriopoda* coexist (Miller et al. 2009), and Cabeza Prieta National Wildlife Refuge (90 ± 8 mm; mean $\pm$ SE), where *O. phaeacantha* and *B. curtipendula* coexist. For *C. imbricata* and *B. eriopoda*, pots were watered with sprinklers 5 mm (i.e., 0.5 cm $\times$ pot area 176 cm^2 = 88 ml) every three days in V1 treatment, 10 mm (176 ml) every six days in V2 treatment and 15 mm (264 ml) every nine days in V3 treatment; for *O. phaeacantha* and *B. curtipendula*, pots were watered 3 mm (53 ml) every three days in V1 treatment, 6 mm (106 ml) every six days in V2 treatment and 9 mm (159 ml) every nine days in V3 treatment. Plants were fertilized with 20-20-20 Peters professional solution (100 ppm nitrogen) every nine days to ensure that plant growth is not nutrient limited. The daily temperatures in the greenhouse ranged from 17°C to 33°C to reflect the natural conditions and the photosynthetically photon flux density (PPFD) was 700-900 umol m^{-2} s^{-1} from 7 am to 7 pm.

1.3.2 Individual gas exchange measurements

Gas exchange measurements were carried out on both CAM plants on August 2nd, August 20th, September 7th, September 25th, October 13th and October 31th. The whole-plant gas exchange of *C. imbricata* and *O. phaeacantha* was measured three times for each of the five replicates in each rainfall treatment at a constant temperature of 25°C using a customized Plexiglas cylindrical chamber (7 cm in diameter and 12.5 cm in height) (Yu et al. 2019) mounted on a Li-Cor 6400XT portable photosynthesis system (Li-Cor, Lincoln, NE). The chamber is closed on one end and has a hole (1.5 cm in diameter) on the other which was sealed after the CAM stem was inserted into the chamber using silicone putty air plugs during gas exchange measurements to exclude soil respiration (see also Yu et al. 2019). The whole-plant net photosynthetic rate (P, nmol s^{-1}) was calculated as the recorded specific photosynthetic rate (umol m^{-2} s^{-1}) multiplied by the area of leaf cuvette (i.e., 2 cm $\times$ 3 cm) (Yu et al. 2019).

1.3.3 Soil moisture measurements

Soil moisture in the upper layer (~ 6 cm) was measured on November 1st in each pot using a soil moisture sensor (Waterscout SMEC300, Spectrum Technologies Inc., Plainfield, IL, USA) to investigate the difference in water consumption capacity of plants under different treatments and growing conditions (monoculture versus mixture). The sensor was inserted into the soil at the center of the pot and the volumetric water content was recorded when the reading became constant.

1.3.4 Biomass and stem volume-to-surface area (V:S) ratio

Plants were then harvested on November 1-4th to measure above- and below-ground biomass. CAM plants and grasses grown in mixture were separated and all plant individuals were then divided into above-ground and below-ground biomass (i.e., shoots and roots, respectively). The soil was carefully removed from the plant root systems to minimize the loss of fine roots. The small amount of roots remaining in the soil were differentiated between CAM and grass species based on color, diameter and shape. All the samples were then prepared to determine the fresh mass (M_f) and then dried at 65°C for 72 h to measure the dry mass (M_d) of shoots and roots, and then aggregated to individual total dry biomass. The root-to-shoot biomass ($R:S$) ratios were calculated for CAM plants and/or grasses in each pot. The stem volume-to-surface area ratio ($V:S$ ratio) varies by nearly two orders of magnitude among cactus species (Mauseth 2000) and

has been suggested to reflect the physiological responses of CAM plants to climate related stresses such as droughts (Williams et al. 2014). Therefore, *V:S* ratio may change in response to environmental stress or strong competition. Since the ribs of 3-month-old columnar cacti *C. imbricata* are negligible, the *V:S* ratio can be estimated by

$$V:S = \frac{\frac{1}{4}\pi D^2 h}{\pi D h} = \frac{1}{4}D,$$

where *h* is the plant height and *D* is the stem diameter (Mauseth 2000; Williams et al. 2014). The stem diameter (mm) of *C. imbricata* was measured using a digital Vernier caliper with a resolution of 0.01 mm at three locations along the stem (top, middle and bottom) and averaged for each individual plant.

1.3.5 Statistical analyses
We conducted data analyses separately for each pair of CAM and grass species. We first compared the variable of interest among rainfall treatments for each combination of species and growing conditions (i.e., monoculture and mixture) to detect whether differences among treatments were significant. Then we compared the variable between monoculture and mixture for each species in each rainfall treatment to test the significance of the difference. In total, 225 pairwise comparisons of the means of individual traits and soil moisture were made. The significance of differences in the mean of each variable between species (C1 versus G1, and C2 versus G2), rainfall treatments (V1, V2 and V3) or time were determined respectively using Tukey's test through TukeyHSD function from R base packages ($\alpha = 0.05$). The effects of rainfall treatment, competition (intra- and interspecific competition) and species as well as their interactions on individual total biomass and *R:S* ratio, were analyzed using the linear mixed-effects models with block as a random factor from the "lme4" package in R (Bates et al. 2015). The effects of rainfall treatment, competition and time as well as their interactions on individual CO_2 exchange rate of CAM plants, were also analyzed using the linear mixed-effects models with individual as a random factor. All the statistical analyses and plots were made in R (version 3.4.3, R Development Core Team 2017).

1.4 Results
1.4.1 The effect of rainfall variability on plant total biomass
The increase in rainfall variability did not affect the total biomass of CAM species *C. imbricata* either in monoculture or mixture (Tukey HSD test, all $P > 0.111$, Figure 1A). Increased rainfall variability from V1 to V2 did not lead to a significant difference in the total biomass of grass species *B. eriopoda* in monoculture (Tukey HSD test, $P = 0.885$) but there was a significant decrease from V2 to V3 treatment (Tukey HSD test, $P = 0.037$). For *B. eriopoda* in mixture, there was a significant increase in biomass in V2 with respect to V1 (Tukey HSD test, $P = 0.003$), and a further significant increase from V2 to V3 (Tukey HSD test, $P = 0.023$, Figure 1A). The biomass of *C. imbricata* was significantly higher in monoculture than that in mixture in V2 and V3 treatments (Tukey HSD test, both $P < 0.025$) but no significant difference was detected in V1 treatment (Tukey HSD test, $P = 0.421$). The biomass of *B. eriopoda* was significantly lower in monoculture than that in mixture regardless of rainfall treatment (Tukey HSD test, all $P < 0.001$). These findings were further corroborated by the result of the linear mixed-effects

model that species, rainfall variability treatment and competition as well as their interactions had all significant effects on the total biomass of *C. imbricata* and *B. eriopoda* (Table 1).
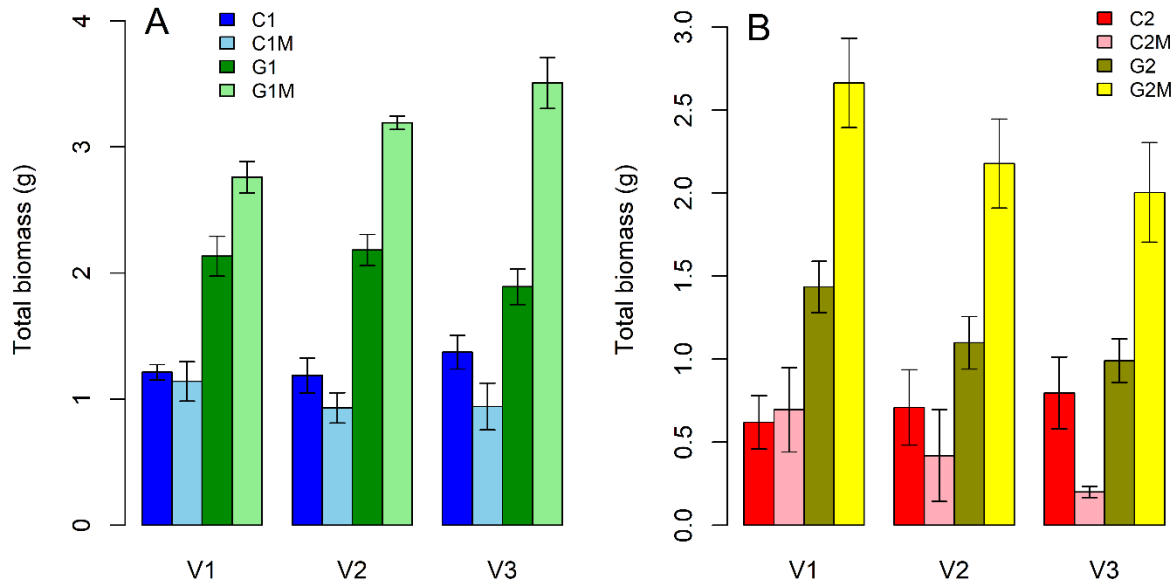
Figure 1. Individual total biomass (TB, g) of two pairs of CAM (C1: *Cylindropuntia imbricata*; C2: *Opuntia phaeacantha*) and C4 grass species (G1: *Bouteloua eriopoda*; G2: *Bouteloua curtipendula*) in monoculture (C1, G1, C2, G2) and mixture (C1M, G1M, C2M, G2M) in each of the three rainfall treatments (V1, V2 and V3). Error bars indicate 95% confidence intervals.

Similarly, the total biomass of CAM species *O. phaeacantha* both in monoculture and mixture was statistically indistinguishable between the V1 and V2 or between the V2 and V3 rainfall treatments (Tukey HSD test, all $P > 0.111$, Figure 1B), whereas a significant decrease in the biomass was found in the V3 treatment with respect to V1 in mixture conditions (Tukey HSD test, $P = 0.021$). A significant lower *B. curtipendula* biomass was found in monoculture in the V2 treatment compared with V1 (Tukey HSD test, $P = 0.021$), while a further increase in rainfall variability (V3) did not significantly influence the *B. curtipendula* biomass with respect to V2 (Tukey HSD test, $P = 0.588$). While in mixture, a moderate increase in rainfall variability (from V1 to V2) did not show a significant effect on the biomass of *B. curtipendula* (Tukey HSD test, $P = 0.078$), a stronger increase in rainfall variability (from V1 to V3) resulted in a significantly lower biomass (Tukey HSD test, $P = 0.017$). The biomass of *O. phaeacantha* in monoculture and mixture were statistically indistinguishable in both the V1 and V2 treatments (Tukey HSD test, both $P > 0.150$) but the biomass was significantly lower in mixture than in monoculture in the V3 treatment (Tukey HSD test, $P < 0.001$). However, the biomass of *B. curtipendula* in mixture was significantly higher than in monoculture regardless of rainfall variability treatment (Tukey HSD test, all $P < 0.001$). The analysis of the linear mixed-effects model showed that the effects of species, rainfall variability treatment and competition as well as their pairwise interactions on the total biomass were all significant (Table 1).

Table 1. Results of the linear mixed-effects model evaluating the effects of species, rainfall variability treatment and competition as well as their interactions on individual total biomass. Block was treated as a random factor.

Source	χ^2	d.f.	*P* value
C. imbricata and *B. eriopoda*			
Species	1646.75	1	< 0.0001 ***
Rainfall treatment	6.75	2	0.0343 *
Competition	129.60	1	< 0.0001 ***
Species: rainfall treatment	17.56	2	0.0002 ***
Species: competition	335.82	1	< 0.0001 ***
Rainfall treatment: competition	13.10	2	0.0014 **
Species: rainfall treatment: competition	57.36	2	< 0.0001 ***
O. phaeacantha and *B. curtipendula*			
Species	407.67	1	< 0.0001 ***
Rainfall treatment	27.27	2	< 0.0001 ***
Competition	53.45	1	< 0.0001 ***
Species: rainfall treatment	8.86	2	0.0119 *
Species: competition	144.88	1	< 0.0001 ***
Rainfall treatment: competition	10.12	2	0.0063 **
Species: rainfall treatment: competition	2.67	2	0.2637

*indicates the degree of significance test by Wald chi-squared test, *$P < 0.05$, **$P < 0.01$, ***$P < 0.001$

1.4.2 The effect of rainfall variability on plant root-to-shoot biomass ratio (R:S ratio)
The *R:S* ratio of *C. imbricata* was not significantly different among rainfall variability treatments both in monoculture and mixture (Tukey HSD test, all *$P > 0.232$*, Figure 2A). The *R:S* ratio of *B. eriopoda* in monoculture decreased significantly when rainfall variability increased from V1 to V2 (Tukey HSD test, *$P < 0.001$*) but no significant difference was detected between V2 and V3 treatments (Tukey HSD test, *$P < 0.941$*). Increasing rainfall variability did not affect the *R:S* ratio of *B. eriopoda* in mixture (Tukey HSD test, all *$P > 0.297$*). In the V1 treatment, the *R:S* ratio of *C. imbricata* in monoculture was significantly lower than that in mixture (Tukey HSD test, *$P = 0.015$*) and by contrast, the *R:S* ratio of *B. eriopoda* in monoculture was significantly higher than that in mixture (Tukey HSD test, *$P < 0.001$*). There was no significant difference in the *R:S* ratio between monoculture and mixture for either species in the V2 treatment (Tukey HSD test, both *$P > 0.071$*). A significantly lower *R:S* ratio of *C. imbricata* was found in monoculture in the V3 treatment (Tukey HSD test, *$P = 0.046$*) while there was no significant difference between monoculture and mixture for *B. eriopoda* (Tukey HSD test, *$P = 0.487$*). The results of linear

mixed-effects model further demonstrated the significant impacts of rainfall variability and its interactions with other factors on the *R:S* ratio of *C. imbricata* (all *P* < 0.010, Table S1).

In monoculture conditions, a moderate increase in rainfall variability (V2) did not cause a significant effect on the *R:S* ratio of *O. phaeacantha* (Tukey HSD test, *P* = 0.051) but a strong increase in rainfall variability (V3) significantly increased the *R:S* ratio with respect to V1 (Tukey HSD test, *P* = 0.001, Figure 2B). The *R:S* ratio of *O. phaeacantha* in mixture was not significantly different among rainfall variability treatments (Tukey HSD test, all *P* > 0.240). The *R:S* ratio of *B. curtipendula* in monoculture decreased significantly as the rainfall variability increased from V1 to V2 (Tukey HSD test, *P* = 0.035) but a further increase from V2 to V3 did not significantly affect the *R:S* ratio (Tukey HSD test, *P* = 0.757). Similar to the case of *O. phaeacantha*, no significant difference in the *R:S* ratio of *B. curtipendula* was observed among rainfall variability treatments in mixture conditions (Tukey HSD test, all *P* > 0.771). The *R:S* ratio of *O. phaeacantha* was significantly lower in monoculture than in mixture in V1 treatment (Tukey HSD test, *P* = 0.043) while no significant difference was observed in V2 and V3 treatments (Tukey HSD test, both *P* > 0.097). The *R:S* ratio of *B. curtipendula* in monoculture was statistically similar to that in mixture in V1 and V2 treatments (Tukey HSD test, both *P* > 0.074) but was significantly higher than that in mixture in V3 treatment (Tukey HSD test, *P* = 0.012). The results of linear mixed-effects model suggested that the overall impact of rainfall variability on the *R:S* ratio of *O. phaeacantha* was significant (*P* = 0.007, Table S1).
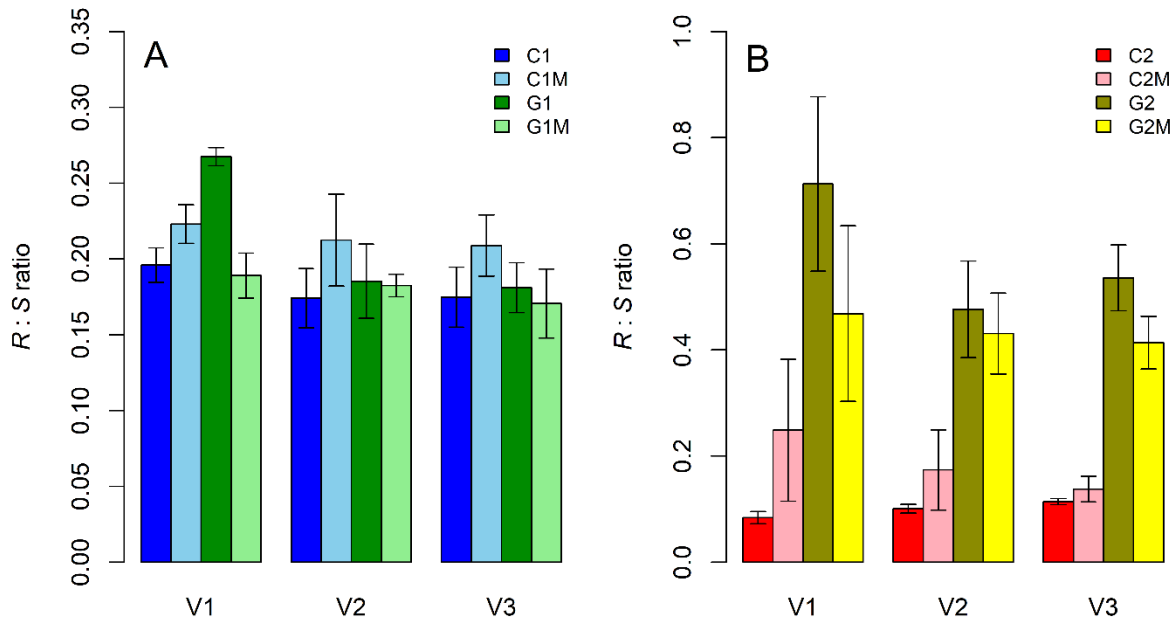
Figure 2. Root-to-shoot biomass ratio (*R:S* ratio) of two pairs of CAM (C1: *Cylindropuntia imbricata*; C2: *Opuntia phaeacantha*) and C4 grass species (G1: *Bouteloua eriopoda*; G2: *Bouteloua curtipendula*) in monoculture (C1, G1, C2, G2) and mixture (C1M, G1M, C2M, G2M) in each of the three rainfall treatments (V1, V2 and V3). Error bars indicate 95% confidence intervals.

1.4.3 The effect of rainfall variability on shallow soil water content

Increasing rainfall variability from V1 to V2 and from V2 to V3 both significantly decreased the soil water content in *C. imbricata* monoculture pots (Tukey HSD test, both $P < 0.002$, Figure 3A), while the decline in soil water content in *B. eriopoda* monoculture pots was only significant when rainfall variability increased from V1 to V3 (Tukey HSD test, $P = 0.010$). The soil water content in mixture pots of *C. imbricata* and *B. eriopoda* decreased from V1 to V2 treatment (Tukey HSD test, $P = 0.001$) and was statistically similar in the V2 and V3 treatments (Tukey HSD test, $P = 0.721$). The soil water content in *C. imbricata* monoculture pots was significantly higher than that in *B. eriopoda* monoculture pots and mixture pots regardless of rainfall treatment (Tukey HSD test, all $P < 0.001$), while there was no significant difference between *B. eriopoda* monoculture pots and mixture pots (Tukey HSD test, all $P > 0.205$).

The soil water content in *O. phaeacantha* monoculture pots was reduced significantly only when rainfall variability increased from V1 to V3 (Tukey HSD test, $P = 0.011$, Figure 3B). In *B. curtipendula* monoculture pots, soil water content did not differ statistically between V1 and V2 treatments but was significantly higher in V3 treatment than in V1 and V2 treatments (Tukey HSD test, both $P < 0.001$). The soil water content in mixture pots declined significantly from V1 to V2 treatment (Tukey HSD test, $P = 0.046$) but remained statistically indistinguishable between V2 and V3 treatments (Tukey HSD test, both $P > 0.131$). The soil water content in *O. phaeacantha* monoculture pots was statistically higher than that in *B. curtipendula* monoculture pots and mixture pots in all rainfall treatments (Tukey HSD test, all $P < 0.037$) except that the difference between *O. phaeacantha* and *B. curtipendula* monoculture pots was statistically insignificant in V3 treatment (Tukey HSD test, $P = 0.498$). The soil water content between *B. curtipendula* monoculture pots and mixture pots was statistically similar regardless of rainfall treatment (Tukey HSD test, all > 0.254).
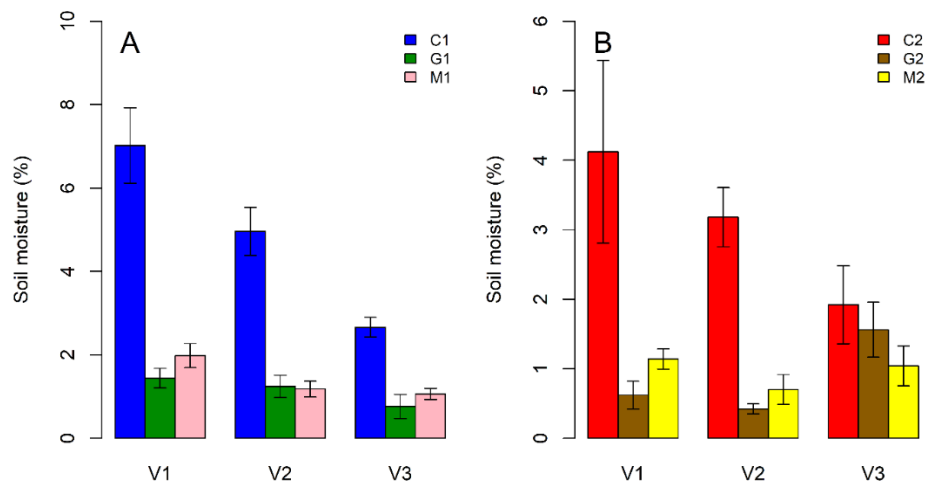
Figure 3. Shallow soil moisture (%) in monoculture (C1, G1, C2, G2) and mixture (M1, M2) in each of the three rainfall variability treatments (V1, V2 and V3). Error bars indicate 95% confidence intervals.

1.4.4 The effect of rainfall variability on CAM CO_2 assimilation rate

The increase in rainfall variability did not have significant effects on the CO_2 assimilation rate of *C. imbricata* in monoculture at all stages examined in this study (Tukey HSD test, all $P > 0.056$) except that the CO_2 assimilation rate was significantly higher in the V3 treatment than in V1 and V2 treatments on October 12 (Tukey HSD test, both $P < 0.001$, Figure 4A). Similarly, the CO_2 assimilation rate of *C. imbricata* in mixture did not differ among the three rainfall treatments at all ontogenetic stages (Tukey HSD test, all $P > 0.216$) except that a strong increase in rainfall variability (V3) led to a significant increase with respect to V1 treatment on October 12 (Tukey HSD test, $P = 0.018$). The difference in CO_2 assimilation rate of *C. imbricata* between monoculture and mixture conditions was not significant among rainfall variability treatments on August 1 and 19 (Tukey HSD test, all $P > 0.090$), but the CO_2 assimilation rate was significantly higher in monoculture than in mixture in V3 treatment on September 7 (Tukey HSD test, $P = 0.018$) and in all rainfall treatments on and after September 25 (Tukey HSD test, all $P < 0.043$). The result of the linear mixed-effects model indicated that rainfall variability, competition and time as well as their interactions all significantly affected CO_2 assimilation rate of *C. imbricata* (all $P < 0.002$, Table S2).
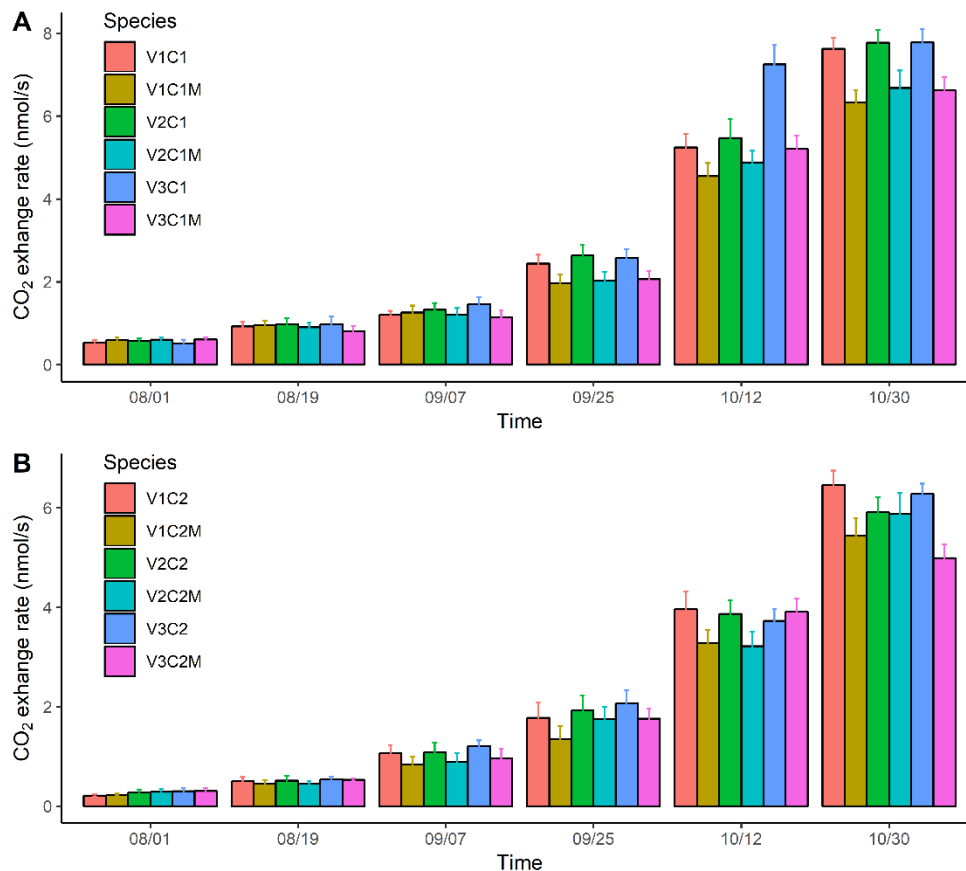
Figure 4. Ontogenetic changes in individual nocturnal CO_2 exchange rate (nmol/s) of two CAM species (C1: *Cylindropuntia imbricata*; C2: *Opuntia phaeacantha*) in monoculture (C1, C2) and mixture (C1M, C2M) in each of the three rainfall treatments (V1, V2 and V3). Error bars indicate 95% confidence intervals.

The effect of rainfall variability treatments on CO_2 assimilation rate of *O. phaeacantha* in monoculture was not significant at all stages (Tukey HSD test, all $P > 0.074$) except that a significant decrease in CO_2 assimilation was found from V1 to V2 treatment on October 30 (Tukey HSD test, $P = 0.025$, Figure 4B). In mixture conditions, the difference in CO_2 assimilation among rainfall treatments was not significant from August 1 to September 25 (Tukey HSD test, all $P > 0.059$), while the CO_2 assimilation rate was significantly higher in V3 treatment than in V1 and V2 treatments on October 12 (Tukey HSD test, both $P < 0.010$) and significantly lower in V3 treatment than in V2 treatment (Tukey HSD test, $P = 0.004$). The difference in CO_2 assimilation rate between monoculture and mixture conditions was not significant regardless of rainfall treatment from August 1 to September 25 (Tukey HSD test, all $P > 0.050$), but the CO_2 assimilation rate was significantly higher in monoculture than in mixture in both V1 and V2 treatments on October 12 (Tukey HSD test, both $P > 0.005$) and in both V1 and V3 treatments on October 30. In general, the analysis of the linear mixed-effects model suggested that the effect of rainfall variability was not significant ($P = 0.139$), while its interactions with competition and time showed significant impacts on CO_2 assimilation of *O. phaeacantha* (all $P < 0.041$, Table S2).

1.4.5 The effect of rainfall variability on stem volume-to-surface area ratio (V:S ratio) of C. imbricata

The *V:S* ratio of *C. imbricata* in monoculture decreased significantly when rainfall variability increased from V1 to V2 (Tukey HSD test, $P = 0.024$), while a further increase in rainfall variability (V3) did not lead to a significant difference between the V2 and V3 treatments (Tukey HSD test, $P = 0.300$, Figure 5). The ratio of *C. imbricata* in mixture decreased significantly when rainfall variability increased from V1 to V2 (Tukey HSD test, $P < 0.001$), and further declined from V2 to V3 (Tukey HSD test, $P = 0.019$). The *V:S* ratio of *C. imbricata* in monoculture was significantly lower than in mixture regardless of rainfall variability treatment (Tukey HSD test, all $P < 0.013$).
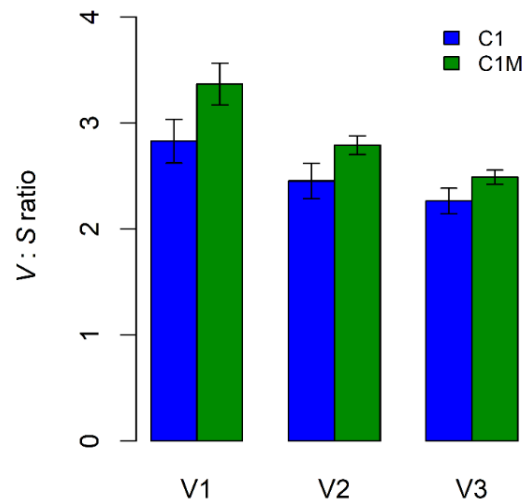
Figure 5. Stem volume-to-surface area ratio (*V:S* ratio, $mm^3 mm^{-2}$) of CAM species *C. imbricata* in monoculture (C1) and mixture (C1M) in each of the three rainfall treatments (V1, V2 and V3). Error bars indicate 95% confidence intervals.

16

1.5 Discussion

The findings in this study show that C4 grasses may outcompete CAM plants under increased rainfall variability. The increase in rainfall variability decreased the biomass of *B. eriopoda* in monoculture. It however, significantly increased the biomass of *B. eriopoda* in mixture (Figure 1A). Although both *O. phaeacantha* and *B. curtipendula* responded negatively to the increase in rainfall variability, only a 24.8% decrease in biomass was found in *B. curtipendula* compared with a 71.3% decline in *O. phaeacantha* (Figure 1B). Additionally, the biomass of both grass species in mixture with CAM plants was significantly higher than that in monoculture while the individual biomass of both CAM species in mixture was significantly lower than that in monoculture (Figure 1), suggesting that grasses benefit from coexisting with CAM plants. The higher *R:S* ratio of both CAM species (in V1 and V3 treatments for *C. imbricata* and V1 treatment for *O. phaeacantha*) and lower *R:S* ratio of both grass species (in V1 treatment for *B. eriopoda* and V3 treatment for *B. curtipendula*) in mixture than in monoculture can be attributed to the fact that CAM plants tend to allocate more biomass to roots for better access to soil water when coexisting with grasses (Yu et al. 2017a) while grasses experience less interspecific competition than intraspecific competition likely due to the spatial niche partitioning of root systems between CAM plants and grasses (Yu et al. 2018).

The high WUE of CAM plants (Lüttge 2004) allows grasses in mixture to absorb more water from the soil and promotes the growth of grasses. The soil moisture in the upper layer generally decreased with increasing rainfall variability (Figure 3), which may result from more rapid infiltration due to the relatively coarse soil texture used in this study and prolonged dry periods between rainfall events under increased rainfall variability conditions. These results suggest that deep-rooted plants can gain a competitive advantage over shallow-rooted plants in acquiring deep soil water under increased rainfall variability, which is consistent with previous studies (Kulmatiski and Beard 2013; Munson et al. 2013). Our study found that although CAM plants have strong drought resistance (Lüttge 2004), more extreme rainfall inputs can alter soil water distribution, increase deeper soil moisture and consequently increase the competitive advantage of grasses over CAM plants. This implies that grasses can fully take advantage of deeper soil moisture caused by increased rainfall variability thereby indirectly reducing CAM plant biomass production. We also note that the decreased biomass of CAM species *C. imbricata* in mixture might be partially attributed to the shading effect of co-existing grass species *B. eriopoda* during the later stage of the experiment, which can negatively affect the daytime carbon assimilation in CAM plants.

The carbon assimilation rate of both CAM species was significantly reduced in mixture versus in monoculture especially at the final measurement stage (Figure 4), which indicates the negative physiological responses of CAM plants to the strong competition for available water with grasses. The lower instantaneous photosynthesis of CAM plants in mixture is responsible for the observed decrease in biomass since photosynthesis directly determines biomass production (Wang et al. 2015). This metabolic difference can be further illustrated by changes in morphological traits. Our results show that the *V:S* ratio of *C. imbricata* was significantly higher in mixture than in monoculture in all rainfall variability scenarios (Figure 5). This may indicate that CAM plants tend to increase their *V:S* ratio in order to reduce transpiration and water loss when they are in competition for soil moisture with grasses, although it decreased photosynthesis

which was confirmed by the significant decline in nocturnal carbon assimilation of *C. imbricata* in mixture compared with *C. imbricata* in monoculture (Figure 4). Variations in stem *V:S* ratio can be considered as a morphological strategy of many CAM species to adapt to soil water dynamics in arid environments because stem surface area determines the photosynthetic capacity while stem volume constrains the storage of carbon, water and nutrients (Williams et al. 2004). Under water stress, a higher stem *V:S* ratio may be favored to ensure high storage of water as well as non-structural carbohydrates to maintain growth and development. However, this reduces carbon assimilation due to restricted surface area and further limit plant growth. Therefore, the functional trade-off in maximum growth versus drought tolerance is related with stem *V:S* ratio and determines the sensitivity of CAM plants to climate change (Mauseth 2000; Williams et al. 2004). Interestingly, increasing rainfall variability decreased the stem *V:S* ratio of *C. imbricata* in both monoculture and mixture (Figure 5), indicating that CAM plants tend to increase their photosynthetic capacity to maximize their survival and growth under higher rainfall variability when grasses show a competitive advantage over CAM plants. Though adjusting *V:S* ratio was suggested as a common strategy when CAM plants encounter long-term drought conditions, our study indicates that strong competition with grasses may also force CAM plants to develop morphological changes under drought stress to minimize water loss.

Previous work has examined the impacts of increasing aridity and CO_2 enrichment on the growth of *C. imbricata* and its competitive relationship with *B. eriopoda* (Yu et al. 2019), but it is still unclear how rainfall variability could affect CAM-grass interactions. This study shows that increasing rainfall variability alone favors C4 grasses over CAM plants. Although CAM plants are drought resistant, large rainfall inputs can cause deeper drainage and significantly reduce soil moisture at shallow depths where roots of CAM plants are mainly distributed (Knapp et al. 2008; Kulmatiski and Beard 2013; Gherardi and Sala 2015). Moreover, the increased deep soil moisture caused by extreme rainfall events can be accessible by grass roots, which promotes grass biomass production and its competitive advantage over CAM plants. Our study suggests that changes in rainfall variability is one of the major climate drivers that can alter plant interactions and species composition in dryland ecosystems given the extremely limited water availability.

It has been widely recognized that while the total amount of precipitation remains constant, the changes in the variability of rainfall regimes can exhibit substantial influences on plant individual growth and interspecific interactions, therefore further impacting community composition as well as ecosystem functioning and services (Fay et al. 2000; Adler et al. 2006; Knapp et al. 2008; Thornton et al. 2014; Gherardi and Sala 2015; Rudgers et al. 2018; March-Salas and Fitze 2019). Despite the importance of mean annual precipitation for plant growth and productivity at large scales (Heisler-White et al. 2008), changes in intra-seasonal rainfall variability may alter ecohydrological processes such as infiltration and evapotranspiration at local scale, and therefore also have significant influences on vegetation dynamics (Knapp et al. 2002; Harper et al. 2005; Yu et al. 2018). Our study indicates that increases in rainfall variability alone may not favor CAM expansion. Instead, more extreme rainfall events can cause deeper infiltration of soil water thereby facilitating grass biomass production. We should note that other climate factors such as global warming and increased CO_2 concentrations may also play an important role in determining the interactions between CAM plants and grasses and therefore their relative abundance. Additionally, plant survival capacity during resource (e.g., water)

interpulse can also affect plant community composition and dynamics in environments with low resource availability (Goldberg and Novoplansky 1997). Finally, we cannot exclude that the results of this study might be affected the pot size, as bigger pots would have allowed to accommodate a greater number of plant individuals. In this study, however, we did not evaluate the sensitivity of our result to the pot size. Further experimental work is needed to test how climate variables jointly impact the CAM-grass coexistence to better predict the structure and dynamics of dryland ecosystems under ongoing climate change.

1.6 Conclusion

Our study provides novel evidence that increasing rainfall variability can suppress CAM biomass production due to decreased shallow soil water availability and thus favor coexisting C4 grasses. Besides the decline in nocturnal carbon assimilation, CAM plants can also develop morphological changes through increasing stem *V:S* ratio when coexisting with grasses to reduce water loss from transpiration and maintain growth, development and reproduction. Stem *V:S* ratio therefore is indicative of the trade-off in growth capacity versus water storage capacity. Our study suggests that soil water distribution significantly regulates the biomass production of CAM plants and its competitive relationships with coexisting grass species and highlights the crucial role of rainfall variability as well as other climate drivers and plant survival capacity under drought stress during rainfall interpulse in shifting the community composition and ecosystem productivity in drylands.

1.7 References

Adler PB, HilleRisLambers J, Kyriakidis PC, Guan QF, Levine JM (2006) Climate variability has a stabilizing effect on the coexistence of prairie grasses. Proc Natl Acad Sci USA 103:12793–12798

Allen CD, Breshears DD, McDowell NG (2015) On underestimation of global vulnerability to tree mortality and forest die-off from hotter drought in the Anthropocene. Ecosphere 6:129

Anderegg WRL, Kane J, Anderegg LDL (2013) Consequences of widespread tree mortality triggered by drought and temperature stress. Nat Clim Chang 3:30–36

Bates D, Maechler M, Bolker B, Walker S (2015) Fitting linear mixed-effects models using lme4. J Stat Softw 67:1–48

Benson L, Walkington DL (1965) The southern Californian prickly pears–invasion, adulteration, and trail-by-fire. Ann Mo Bot Gard 52:262–273

Borland AM, Griffiths H, Hartwell J, Smith JAC (2009) Exploiting the potential of plants with crassulacean acid metabolism for bioenergy production on marginal lands. J Exp Bot 60:2879–2896

Borland AM, Barrera Zambrano VA, Ceusters J, Shorrock K (2011) The photosynthetic plasticity of crassulacean acid metabolism: an evolutionary innovation for sustainable productivity in a changing world. New Phytol 191:619–633

Cushaman JC, Borland AM (2002) Induction of crassulacean acid metabolism by water limitation. Plant Cell Environ 25:295–310

Davis S, LeBauer D, Long S (2014) Light to liquid fuel: theoretical and realized energy conversion efficiency of plants using Crassulacean Acid Metabolism (CAM) in arid conditions. J Exp Bot 65:3471–3478

D'Odorico P, Okin GS, Bestelmeyer BT (2012) A synthetic review of feedbacks and drivers of shrub encroachment in arid grasslands. Ecohydrology 5:520–530

D'Odorico P, Bhattachan A (2012) Hydrologic variability in dryland regions: impacts on ecosystem dynamics and food security. Phyl Trans R Soc B 367:3145–3157

Drennan PM, Nobel PS (2000) Responses of CAM species to increasing atmospheric CO_2 concentrations. Plant Cell Environ 23:767–781

Fan Y, Li XY, Huang H, Wu XC, Yu KL, Wei JQ, Zhang CC, Wang P, Hu X, D'Odorico P (2019) Does phenology play a role in the feedbacks underlying shrub encroachment? Sci Total Environ 657:1064–1073

Fay PA, Carlisle JD, Knapp AK, Blair JM, Collins SL (2000) Altering rainfall timing and quantity in a mesic grassland ecosystem: design and performance of rainfall manipulations shelters. Ecosystems 3:308–319

Fischer EM, Beyerle U, Knutti R (2013) Robust spatially aggregated projections of climate extremes. Nat Clim Chang 3:1033–1038

Gherardi LA, Sala OE (2015) Enhanced precipitation variability decreases grass- and increases shrub- productivity. Proc Natl Acad Sci USA 112:12735–12740

Goldberg D, Novoplansky A (1997) On the relative importance of competition in unproductive environments. J Ecol 85:409–418

Harper CW, Blair JM, Fay PA, Knapp AK, Carlisle JD (2005) Increased rainfall variability and reduced rainfall amount decreases soil CO_2 flux in a grassland ecosystem. Glob Chang Biol 11:322–334

Heisler-White J, Knapp A, Kelly E (2008) Increasing precipitation event size increases aboveground net primary productivity in a semi-arid grassland. Oecologia 158:129–140

Hillel D, Rosenzweig C (2002) Desertification in relation to climate variability and change. Adv Agron 77:1-38

IPCC (2013) Summary for policymakers. In: Stocker TF, Qin D, Plattner G-K, Tignor M, Allen SK, Boschung J, Nauels A, Xia Y, Bex V, Midgley PM (eds) Climate Change 2013: The Physical Science Basis. Contribution of Working Group I to the Fifth Assessment Report of the Intergovernmental Panel on Climate Change. Cambridge University Press, Cambridge, UK and New York, NY, pp 3–29

Knapp AK, Fay PA, Blair JM, Collins SL, Smith MD, Carlisle JD, Harper CS, Danner BT, Lett MS, McCarron JK (2002) Rainfall variability, carbon cycling, and plant species diversity in a mesic grassland. Science 298:2202–2205

Knapp AK, Beier C, Briske DD, Classen AT, Luo Y, Reichstein M, Smith MD, Smith SD, Bell JE, Fay PA, Heisler JL, Leavitt SW, Sherry R, Smith B, Weng E (2008) Consequences of more extreme precipitation regimes for terrestrial ecosystems. Bioscience 58:811–821

Kulmatiski A, Beard K (2013) Woody plant encroachment facilitated by increased precipitation intensity. Nat Clim Chang 3:833–837

Lüttge U (2004) Ecophysiology of crassulacean acid metabolism (CAM). Ann Bot 93:629–652

Maestre FT, Salguero-Gomez R, Quero JL (2012) It's getting hotter in here: determining and projecting the impacts of global change on drylands. Phyl Trans R Soc B 367:3062–3075

March-Salas M, Fitze PS (2019) A multi-year experiment shows that lower precipitation predictability encourages plants' early life stages and enhances population viability. PeerJ 7:e6443

Mauseth JD (2000) Theoretical aspects of surface-to-volume ratios and water-storage capacities of succulent shoots. Am J Bot 87:1107–1115

Miller TEX, Louda SM, Rose KA, Eckberg JO (2009) Impacts of insect herbivory on cactus population dynamics: experimental demography across an environmental gradient. Ecol

Monogr 79:155–172

Munson SM, Muldavin EH, Belnap J, Peters DPC, Anderson JP, Reiser MH, Melgoza-Castillo A, Herrick JE, Christiansen TA (2013) Regional signatures of plant response to drought and elevated temperature across a desert ecosystem. Ecology 94: 2030–2041

Ogburn RM, Edwards EJ (2010) The ecological water-use strategies of succulent plants. Adv Bot Res 55:179–225

Osmond C, Neales T, Stange G (2008) Curiosity and context revisited: crassulacean acid metabolism in the Anthropocene. J Exp Bot 59:1489–1502

Petrie MD, Collins SL, Gutzler DS, Moore DM (2014) Regional trends and local variability in monsoon precipitation in the northern Chihuahuan Desert, USA. J Arid Environ 103:63–70

Poorter H, Navas ML (2003) Plant growth and competition at elevated CO_2: on winners, losers and functional groups. New Phytol 157:175–198

R Development Core Team (2017) R: A language and environment for statistical computing. R Foundation for Statistical Computing, Vienna, Austria. URL https://www.R-project.org/

Ravi S, D'Odorico P, Wang L, White C, Okin GS, Collins SL (2009) Post-fire resource redistribution in desert grasslands: A possible negative feedback on land degradation. Ecosystems 12:434–444

Reyes-García C, Andrade JL (2009) Crassulacean acid metabolism under global climate change. New Phytol 181:754–757

Reynolds JF, Stafford Smith DM, Lambin EF, Turner II BL, Mortimore M, Batterbury SP, Downing TE, Dowlatabadi H, Fernández RJ, Herrick JE, Huber-Sannwald E, Jiang H, Leemans R, Lynam T, Maestre FT, Ayarza M, Walker B (2007). Global desertification: building a science for dryland development. Science 316:847–851

Rudgers JA, Chung AY, Maurer GE, Moore DI, Muldavin EH, Litvak ME, Collins SL (2018) Climate sensitivity functions and net primary production: A framework for incorporating climate mean and variability. Ecology 99:576–582

Seager R, Ting M, Held I, Kushnir Y, Lu J, Vecchi G, Huang HP, Harnik N, Leetmaa A, Lau NC, Li CH, Velez J, Naik N (2007) Model projections of an imminent transition to a more arid climate in Southwestern North America. Science 16:1181–1184

Smith MD (2011) The ecological role of climate extremes: current understanding and future prospects. J Ecol 99:651–655

Thomey ML, Collins SL, Vargas R, Johnson JE, Brown RF, Natvig DO, Friggens MT (2011) Effect of precipitation variability on net primary production and soil respiration in a Chihuahuan desert grassland. Glob Chang Biol 17:1505–1515

Thornton PK, Ericksen PJ, Herrero M, Challinor AJ (2014) Climate variability and vulnerability to climate change: a review. Glob Chang Biol 20:3313–3328

Van Mantgem PJ, Stephenson NL, Byrne JC, Daniels LD, Franklin JF, Fulé PZ, Harmon ME, Larson AJ, Smith JM, Taylor AH, Veblen TT (2009) Widespread increase of tree mortality rates in the western United States. Science 323:521–524

Wang Z, Ji M, Deng J, Milne RI, Ran J, Zhang Q, Fan Z, Zhang X, Li J, Huang H, Cheng D, Niklas KJ (2015) A theoretical framework for whole-plant carbon assimilation efficiency based on metabolic scaling theory: a test case using *Picea* seedlings. Tree Physiol 35:599–607

Williams CA, Albertson JD (2006) Dynamical effects of the statistical structure of annual rainfall on dryland vegetation. Glob Chang Biol 12:777–792

Williams DG, Hultine KR, Dettman DL (2014) Functional trade-offs in succulent stems predict

responses to climate change in columnar cacti. J Exp Bot 65:3405–3413

Weltzin JF, Loik ME, Schwinning S, Williams DG, Fay PA, Haddad BM, Harte J, Huxman TE, Knapp AK, Lin GH, Pockman WT, Shaw MR, Small EE, Smith MD, Smith SD, Tissue DT, Zak JC (2003) Assessing the response of terrestrial ecosystems to potential changes in precipitation. Bioscience 53:941–952

Wu Z, Dijkstra P, Koch GW, Pañuelas J, Hungate BA (2011) Responses of terrestrial ecosystems to temperature and precipitation change: A meta-analysis of experimental manipulation. Glob Chang Biol 17:927–942

Yu K, Foster A (2016) Modeled hydraulic redistribution in tree-grass, CAM-grass, and tree-CAM associations: the implications of crassulacean acid metabolism (CAM). Oecologia 180:1113–1125

Yu K, D'Odorico P, Carr DE, Personius A, Collins SL (2017a) The effect of nitrogen availability and water conditions on competition between a facultative CAM plant and an invasive grass. Ecol Evol 7:7739–7749

Yu K, D'Odorico P, Li W, He YL (2017b) Effects of competition on induction of crassulacean acid metabolism in a facultative CAM plant. Oecologia 184:351–361

Yu K, Carr D, Anderegg W, Tully K, D'Odorico P (2018) Response of a facultative CAM plant and its competitive relationship with a grass to changes in rainfall regime. Plant Soil 427:321–333

Yu K, D'Odorico P, Collins SL, Carr D, Porporato A, Anderegg WRL, Gilhooly III WP, Wang L, Bhattachan A, Bartlett M, Hartzell S, Yin J, He Y, Li W, Tatlhego M, Fuentes JD (2019) The competitive advantage of a constitutive CAM species over a C4 grass species under drought and CO2 enrichment. Ecosphere 10:e02721

Zhang RD (1997) Determination of soil sorptivity and hydraulic conductivity from the disk infiltrometer. Soil Sci Soc Am J 61:1024–30

1.8 Supplemental information

Figure S1. The randomized block design in this study illustrated by one of the five blocks (90 pots in total). Each block consisted of 18 randomly distributed pots representing different species and treatment combinations. V1, V2 and V3 represent three levels of rainfall treatments as shown by different colors. C and G refer to CAM and grass monoculture pots, respectively. C1: *Cylindropuntia imbricata*; G1: *Bouteloua eriopoda*; M1: C1 and G1 in mixture; C2: *Opuntia phaeacantha*; G2: *Bouteloua curtipendula*; M2: C2 and G2 in mixture.
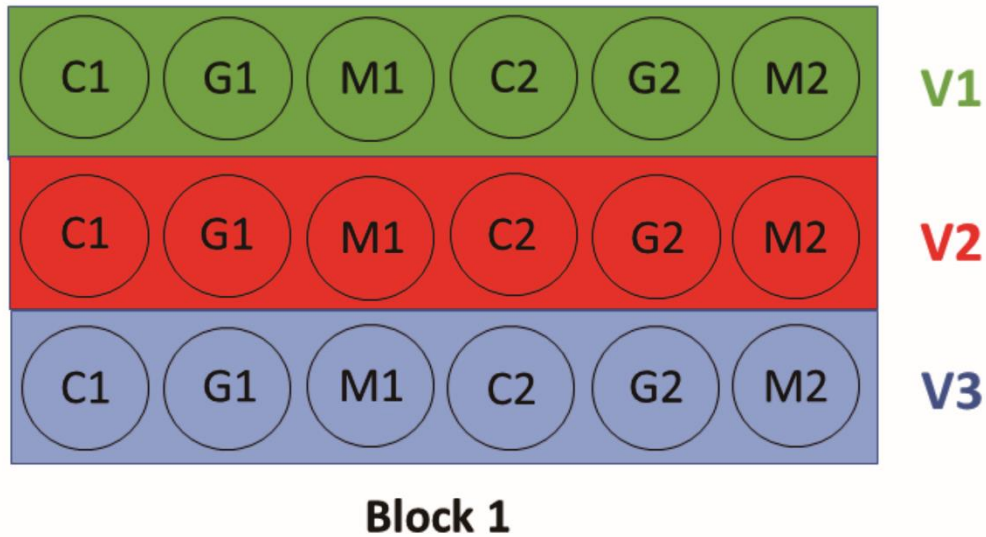
Table S1. Results of the linear mixed-effects model evaluating the effects of species, rainfall variability treatment and competition as well as their interactions on belowground to aboveground biomass ratio (*R:S* ratio). Block was treated as a random factor.

Source	χ^2	d.f.	*P* value
C. imbricata and *B. eriopoda*			
Species	0.20	1	0.6512
Rainfall treatment	40.63	2	< 0.0001 ***
Competition	0.07	1	0.7877
Species: rainfall treatment	9.63	2	0.0081 **
Species: competition	42.89	1	< 0.0001 ***
Rainfall treatment: competition	15.63	2	0.0004 ***
Species: rainfall treatment: competition	9.26	2	0.0097 **
O. phaeacantha and *B. curtipendula*			
Species	229.86	1	< 0.0001 ***
Rainfall treatment	10.06	2	0.0065 **
Competition	1.10	1	0.2943
Species: rainfall treatment	3.57	2	0.1680
Species: competition	21.99	1	< 0.0001 ***
Rainfall treatment: competition	1.34	2	0.5118
Species: rainfall treatment: competition	7.48	2	0.0238 *

*indicates the degree of significance test by Wald chi-squared test, *$P < 0.05$, **$P < 0.01$, ***$P < 0.001$

Table S2. Results of the linear mixed-effects model evaluating the effects of rainfall variability treatment, competition and time as well as their interactions on nocturnal CO$_2$ exchange rate of *C. imbricata* and *O. phaeacantha*. Individual was treated as a random factor.

Source	χ^2	d.f.	*P* value
C. imbricata			
Rainfall treatment	36.30	2	< 0.0001 ***
Competition	166.15	1	< 0.0001 ***
Time	16683.74	5	< 0.0001 ***
Rainfall treatment: Competition	12.58	2	0.0019 **
Rainfall treatment: Time	119.91	10	< 0.0001 ***
Competition: Time	166.79	5	< 0.0001 ***
Rainfall treatment: Competition: Time	41.67	10	< 0.0001 ***
O. phaeacantha			
Rainfall treatment	3.94	2	0.1391
Competition	66.30	1	< 0.0001 ***
Time	12643.97	5	< 0.0001 ***
Rainfall treatment: Competition	6.41	2	0.0405 *
Rainfall treatment: Time	28.12	10	0.0017**
Competition: Time	54.21	5	< 0.0001 ***
Rainfall treatment: Competition: Time	56.49	10	< 0.0001 ***

*indicates the degree of significance test by Wald chi-squared test, *$P < 0.05$, **$P < 0.01$, ***$P < 0.001$

CHAPTER 2

CAM plant expansion favored indirectly by asymmetric climate warming and increased rainfall variability

2.1 Abstract

Recent observational evidence suggests that nighttime temperatures are increasing faster than daytime temperatures while in some regions precipitation events are becoming less frequent and more intense. The combined ecological impacts of these climatic changes on crassulacean acid metabolism (CAM) plants and their interactions with other functional groups (i.e., grass communities) remain poorly understood. Here we developed a growth chamber experiment to investigate how two CAM-grass communities in desert ecosystems of the southwestern United States and northern Mexico respond to asymmetric warming and increasing rainfall variability. Grasses generally showed competitive advantages over CAM plants with increasing rainfall variability under ambient temperature conditions. In contrast, asymmetric warming caused mortality of both grass species (*Bouteloua eriopoda* and *Bouteloua curtipendula*) in both rainfall treatments due to enhanced drought stress. Grass mortality indirectly favored CAM plants even though the biomass of both CAM species *Cylindropuntia imbricata* and *Opuntia phaeacantha* significantly decreased. The stem's volume-to-surface ratio of *C. imbricata* was significantly higher in mixture than in monoculture under ambient temperature (both $P < 0.0014$); however the difference became insignificant under asymmetric warming (both $P > 0.1625$), suggesting that warming weakens the negative effects of interspecific competition on CAM plant growth. Our findings suggest that while the increase in intra-annual rainfall variability enhances grass productivity, asymmetric warming may lead to grass mortality, thereby indirectly favoring the expansion of co-existing CAM plants. This study provides novel experimental evidence showing how the ongoing changes in global warming and rainfall variability affect CAM-grass growth and interactions in dryland ecosystems.

2.2 Introduction

Future climate projections indicate the occurrence of changes in variability of weather variables at multiple scales (IPCC, 2013). For example, empirical observations suggest that in many regions of the world the minimum nighttime temperature (T_{min}) is increasing more rapidly than the maximum daytime temperature (T_{max}), causing a decrease in the diurnal temperature range (i.e., the difference between T_{max} and T_{min}) (Karl et al., 1993; Vose et al., 2005; Alexander et al., 2006; Peng et al., 2013; Davy et al., 2016). As a result of climate warming, rainfall events tend to become fewer but greater (Huntington, 2006; Durack et al., 2012) which can significantly alter soil moisture distribution and create longer dry spells. However, few ecological studies have investigated the consequences of altered variability, relative to the large number of studies focusing on changes in the mean of climate variables (Parmesan & Yohe, 2003; Heisler-White et al. 2008; D'Odorico & Bhattachan, 2012; Rudgers et al., 2018).

Drylands cover more than 40% of the global terrestrial land surface and account for nearly 40% of the global net primary productivity (Hillel & Rosenzweig, 2002). Because of the limited soil

water and nutrients as well as the sparse vegetation cover, drylands are particularly vulnerable to changes in climate variables (Reynolds et al., 2007; Maestre et al., 2012). Land degradation and desertification have been intensified in drylands over the last century due to climate warming and anthropogenic activities (Fu et al., 2008; Huang et al., 2016). Climate models forecast a warming of up to 4°C in these regions by 2100 (IPCC, 2013; Huang et al., 2016). This large scale warming along with increased precipitation variability will cause a significant shift in species composition and ecological resilience in dryland ecosystems (D'Odorico & Bhattachan, 2012; Maestre et al., 2012). For example, it has been found that increasing precipitation variability caused a dramatic decline in grass productivity but a significant increase in shrub productivity in a Chihuahuan desert grassland (Gherardi & Sala, 2015).

Previous studies have primarily emphasized the ecological impacts of homogeneous climatic warming or changes in rainfall amount (Sala et al., 1988; Knapp et al., 2002; Heisler-White et al., 2008; D'Odorico & Bhattachan, 2012; Maestre et al., 2012), with little attention paid on how ecosystems respond to the combined effects of asymmetric diurnal warming and increased intra-seasonal rainfall variability. The asymmetric warming can significantly affect plant carbon assimilation and productivity through the regulation of temperature-dependent biological rates such as photosynthesis and respiration (Brown et al., 2004; McCormick et al., 2006; Peng et al., 2013; Wang et al., 2015). It has been proposed that nighttime warming increases plant respiration (Ryan, 1991; Griffin et al., 2002), but the associated greater consumption of carbohydrates can stimulate photosynthesis during the following day thereby leading to a net positive carbon fixation in plants (Paul et al., 2001; McCormick et al., 2006), as evidenced by a field warming experiment in a semi-arid steppe (Wan et al., 2009). However, the net effects of asymmetric diurnal warming may vary among ecosystem types and also depend on the interactive effects between global warming and other climate variables such as rainfall (Xia et al., 2014; Collins et al., 2017). For instance, the increased precipitation variability is likely to favor species with deep root systems such as woody plants with respect to shallow-rooted plants (Kulmatiski & Beard, 2013; Gherardi & Sala, 2015), which may interfere with plant responses to climate warming. Therefore, the combined effects of asymmetric diurnal warming and intra-seasonal rainfall variability on vegetation growth and relative abundance among plant functional groups remain highly uncertain.

Previous work on dryland vegetation response to climate change typically concentrated on the dynamics of woody or grass species (Knapp et al., 2008; D'Odorico & Bhattachan, 2012; Kulmatiski & Beard, 2013; Fan et al., 2019), while the response of plants with crassulacean acid metabolism (CAM) and its interactions with other functional groups (i.e., grasses) has remained poorly understood (Yu et al., 2017a, 2018, 2019; Huang et al. 2019). CAM plants are ecologically important for maintaining ecosystem productivity in drylands and economically valuable as food and bioenergy sources (Borland et al., 2009; Davis et al, 2014; Yu et al., 2018). One of the key features in CAM plants is the nocturnal carbon assimilation, which allows them to minimize water loss from transpiration. In addition, the adjustment of stem *V:S* ratio was proposed as a morphological strategy of columnar cacti in response to environmental stresses such as drought, as supported by the large variation in stem *V:S* ratio among cacti species (Williams et al., 2014). The stem's volume-to-surface area (*V:S*) ratio is indicative of the critical trade-off between maximization of growth and minimization of water loss through transpiration (Williams et al., 2014). Under relatively favorable hydrologic conditions, CAM stems tend to

have lower *V:S* ratios to maximize photosynthetic assimilation, but this constrains the water storage capacity due to the relatively limited stem volume. Likewise, climate-induced stresses may induce CAM stems to optimize water use at the expense of declined photosynthesis and growth through increasing *V:S* ratio (Mauseth, 2000; Williams et al., 2014; Hultine et al., 2016). With high water use efficiency (WUE) and strong ability to tolerate drought, CAM plants are expected to outcompete many other functional groups including C4 grasses in highly water limited environments, especially under global climate change (Cushaman & Borland, 2002; Borland et al., 2009; Yu et al., 2017a,b).

The effect of asymmetric nocturnal warming on CAM-grass communities can be intriguing because of the ability of CAM plants to perform nocturnal carbon assimilation. Warming trends may overall favor CAM plants because of the higher optimal temperature for nighttime photosynthesis (Reyes-García & Andrade, 2009) and/or their reduced likelihood of freezing damage during winter (Nobel, 1996) (direct effects). Moreover, CAM productivity can increase as an indirect effect of the decreased productivity of other functional groups such as grasses, and the consequent enhanced availability of moisture and other soil resources for CAM plants (indirect effects). However, increasing nighttime temperatures may also cause stomatal closure in CAM plants when temperature exceeds the optimal range (Osmond, 1978). As discussed earlier, nighttime warming increases nocturnal respiration of grasses but may further stimulate photosynthesis during the following day. In addition, increased rainfall variability pushes more water into deep soil and favors the growth of deep-rooted grasses. However, on the other side, it creates longer dry periods between rainfall events, which likely benefits CAM plants since grasses are more vulnerable to drought and water stress (Yu et al., 2019). Therefore, the impact of asymmetric warming in combination with increasing rainfall variability on the competitive interactions between CAM plants and coexisting grasses remains elusive and experimental evidence is extremely lacking. This has limited our accurate prediction of the whole-ecosystem dynamics in response to global environmental change.

Empirical observations suggest that both of CAM species *Cylindropuntia imbricata* and *Opuntia phaeacantha* are expanding their distribution range across the Chihuahuan desert (Benson & Walkington, 1965; Yu et al., 2019). However, it is still unknown whether this phenomenon results directly from the positive effects of climate change on CAM plant growth or indirectly from negative climate impacts on other coexisting plant functional types such as grasses. In this study, we experimentally investigated the growth of *C. imbricata* and *O. phaeacantha* and their interactions with coexisting C4 grass species (*Bouteloua eriopoda* and *Bouteloua curtipendula* respectively) under future temperature and rainfall patterns. Specifically, we asked: (1) Does increasing rainfall variability promote the growth of grasses due to enhanced deep soil water availability? (2) Does asymmetric warming favor CAM plant growth and counteract the possible positive effect of increasing rainfall variability on grasses given that CAM plants are more drought tolerant? (3) Can *C. imbricata* increase the stem *V:S* ratio when grown in mixture with *B. eriopoda* to minimize water loss?

2.3 Materials and methods
2.3.1 Experimental design
Seeds of two CAM species, *C. imbricata* and *O. phaeacantha* and two C4 grass species, *B. eriopoda* and *B. curtipendula*, were purchased from http://www.cactusstore.com and

http://www.seedsource.com, respectively. Seeds of both CAM species were soaked in warm water overnight and then sown on the soil surface and covered by a thin layer of soil in plastic trays on 15 June 2018. Trays were incubated in a Temperature Incubator 815 (Precision Scientific, Chicago, IL, USA) at 33/22°C day/night to improve seed germination success of CAM plants. Seeds of both C4 grass species were germinated in plastic trays filled with potting mix on 20 June 2018 in the Oxford Tract Greenhouse at University of California, Berkeley. The daily temperatures in the greenhouse ranged from 17°C to 33°C and the photosynthetically photon flux density (PPFD) was 700-900 umol m^{-2} s^{-1} from 7 am to 7 pm. Trays were watered regularly during seed germination to avoid water stress. CAM seedlings were transported to the greenhouse two weeks before transplantation. On 5 August 2018, all CAM and grass seedlings were transplanted into plastic pots (15 cm in diameter and 13 cm in height) filled with potting mix. 6:1 Metromix 200:Turface was selected in our study because its hydraulic conductivity ($\approx$ 3.72×10^{-5} m/s) was close to the values measured in the field in areas of the Northern Chihuahuan Desert where these species coexist (Ravi et al., 2009). Monoculture pots included four conspecific individuals and mixture pots contained two individuals of CAM species and two individuals of co-existing grass species.

2.3.2 Temperature and rainfall treatments
Plants were moved to growth chambers (Conviron E15; Controlled Environments, Winnipeg, Manitoba, Canada) on 6 August 2018 for temperature and rainfall treatments. The experiment consisted of 120 pots with five replicates in both monoculture and mixture. Pots were randomly assigned to each of the two growth chambers with different daily temperature regimes (T1 and T2 respectively) and pots within each growth chamber were randomly subject to two levels of intra-seasonal rainfall variability treatments (V1 and V2) over 90 days. Due to the limited availability of growth chambers, we only included one growth chamber for each temperature treatment following other studies (e.g., Hoekman, 2010). The temperatures in the control group (T1) were set to 33/17°C day/night based on the average daytime and nighttime temperatures observed during growing season in Northern Chihuahuan Desert where some of these species are found to coexist (http://sev.lternet.edu/data). Considering a 4°C warming of the global drylands by the end of 21st century (IPCC, 2013; Huang et al., 2016), the temperatures were increased to 36/22°C day/night in the T2 treatment to simulate future asymmetric warming scenario. V1 is the control rainfall variability treatment which represents the current natural precipitation regime, and V2 simulates the increased rainfall variability under future climate scenario. Watering intensity and frequency were determined based on 30-year records of growing season precipitation in Sevilleta National Wildlife Refuge (150 mm, Petrie et al., 2014) where *C. imbricata* and *B. eriopoda* coexist (Miller et al., 2009), and Cabeza Prieta National Wildlife Refuge (90 mm), where *O. phaeacantha* and *B. curtipendula* co-occur. For *C. imbricata* and *B. eriopoda*, pots were watered with an intensity of 5 mm every three days in the V1 treatment and 10 mm every six days in the V2 treatment; for *O. phaeacantha* and *B. curtipendula*, pots were watered with an intensity of 3 mm every three days in the V1 treatment and 6 mm every six days in the V2 treatment. Plants were fertilized with 20-20-20 Peters professional solution (100 ppm nitrogen) every nine days during the experiment to avoid nutrient stress on plant growth. The daily PPFD in the growth chambers was set to 700 umol m^{-2} s^{-1} from 7 am to 7 pm.

2.3.3 Soil moisture, plant biomass and stem volume-to-surface area (V:S) ratio
Before harvest, soil volumetric water content in the upper layer (~ 6 cm) was determined for each pot on 5 November 2018 using a soil moisture sensor (Waterscout SMEC300, Spectrum Technologies Inc., Plainfield, IL, USA). The grass mortality in the warming treatment was observed in mid-October. Plants were then harvested to measure biomass. CAM plants and grasses in mixture pots were separated and all plant individuals were divided into shoots and roots. Plant roots were removed from pots and carefully washed to minimize the loss of fine roots. The small proportion of remaining roots of CAM plants and grasses in the soil were differentiated based on color, diameter and shape and collected. After fresh mass measurements, all plant samples were oven-dried at 65°C for 72 h to determine dry mass. The shoot and root dry biomass were then aggregated to individual total dry biomass. The CAM/grass individual fresh (M_f) and dry biomass (M_d) were calculated by the CAM/grass total fresh and dry mass in each pot divided by the number of CAM/grass individuals. The individual root-to-shoot biomass ($R:S$) ratios were calculated. The stem *V:S* ratio has been considered as an effective indicator of CAM plant responses to environmental stress because the stem surface area determines the rates of both photosynthetic assimilation and transpirational water loss (Williams et al., 2014). In this study, we also investigated how the stem *V:S* ratio of columnar cacti *C. imbricata* responds to climate change as well as competition. Given that the ribs of 3-month-old cacti are negligible, the stem *V:S* ratio ($mm^3 \ mm^{-2}$) can be roughly determined as following (Mauseth, 2000)

$$V:S = \frac{\frac{1}{4}\pi D^2 h}{\pi D h} = \frac{1}{4}D,$$

where *h* is plant height and *D* is the stem diameter. The stem diameter (mm) of each *C. imbricata* individual was measured at the top, middle and bottom of the stem using a digital Vernier caliper with a resolution of 0.01 mm and then averaged to calculate the mean stem diameter. We clarify here that we were unable to measure the stem *V:S* ratio of *O. phaeacantha* due to the irregular shape of the stems.

2.3.4 Statistical analyses
Data analyses were conducted separately for each pair of CAM and grass species. We first conducted multivariate analysis of variance (MANOVA) using manova function in stats package to examine the effects of growth type (monoculture versus mixture), temperature (T1 versus T2), rainfall treatments (V1 versus V2), and their interactions on measured variables including individual biomass, the *R:S* ratio, and soil water content. Then 156 pairwise comparisons were made to test the significance of differences in individual biomass, the *R:S* ratio, soil water content and the stem *V:S* ratio between growth type, temperature, and rainfall treatments using Tukey's HSD post hoc test through TukeyHSD function in stats package ($\alpha = 0.05$). For each trait, we compared the mean value (i) between T1 and T2 treatments in each rainfall treatment for monoculture and mixture of each species respectively; (ii) between V1 and V2 treatments in each temperature treatment for monoculture and mixture of each species respectively; and (iii) between monoculture and mixture in each combination of rainfall and temperature treatments. The effects of temperature, rainfall, competition (intraspecific versus interspecific) and species as well as their interactions on individual biomass and *R:S* ratio were analyzed using the linear mixed-effects models through lmer function in lme4 package (Bates et al., 2015) and Anova function in car package. Block was treated as a random factor. All the analyses were conducted in R (R Core Team, 2017).

2.4 Results

2.4.1 Responses of plant total biomass

The asymmetric warming (T2 treatment) caused a 34.3–89.9% decline in the biomass of CAM species *C. imbricata* and C4 grass species *B. eriopoda* regardless of growth type and rainfall variability treatment (all $P < 0.0034$, Figure 1a, b). Specifically, *B. eriopoda* in both monoculture and mixture died during the experiment under asymmetric warming regardless of rainfall treatment. The biomass of *C. imbricata* in both monoculture and mixture did not significantly change when rainfall variability increased from V1 to V2 regardless of temperature treatment (all $P > 0.1224$) except for the case of *C. imbricata* biomass in mixture, which declined 31.7% with increased rainfall variability under ambient temperature conditions ($P = 0.0066$). Interestingly, under ambient temperature conditions the increase in rainfall variability resulted in a 19.8% increase in the biomass of *B. eriopoda* in monoculture and a 25.1% increase in mixture (both $P < 0.0091$) while the *B. eriopoda* biomass decreased 40.5% and 43.4% with increasing rainfall variability under asymmetric warming in monoculture and mixture (both $P < 0.0149$), respectively. The biomass of *C. imbricata* in monoculture and mixture were not significantly different in most treatments (all $P > 0.1743$) except for the case of increased rainfall variability and ambient temperature conditions, which exhibited a 34.6% higher *C. imbricata* biomass in monoculture than in mixture ($P = 0.0101$). *B. eriopoda* exhibited a 29.3–44.7% higher biomass in mixture than in monoculture (all $P < 0.0356$) except for the T2V2 treatment in which no significant difference was detected ($P = 0.0866$). The linear mixed-effects model results showed that although the effect of rainfall variability alone on biomass of *C. imbricata* and *B. eriopoda* was not significant ($P = 0.536$), temperature and its interaction with rainfall variability exhibited significant impacts (both $P < 0.001$, Table 1).

Table 1. Results of the linear mixed-effects model evaluating the effects of species, temperature, rainfall variability and competition as well as their interactions on individual total biomass of *C. imbricata* and *B. eriopoda*. Block was treated as a random factor. *P* value was calculated by Wald chi-squared test.

Source	χ^2	*df*	*P* value
Species	1047.291	1	< 0.001
Temperature	1994.947	1	< 0.001
Rainfall	0.382	1	0.536
Competition	36.316	1	< 0.001
Species: temperature	955.789	1	< 0.001
Species: rainfall	23.486	1	< 0.001
Species: competition	30.459	1	< 0.001
Temperature: rainfall	78.318	1	< 0.001
Temperature: competition	21.151	1	< 0.001

Rainfall: competition	0.084	1	0.772
Species: temperature: rainfall	53.570	1	< 0.001
Species: temperature: competition	30.078	1	< 0.001
Species: rainfall: competition	2.943	1	0.086
Temperature: rainfall: competition	0.931	1	0.335
Species: temperature: rainfall: competition	4.212	1	0.040

Similarly, the asymmetric warming was associated with a 39.2–88.5% decline in the biomass of CAM species *O. phaeacantha* and C4 grass species *B. curtipendula* in both monoculture and mixture irrespective of rainfall treatment (all $P < 0.0019$) except that no significant difference in the biomass of *O. phaeacantha* in mixture was found between T1 and T2 treatments under increased rainfall variability ($P = 0.1245$, Figure 1c, d). Asymmetric warming led to the mortality of *B. curtipendula* in both monoculture and mixture regardless of rainfall treatment. Increasing rainfall variability had no significant effects on the biomass of *O. phaeacantha* and *B. curtipendula* both in monoculture and mixture in the two temperature treatments (all $P > 0.0710$). The biomass of *O. phaeacantha* was 52.3% and 118.7% higher in monoculture than in mixture under ambient temperature conditions in both rainfall treatments (both $P < 0.0110$) respectively, while the biomass in monoculture was statistically indistinguishable from that in mixture in both rainfall treatments under asymmetric warming (both $P > 0.1598$). A 43.3–82.5% higher biomass of *B. curtipendula* in mixture than in monoculture was observed across all treatments (all $P < 0.0318$). The results of the linear mixed-effects model suggested strong effects of temperature, rainfall and their interaction on biomass of *O. phaeacantha* and *B. curtipendula* (all $P < 0.020$, Table 2).

Table 2. Results of the linear mixed-effects model evaluating the effects of species, temperature, rainfall variability and competition as well as their interactions on individual total biomass of *O. phaeacantha* and *B. curtipendula*. Block was treated as a random factor. *P* value was calculated by Wald chi-squared test.

Source	χ^2	df	P value
Species	1232.741	1	< 0.001
Temperature	1351.159	1	< 0.001
Rainfall	5.439	1	0.020
Competition	98.208	1	< 0.001
Species: temperature	858.205	1	< 0.001
Species: rainfall	8.042	1	0.005
Species: competition	9.554	1	0.002
Temperature: rainfall	200.014	1	< 0.001

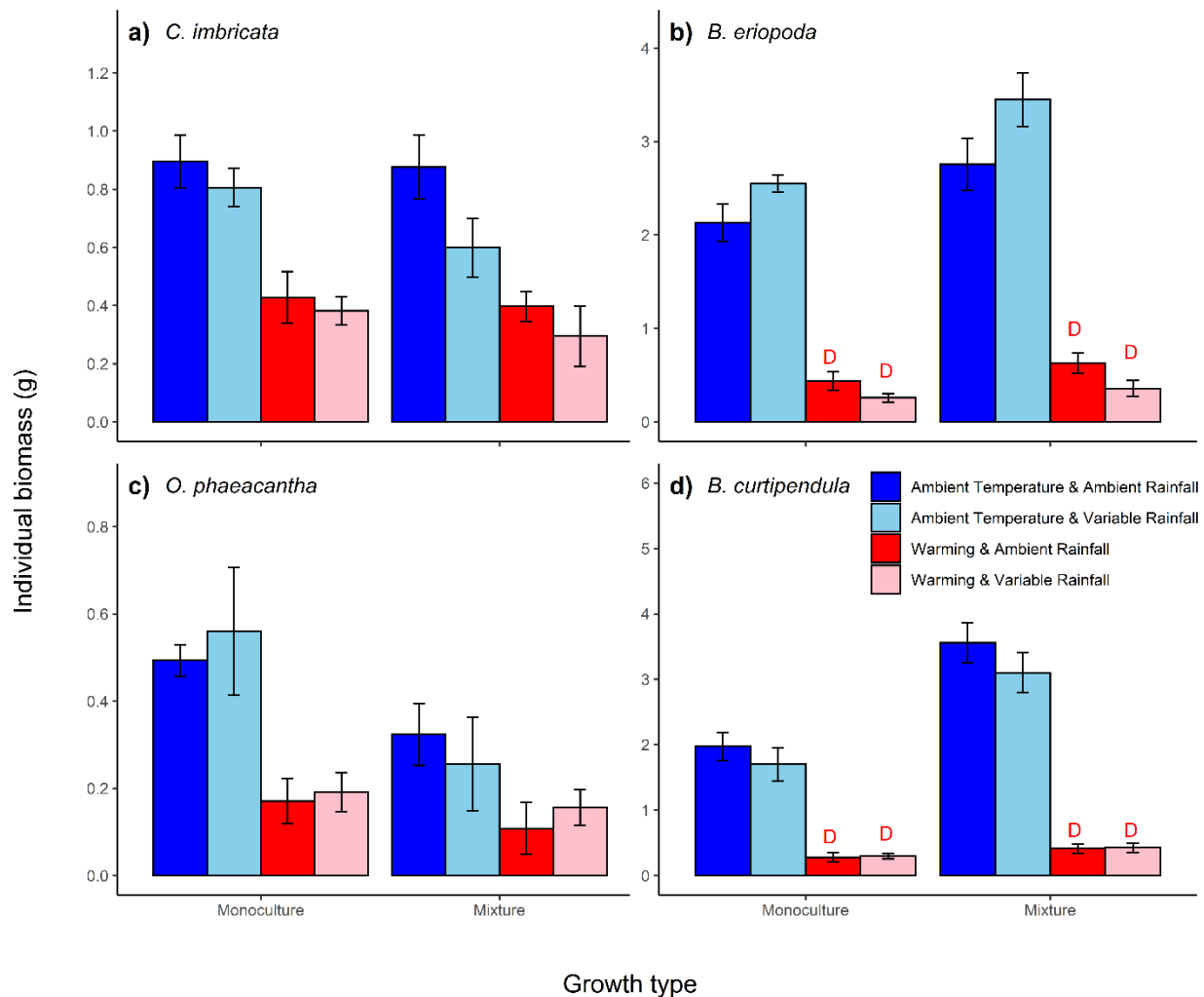| Temperature: competition	75.751	1	< 0.001
Rainfall: competition	1.195	1	0.274
Species: temperature: rainfall	6.666	1	0.001
Species: temperature: competition	131.881	1	< 0.001
Species: rainfall: competition	0.088	1	0.767
Temperature: rainfall: competition	1.602	1	0.206
Species: temperature: rainfall: competition	0.004	1	0.949

Figure 1. Individual total biomass (g, mean 95% confidence internals) of a-d) four species (*C. imbricata*, *B. eriopoda*, *O. phaeacantha*, and *B. curtipendula*, respectively) in monoculture and mixture in each combination of temperature and rainfall treatments. Groups in which plants were dead at harvest were labeled by letter "D".

2.4.2 Responses of plant R:S ratio

Asymmetric warming did not significantly affect the *R:S* ratio of CAM species *C. imbricata* in monoculture in either rainfall treatment (both $P > 0.4577$) but significantly decreased the *R:S* ratio of *C. imbricata* in mixture in both rainfall conditions (both $P < 0.0106$, Figure 2). Under asymmetric warming, the *R:S* ratio of grass species *B. eriopoda* in both monoculture and mixture decreased with respect to the ambient temperature scenario in the V1 treatment (both $P < 0.0086$) but did not significantly change in the V2 treatment (both $P > 0.1680$). The *R:S* ratio of *C. imbricata* was significantly higher in mixture than in monoculture in both rainfall conditions in the ambient temperature treatment (both $P < 0.0011$). Conversely, under asymmetric warming the *R:S* ratio of *C. imbricata* in monoculture and mixture was statistically similar in either rainfall treatment (both $P > 0.1564$). The *R:S* ratio of *B. eriopoda* did not statistically differ between monoculture and mixture conditions regardless of rainfall and temperature treatments (all $P > 0.0520$) except that a higher *R:S* ratio was observed in monoculture than in mixture in the T1V1 treatment ($P = 0.0001$). The linear mixed-effects model results confirmed the significant effects of temperature and its interactions with other factors on *R:S* ratio though the effect of rainfall variability alone was weak (Table S1).
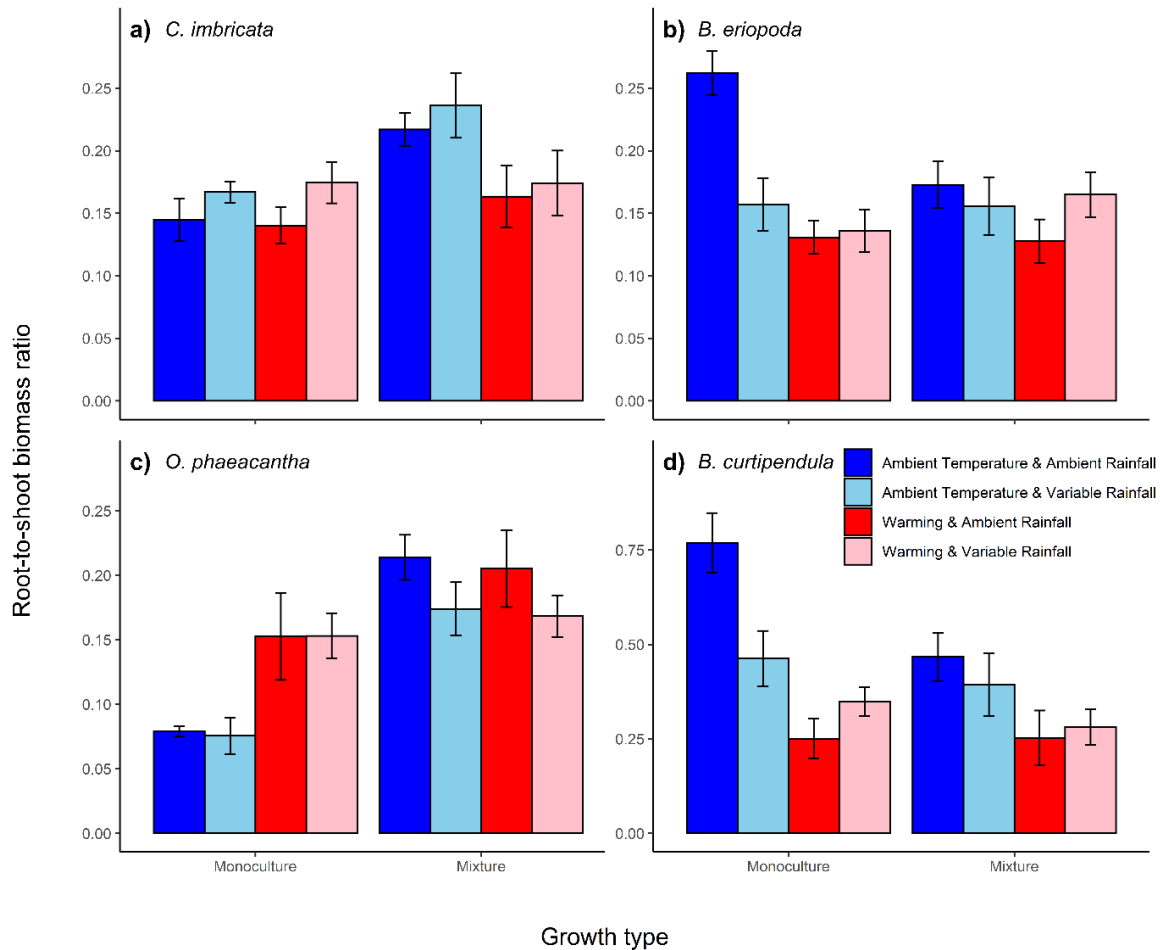

Figure 2. Root-to-shoot biomass (*R:S*) ratio (mean 95% confidence internals) of a-d) four species (*C. imbricata*, *B. eriopoda*, *O. phaeacantha*, and *B. curtipendula*, respectively) in monoculture and mixture in each combination of temperature and rainfall treatments.

Asymmetric warming significantly increased the *R:S* ratio of *O. phaeacantha* grown alone (both *P* < 0.0028) but didn't show a significant effect when it was in mixture regardless of rainfall treatment (both *P* > 0.6329). However, the *R:S* ratio of *B. curtipendula* in both monoculture and mixture was significantly reduced under asymmetric warming with respect to ambient temperature conditions, regardless of rainfall treatment (all *P* < 0.0268) except that no significant difference between the two temperature treatments was observed for *B. curtipendula* in mixture in the V2 rainfall treatment (*P* = 0.0509). The *R:S* ratio of *O. phaeacantha* was significantly higher in mixture than in monoculture under ambient temperature conditions in both rainfall treatments (both *P* < 0.0001). In ambient temperature treatment, a significantly higher *B. curtipendula R:S* ratio was detected in monoculture than in mixture in the V1 treatment (*P* = 0.0004), while the difference was not significant in the V2 treatment (*P* = 0.2595). The *R:S* ratio was not significantly different between monoculture and mixture conditions under asymmetric warming for both *O. phaeacantha* and *B. curtipendula* irrespective of rainfall treatment (all *P* > 0.0511). The strong effects of warming and rainfall treatments were further demonstrated by results of the linear mixed-effects model (Table S2).

2.4.3 Responses of shallow soil moisture
Similar patterns of shallow soil moisture in response to temperature and rainfall treatments were found in the two CAM-grass communities (Figure 3). The soil moisture of all CAM monoculture pots decreased 2.1–5.5% under asymmetric warming in both rainfall treatments (both *P* < 0.0001), while soil moisture of all grass monoculture pots as well as all mixture pots increased 1.4–7.3% under elevated temperature (all *P* < 0.0022) except for *B. curtipendula* monoculture pots in the V2 treatment (*P* = 0.0833). The increased rainfall variability caused a 0.6–8.2% reduction in shallow soil moisture in all monoculture and mixture pots regardless of temperature treatment and species (all *P* < 0.0080).

Under ambient temperature conditions, the shallow soil moisture was 3.1–12.4% higher in all CAM monoculture pots than in grass monoculture pots as well as all mixture pots irrespective of rainfall treatments (all *P* < 0.0001). Under asymmetric warming, the CAM monoculture pots shared statistically similar shallow soil water content with grass monoculture pots and mixture pots regardless of rainfall treatment (all *P* > 0.0997) except that soil water content in *C. imbricata* monoculture pots was 1.7% lower than that in *B. eriopoda* monoculture pots in the V2 treatment (*P* = 0.0435).
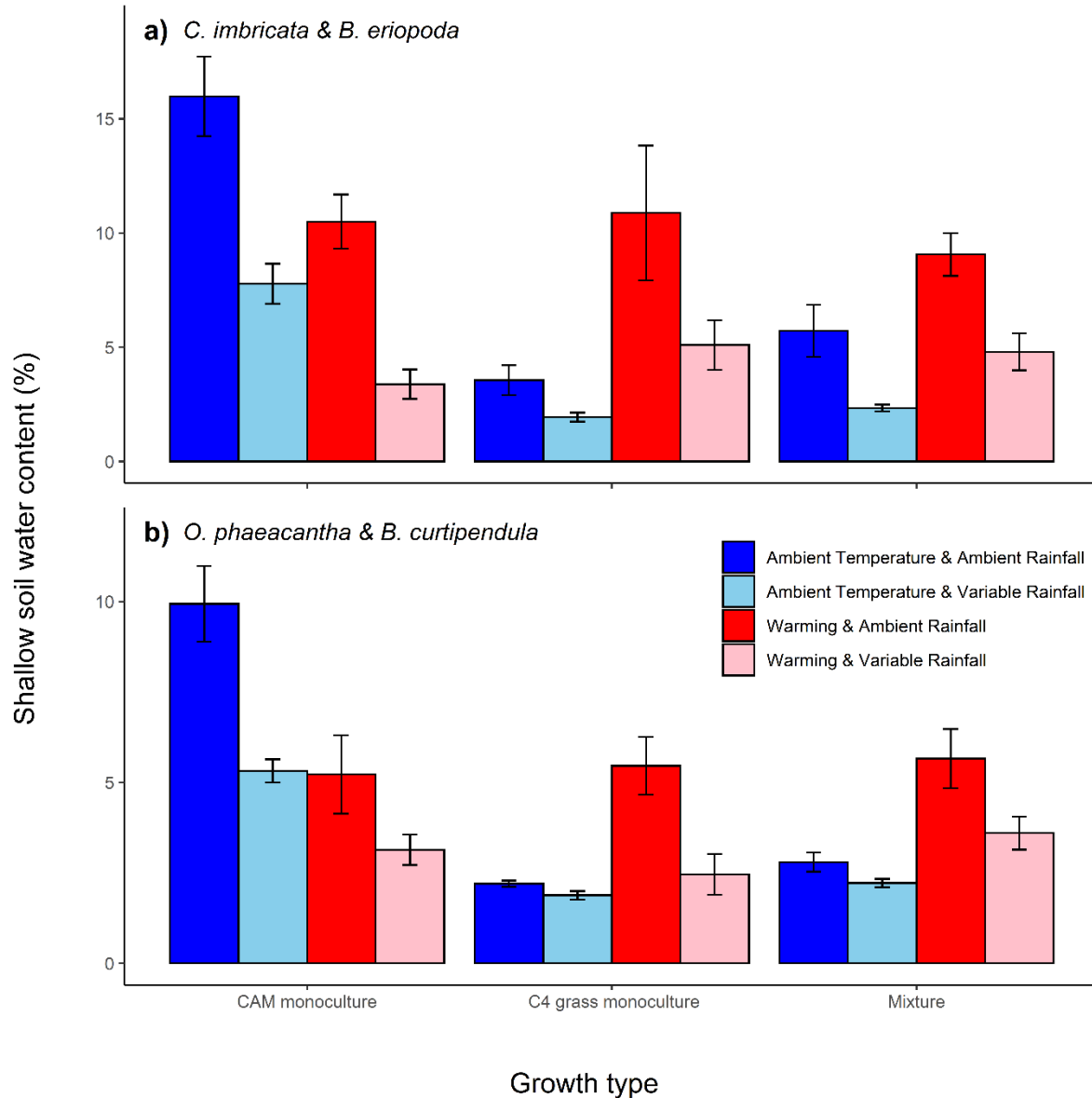
Figure 3. Shallow soil water content (% , mean 95% confidence internals) in monoculture and mixture pots in each combination of temperature and rainfall treatments for both pairs of species.

2.4.4 Responses of stem V:S ratio of C. imbricata

The stem *V:S* ratio of *C. imbricata* was significantly higher in mixture (2.59 and 2.41) than in monoculture (2.30 and 2.12) under ambient temperature conditions in both rainfall treatments (both *P* < 0.0014, Figure 4), respectively. However, the stem *V:S* ratios in monoculture and mixture were not significantly different under asymmetric warming in either rainfall treatment (both *P* > 0.1625). In addition, asymmetric warming caused a significant decline in stem *V:S* ratio of *C. imbricata* in both monoculture and mixture, regardless of rainfall treatment (all *P* < 0.0001). The stem *V:S* ratio of *C. imbricata* in both monoculture and mixture decreased under increased rainfall variability regardless of temperature treatment (all *P* < 0.0163), except for the

case of *C. imbricata* in mixture under asymmetric warming, which did not show a significant difference in *V:S* ratio ($P = 0.1818$).
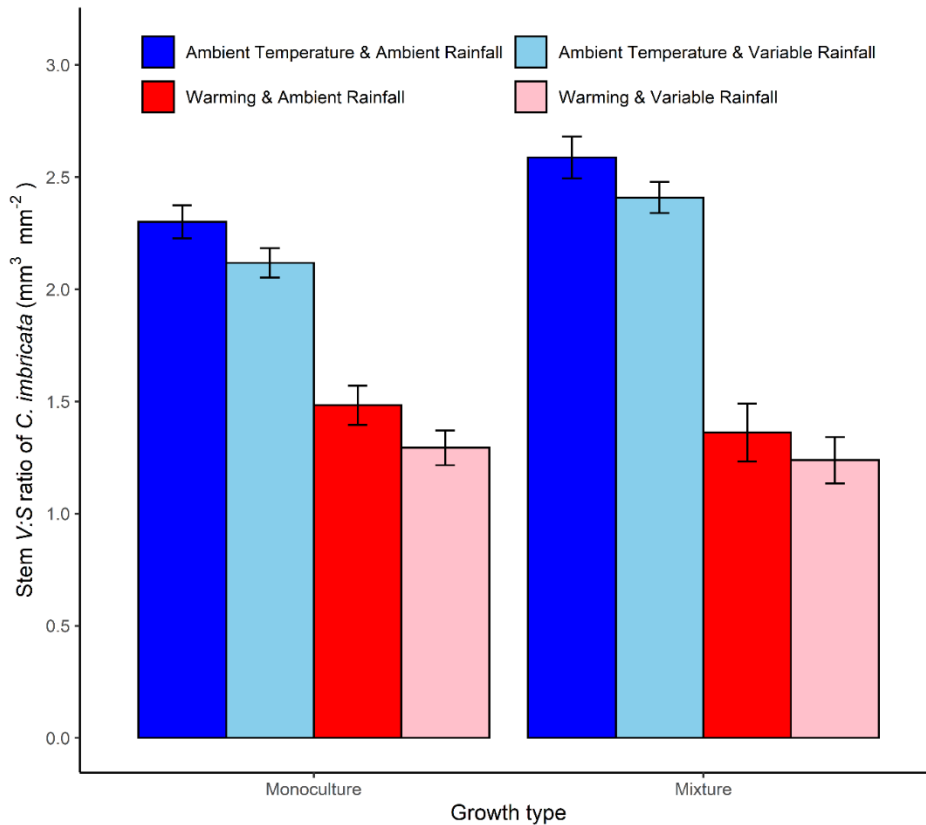
Figure 4. Stem volume-to-surface area (*V:S*) ratio (mm^3 mm^{-2}, mean 95% confidence internals) of CAM species *C. imbricata* in monoculture and mixture in each combination of temperature and rainfall treatments.

2.5 Discussion

This study shows a similar pattern in responses of two CAM-grass communities to asymmetrical warming and increasing intra-annual rainfall variability. The MANOVA results show that temperature, rainfall treatments, and growth type have significant effects on plant biomass, *R:S* ratio, and soil moisture for both pairs of species (all *Pillai* > 0.66, all $P < 0.0001$). Specifically, the combined effects of these two treatments favor CAM plant expansion indirectly through intensified drought stress that suppressed grass growth or led to grass mortality. Under ambient temperature conditions, the biomass of both CAM species *C. imbricata* and *O. phaeacantha* was 2-54% lower in mixture with grasses than in monoculture regardless of rainfall treatment, while the biomass of both grass species increased by 30-82% in mixture with respect to the cases in which they were grown alone (Figure 1). However, both grass species died under asymmetric warming in both rainfall treatments, suggesting that grasses are less drought tolerant than CAM species, likely because of their lower (negligible) water storage capacity; therefore, the competitive advantage is likely to shift from grasses to CAM plants with increasing drought stress. Nighttime warming can accelerate carbohydrate consumption and respiration in grasses, while the limited water availability may cause stomatal closure in grasses during the following

day to avoid drought induced damage therefore constraining their ability to compensate for the nocturnal carbon loss through photosynthetic assimilation (McDowell et al., 2008). This study also indicates that asymmetric warming may decrease CAM plant growth probably due to the negative effects of the greater increase in nighttime temperatures. Few experimental studies have examined the effect of asymmetric daytime and nighttime warming on CAM growth, while some authors have found that a daily temperature regime with lower nighttime and higher daytime temperatures will favor CAM plant growth (Osmond, 1978; Yamori et al., 2014). For instance, nighttime temperatures below 20°C are optimal for acid production and carbon fixation in CAM species (Lüttge, 2004). Increasing daytime temperatures may promote malic acid consumption and thus carbon assimilation, but higher nighttime temperatures can possibly cause a significant increase in dark respiration and induce stomatal closure thereby inhibiting carbon assimilation (Osmond, 1978).

Ecological theory predicts that coexisting species in stable communities should experience weaker interspecific competition compared to intraspecific competition due to niche differentiation, which has been confirmed by numerous empirical studies (Chesson, 2000; Chu et al., 2008; Adler et al., 2018). Our study found a unique pattern in CAM-grass communities that both grass species significantly improved their biomass production when coexisting with CAM species with respect to monoculture conditions likely because of the high WUE of CAM plants (Cushaman & Borland, 2002; Borland et al., 2009), while interspecific competition generally resulted in the decreased growth of both CAM species under ambient temperature conditions. It has been well recognized that under high environmental stress plant species may promote their own survival and growth through less competitive and more facilitative interactions with other species in the same community (Callaway et al., 2002; He et al., 2013). For example, the plant-plant interaction in a Mediterranean mountain shifted from intraspecific competition to interspecific facilitation when environmental conditions became harsher (García-Cervigón et al., 2013). Our results suggest that the interspecific interaction between CAM plants and grasses is weaker than intraspecific competition within grasses, which allows grasses in mixture to have greater access to soil water. However, the strength of CAM-grass interactions dramatically shifted in response to asymmetric climate warming; in fact, both grass species experienced mortality in both monoculture and mixture, and CAM plant growth was not affected by interaction with grasses after grass death (Figure 1). We also found the opposite effect of increasing rainfall variability on the biomass of *B. eriopoda* under ambient temperature and warming conditions, suggesting strong interactions between the effects of warming and increased rainfall variability.

Soil moisture distribution plays a crucial role in driving CAM-plant interactions. Due to the high WUE of CAM plants, shallow soil moisture in CAM monoculture pots was significantly higher compared with other pots under ambient temperature conditions (Figure 3). However, soil moisture did not substantially change with the rainfall treatments under asymmetric warming, which can be ascribed to grass mortality, which ended the interspecific competition for soil water. This is consistent with our finding that the *R:S* ratio of both CAM species was significantly higher in mixture than in monoculture under ambient temperature conditions while no significant difference was detected in warming treatment (Figure 2), which further confirms that CAM plants encountered stronger interspecific competition than intraspecific competition under ambient temperature conditions. However, the occurrence of grass mortality in the

warming treatment released CAM plants from competition for water with grasses. The increase in rainfall variability caused deeper infiltration and reduced shallow soil water availability in all pots regardless of species and temperature treatment. Previous studies suggest that increasing rainfall variability favors the growth of deep-rooted plants through better access to deep soil water and thus suppresses plants with shallow root systems especially in water limited environments (Kulmatiski & Beard, 2013; Munson et al., 2013; Huang et al., 2019). Our results indicate that grasses are more sensitive to changes in soil moisture distribution than CAM plants, but drought stress aggravated by asymmetric warming severely limits the ability of grasses to take advantage of deep soil water under increasing rainfall variability and maintain their survival and growth. Therefore, climate warming also influences CAM-grass interactions and may counteract the positive impacts of more extreme rainfall inputs on deep-rooted grasses.

Our study shows that *C. imbricata* had a significantly higher *V:S* ratio in mixture with *B. eriopoda* than in monoculture under ambient temperature irrespective of rainfall treatments (Figure 4), suggesting that *C. imbricata* experienced much stronger inter- than intraspecific competition primarily for soil water and thus CAM species tend to increase the stem *V:S* ratio when coexisting with C4 grasses to minimize transpirational water loss. However, stem *V:S* ratios of *C. imbricata* in monoculture and mixture were not statistically different in both rainfall treatments under asymmetric warming, which may result from the dramatic decline in interspecific competition due to drought-induced grass mortality. These findings suggest that asymmetric warming and the associated changes in CAM-grass competition dominated the morphological changes in CAM stems and the effect of increasing rainfall variability on stem *V:S* ratio was relatively weak.

These findings suggest that climate change can significantly alter the magnitude and even direction of plant interactions and thus their relative competitive advantages which may lead to rapid shifts in species composition and ecosystem structure in arid ecosystems. Such a transition can also be influenced by other climate factors such as increasing atmospheric CO_2 concentrations which has also been shown to contribute to the rapid expansion of CAM species in drylands (Yu et al., 2019), and the capacity of plant species to survive drought during resource (e.g., rainfall) interpulse outside the growing season (Goldberg & Novoplansky, 1997). Previous studies also found that soil biota such as microbes could also play an important role in driving species interactions in Chihuahuan desert grasslands through plant-soil feedbacks (Chung & Rudgers, 2016; Chung et al., 2019). Future work involving the role of soil microbes and measurements of physiological traits of CAM plants and coexisting grasses such as respiration and photosynthetic rates is needed to provide more direct evidence of the mechanisms underlying how altered global environmental change affects CAM-grass growth and interaction. In addition, given that the environmental conditions in greenhouse or growth chambers often strengthen the plant water stress with shallow pots, we should also note that long-term field manipulative experiments are needed to better understand and predict how CAM-grass communities in drylands respond to the ongoing global changes.

2.6 Conclusion
Our study provides novel experimental evidence that asymmetric warming along with changes in rainfall regimes can strongly affect CAM-grass interactions. Grasses may outcompete CAM plants with increasing rainfall variability under current temperatures due to the deeper drainage

and increased deep (i.e., grass-accessible) soil moisture. However asymmetric warming lead to grass mortality thereby indirectly favoring CAM growth. This pattern was observed in both pairs of CAM and grass species examined in this study, which indicates that these impacts of asymmetric warming on grasses may be general and occur in other dryland CAM-grass communities. Therefore, we expect that the ongoing asymmetric climate warming and changes in precipitation variability would cause dramatic shifts in species interactions, community composition and ecosystem resilience in drylands, potentially leading to the replacement of desert grasslands by "camland" landscapes. Recent work has also shown that nighttime warming may accelerate egg development in grasshoppers (Wu et al., 2012), promote woody plant encroachment in woodland-grassland ecotones (Huang et al., 2018), and have cascading effects on plant diversity by altering predator-prey interactions (Barton & Schmitz, 2018), suggesting the complex impacts of asymmetric warming on ecosystem structure and dynamics. Our study highlights the need of incorporating the effects of asymmetric diurnal warming and changes in rainfall regimes into ecological studies to accurately predict the responses of plant communities to climate change in dryland ecosystems.

2.7 References

Adler PB, Smull D, Beard KH, Choi RT, Furniss T, Kulmatiski A, Meiners JM, Tredennick AT, Veblen KE (2018) Competition and coexistence in plant communities: intraspecific competition is stronger than interspecific competition. Ecol Lett 21:1319–1329. https://doi.org/10.1111/ele.13098

Alexander LV, Zhang X, Peterson TC, Caesar J, Gleason B, Klein Tank AMG, Haylock M, Collins D, Trewin B, Rahimzadeh F, Tagipour A, Kumar RK, Ravedekar J, Griffiths G, Vincent L, Stephenson DB, Burn J, Aguilar E, Brunet M, Taylor M, New M, Zhai P, Rusticucci M, Vazquez-Aguirre JL (2006) Global observed changes in daily climate extremes of temperature and precipitation. J Geophys Res Atmos 111:D05109. https://doi.org/10.1029/2005JD006290

Barton BT, Schmitz OJ (2018) Opposite effects of daytime and nighttime warming on top-down control of plant diversity. Ecology 99:13–20. https://doi.org/10.1002/ecy.2062

Bates D, Maechler M, Bolker B, Walker S (2015) Fitting linear mixed-effects models using lme4. J Stat Softw 67:1–48. https://doi.org/10.18637/jss.v067.i01

Benson L, Walkington DL (1965) The southern Californian prickly pears–invasion, adulteration, and trial-by-fire. Ann Mo Bot Gard 52:262–273. https://doi.org/10.2307/2394792

Borland AM, Griffiths H, Hartwell J, Smith JAC (2009) Exploiting the potential of plants with crassulacean acid metabolism for bioenergy production on marginal lands. J Exp Bot 60:2879–2896. https://doi.org/10.1093/jxb/erp118

Brown JH, Gillooly JE, Allen AP, Savage VM, West GB (2004) Toward a metabolic theory of ecology. Ecology 85:1771–1789. https://doi.org/10.1890/03-9000

Callaway RM, Brooker RW, Choler P, Kikvidze Z, Lortie CJ, Michalet R, Paolini L, Pugnaire FL, Newingham B, Aschehoug ET, Armas C, Kikodze D, Cook BJ (2002) Positive interactions among alpine plants increase with stress. Nature 417:844–848. https://doi.org/10.1038/nature00812

Chesson P (2000) Mechanisms of maintenance of species diversity. Annu Rev Ecol Evol Syst 31:343–366. https://doi.org/10.1146/annurev.ecolsys.31.1.343

Chu CJ, Maestre FT, Xiao S, Weiner J, Wang Y, Duan X, Wang G (2008) Balance between

facilitation and resource competition determines biomass-density relationship in plant populations. Ecol Lett 11:1189–1197. https://doi.org/10.1111/j.1461-0248.2008.01228.x

Chung YA, Rudgers JA (2016) Plant–soil feedbacks promote negative frequency dependence in the coexistence of two aridland grasses. Proc R Soc B 283:20160608. https://doi.org/10.1098/rspb.2016.0608

Chung YA, Collins SL, Rudgers JA (2019) Connecting plant–soil feedbacks to long-term stability in a desert grassland. Ecology 100:e02756. https://doi.org/10.1002/ecy.2756

Collins SL, Ladwig LM, Petrie MD, Jones SK, Mulhouse JM, Thibault JR, Pockman WT (2017) Press-pulse interactions: effects of warming, N deposition, altered winter precipitation, and fire on desert grassland community structure and dynamics. Glob Change Biol 23: 1095–1108. https://doi.org/10.1111/gcb.13493

Cushaman JC, Borland AM (2002) Induction of crassulacean acid metabolism by water limitation. Plant Cell Environ 25:295–310. https://doi.org/10.1046/j.0016-8025.2001.00760.x

Davis S, LeBauer D, Long S (2014) Light to liquid fuel: theoretical and realized energy conversion efficiency of plants using Crassulacean Acid Metabolism (CAM) in arid conditions. J Exp Bot 65:3471–3478. https://doi.org/10.1093/jxb/eru163

Davy R, Esau I, Chernokulsky A, Outten S, Zilitinkevich S (2016) Diurnal asymmetry to the observed global warming. Int J Climatol 37:79–93. https://doi.org/10.1002/joc.4688

Durack PJ, Wijffels SE, Matear RJ (2012) Ocean salinities reveal strong global water cycle intensification during 1950 to 2000. Science 336:455–458. https://doi.org/10.1126/science.1212222

D'Odorico P, Bhattachan A (2012) Hydrologic variability in dryland regions: impacts on ecosystem dynamics and food security. Phyl Trans R Soc B 367:3145–3157. https://doi.org/10.1098/rstb.2012.0016

Fan Y, Li XY, Huang H, Wu XC, Yu KL, Wei JQ, Zhang CC, Wang P, Hu X, D'Odorico P (2019) Does phenology play a role in the feedbacks underlying shrub encroachment? Sci Total Environ 657:1064–1073. https://doi.org/10.1016/j.scitotenv.2018.12.125

Fay PA, Carlisle JD, Knapp AK, Blair JM, Collins SL (2000) Altering rainfall timing and quantity in a mesic grassland ecosystem: design and performance of rainfall manipulations shelters. Ecosystems 3:308–319. https://doi.org/10.1007/s100210000028

Fu CB, Ma ZG (2008) Global change and regional aridification. Chin J Atmos Sci 32:752–760

García-Cervigón AI, Gazol A, Sanz V, Camarero JJ, Olano JM (2013) Intraspecific competition replaces interspecific facilitation as abiotic stress decreases: the shifting nature of plant-plant interactions. Perspect Plant Ecol Evol Syst 15:226–236. https://doi.org/10.1016/j.ppees.2013.04.001

Gherardi LA, Sala OE (2015) Enhanced precipitation variability decreases grass- and increases shrub- productivity. Proc Natl Acad Sci USA 112:12735–12740. https://doi.org/10.1073/pnas.1506433112

Goldberg D, Novoplansky A (1997) On the relative importance of competition in unproductive environments. J Ecol 85:409–418. https://doi.org/10.2307/2960565

Griffin KL, Turnbull M, Murthy R, Lin GH, Adams J, Farnsworth B, Mahato T, Bazin G, Potasnak M and Berry JA (2002) Leaf respiration is differentially affected by leaf vs. stand-level night time warming. Glob Chang Biol 8:479–485. https://doi.org/10.1046/j.1365-2486.2002.00487.x

He Q, Bertness MD, Altieri AH, Vila M (2013) Global shifts towards positive species

interactions with increasing environmental stress. Ecol Lett 16:695–706. https://doi.org/10.1111/ele.12080

Heisler-White J, Knapp A, Kelly E (2008) Increasing precipitation event size increases aboveground net primary productivity in a semi-arid grassland. Oecologia 158:129–140. https://doi.org/10.1007/s00442-008-1116-9

Hillel D, Rosenzweig C (2002) Desertification in relation to climate variability and change. Adv Agron 77:1–38. https://doi.org/10.1016/S0065-2113(02)77012-0

Hoekman D (2010) Turning up the heat: Temperature influences the relative importance of top-down and bottom-up effects. Ecology 91:2819–2825. https://doi.org/10.1890/10-0260.1

Huang H, Zinnert JC, Wood LK, Young DR, D'Odorico P (2018) Non-linear shift from grassland to shrubland in temperate barrier islands. Ecology 99:1671–1681. https://doi.org/10.1002/ecy.2383

Huang H, Yu KL, Fan Y, D'Odorico P (2019) The competitive advantage of C4 grasses over CAM plants under increased rainfall variability. Plant Soil 442:483–495. https://doi.org/10.1007/s11104-019-04216-5

Huang J, Yu H, Guan X, Wang G, Guo R (2016) Accelerated dryland expansion under climate change. Nat Clim Chang 6:166–171. https://doi.org/10.1038/nclimate2837

Hultine KR, Williams DG, Dettman DL, Butterfield BJ, Puente-Martinez R (2016) Stable isotope physiology of stem succulents across a broad range of volume to surface area ratio. Oecologia 182:679–690. https://doi.org/10.1007/s00442-016-3690-6

Huntington TG (2006) Evidence for intensification of the global water cycle: review and synthesis. J Hydrol 319:83–95. https://doi.org/10.1016/j.jhydrol.2005.07.003

IPCC (2013) Summary for policymakers. In: Stocker TF, Qin D, Plattner G-K, Tignor M, Allen SK, Boschung J, Nauels A, Xia Y, Bex V, Midgley PM (eds) Climate Change 2013: The Physical Science Basis. Contribution of Working Group I to the Fifth Assessment Report of the Intergovernmental Panel on Climate Change. Cambridge University Press, Cambridge, UK and New York, NY, pp 3–29

Karl TR, Jones PD, Knight RW, Kukla G, Plummer N, Razuvayev V, Gallo KP, Lindseay J, Charlson RJ, Peterson TC (1993) A new perspective on recent global warming: asymmetric trends of daily maximum and minimum temperature. Bull Am Meteor Soc 74:1007–1023. https://doi.org/10.1175/1520-0477(1993)074<1007:ANPORG>2.0.CO;2

Knapp AK, Fay PA, Blair JM, Collins SL, Smith MD, Carlisle JD, Harper CS, Danner BT, Lett MS, McCarron JK (2002) Rainfall variability, carbon cycling, and plant species diversity in a mesic grassland. Science 298:2202–2205. https://doi.org/10.1126/science.1076347

Knapp AK, Beier C, Briske DD, Classen AT, Luo Y, Reichstein M, Smith MD, Smith SD, Bell JE, Fay PA, Heisler JL, Leavitt SW, Sherry R, Smith B, Weng E (2008) Consequences of more extreme precipitation regimes for terrestrial ecosystems. Bioscience 58:811–821. https://doi.org/10.1641/B580908

Kulmatiski A, Beard K (2013) Woody plant encroachment facilitated by increased precipitation intensity. Nat Clim Chang 3:833–837. https://doi.org/10.1038/nclimate1904

Luo YQ (2007) Terrestrial carbon-cycle feedback to climate warming. Annu Rev Ecol Evol Syst 38:683–712. https://doi.org/10.1146/annurev.ecolsys.38.091206.095808

Lüttge U (2004) Ecophysiology of crassulacean acid metabolism (CAM). Ann Bot 93:629–652. https://doi.org/10.1093/aob/mch087

Maestre FT, Salguero-Gomez R, Quero JL (2012) It's getting hotter in here: determining and projecting the impacts of global change on drylands. Phyl Trans R Soc B 367:3062–3075. https://doi.org/10.1098/rstb.2011.0323

Mauseth JD (2000) Theoretical aspects of surface-to-volume ratios and water-storage capacities of succulent shoots. Am J Bot 87:1107–1115. https://doi.org/10.2307/2656647

McCormick AJ, Cramer MD, Watt DA. (2006) Sink strength regulates photosynthesis in sugarcane. New Phytol 171:759–770. https://doi.org/10.1111/j.1469-8137.2006.01785.x

McDowell N, Pockman WT, Allen CD, Breshears DD, Cobb N, Kolb T, Plaut J, Sperry J, West A, Williams DG, Yepez EA (2008) Mechanisms of plant survival and mortality during drought: why do some plants survive while others succumb to drought? New Phytol 178:719–739. https://doi.org/10.1111/j.1469-8137.2008.02436.x

Miller TEX, Louda SM, Rose KA, Eckberg JO (2009) Impacts of insect herbivory on cactus population dynamics: experimental demography across an environmental gradient. Ecol Monogr 79:155–172. https://doi.org/10.1890/07-1550.1

Munson SM, Muldavin EH, Belnap J, Peters DPC, Anderson JP, Reiser MH, Melgoza-Castillo A, Herrick JE, Christiansen TA (2013) Regional signatures of plant response to drought and elevated temperature across a desert ecosystem. Ecology 94: 2030–2041. https://doi.org/10.1890/12-1586.1

Nobel PS (1996) Responses of some North American CAM plants to freezing temperatures and doubled CO_2 concentrations: implications of global climate change for extending cultivation. J Arid Environ 34:187–196. https://doi.org/10.1006/jare.1996.0100

Osmond CB (1978) Crassulacean acid metabolism: a curiosity in context. Annu Rev Ecol Evol Syst 29:379–414. https://doi.org/10.1146/annurev.pp.29.060178.002115

Parmesan C, Yohe G (2003) A globally coherent fingerprint of climate change impacts across natural systems. Nature 421:37–42. https://doi.org/10.1038/nature01286

Paul MJ, Pellny TK, Goddijn O (2001) Enhancing photosynthesis with sugar signals. Trends Plant Sci 6:197–200. https://doi.org/10.1016/S1360-1385(01)01920-3

Peng S, Piao S, Ciais P, Myneni RB, Chen A, Chevallier F, Vicca S (2013) Asymmetric effects of daytime and night-time warming on Northern Hemisphere vegetation. Nature 501:88–92. https://doi.org/10.1038/nature12434

Petrie MD, Collins SL, Gutzler DS, Moore DM (2014) Regional trends and local variability in monsoon precipitation in the northern Chihuahuan Desert, USA. J Arid Environ 103:63–70. https://doi.org/10.1016/j.jaridenv.2014.01.005

R Development Core Team (2017) R: A language and environment for statistical computing. R Foundation for Statistical Computing, Vienna, Austria. URL https://www.R-project.org/

Ravi S, D'Odorico P, Wang L, White C, Okin GS, Collins SL (2009) Post-fire resource redistribution in desert grasslands: A possible negative feedback on land degradation. Ecosystems 12:434–444. https://doi.org/10.1007/s10021-009-9233-9

Reyes-García C, Andrade JL (2009) Crassulacean acid metabolism under global climate change. New Phytol 181:754–757. https://doi.org/10.1111/j.1469-8137.2009.02762.x

Reynolds JF, Stafford Smith DM, Lambin EF, Turner BL, Mortimore M, Batterbury SPJ et al. (2007). Global desertification: building a science for dryland development. Science 316:847–851. https://doi.org/10.1126/science.1131634

Rudgers JA, Chung AY, Maurer GE, Moore DI, Muldavin EH, Litvak ME, Collins SL (2018) Climate sensitivity functions and net primary production: A framework for incorporating

climate mean and variability. Ecology 99:576–582. https://doi.org/10.1002/ecy.2136

Ryan MG (1991) Effects of climate change on plant respiration. Ecol Appl 1:157–167. https://doi.org/10.2307/1941808

Sala OE, Parton WJ, Joyce LA, Lauenroth WK (1988) Primary production of the central grassland region of the United States. Ecology 69:40–45. https://doi.org/10.2307/1943158

Thornton PK, Ericksen PJ, Herrero M, Challinor AJ (2014) Climate variability and vulnerability to climate change: a review. Glob Chang Biol 20:3313–3328. https://doi.org/10.1111/gcb.12581

Vose RS, Easterling DR, Gleason B (2005) Maximum and minimum temperature trends for the globe: an update through 2004. Geophys Res Lett 32:L23822. https://doi.org/10.1029/2005GL024379

Wan S, Xia J, Liu W, Niu S (2009) Photosynthetic overcompensation under nocturnal warming enhances grassland carbon sequestration. Ecology 90:2700–2710. https://doi.org/10.1890/08-2026.1

Wang Z, Ji M, Deng J, Milne RI, Ran J, Zhang Q, Fan Z, Zhang X, Li J, Huang H, Cheng D, Niklas KJ (2015) A theoretical framework for whole-plant carbon assimilation efficiency based on metabolic scaling theory: a test case using *Picea* seedlings. Tree Physiol 35:599–607. https://doi.org/10.1093/treephys/tpv030

Williams DG, Hultine KR, Dettman DL (2014) Functional trade-offs in succulent stems predict responses to climate change in columnar cacti. J Exp Bot 65:3405–3413. https://doi.org/10.1093/jxb/eru174

Wu T, Hao S, Sun OJ, Kang L (2012) Specificity responses of grasshoppers in temperate grasslands to diel asymmetric warming. PLoS One 7:e41764. https://doi.org/10.1371/journal.pone.0041764

Xia JY, Chen, JQ, Piao SL, Ciais P, Luo YQ, Wan SQ (2014) Terrestrial carbon cycle affected by non-uniform climate warming. Nat Geosci 7:173–180. https://doi.org/10.1038/ngeo2093

Yamori W, Hikosaka K, Way DA (2014) Temperature response of photosynthesis in C3, C4, and CAM plants: temperature acclimation and temperature adaptation. Photosynth Res 119:101–117. https://doi.org/10.1007/s11120-013-9874-6

Yu KL, D'Odorico P, Carr DE, Personius A, Collins SL (2017a) The effect of nitrogen availability and water conditions on competition between a facultative CAM plant and an invasive grass. Ecol Evol 7:7739–7749. https://doi.org/10.1002/ece3.3296

Yu KL, D'Odorico P, Li W, He YL (2017b) Effects of competition on induction of crassulacean acid metabolism in a facultative CAM plant. Oecologia 184:351–361. https://doi.org/10.1007/s00442-017-3868-6

Yu KL, Carr D, Anderegg W, Tully K, D'Odorico P (2018) Response of a facultative CAM plant and its competitive relationship with a grass to changes in rainfall regime. Plant Soil 427:321–333. https://doi.org/10.1007/s11104-018-3657-y

Yu KL, D'Odorico P, Collins SL, Carr D, Porporato A, Anderegg WRL, Gilhooly III WP, Wang L, Bhattachan A, Bartlett M, Hartzell S, Yin J, He Y, Li W, Tatlhego M, Fuentes JD (2019) The competitive advantage of a constitutive CAM species over a C4 grass species under drought and CO_2 enrichment. Ecosphere 10:e02721. https://doi.org/10.1002/ecs2.2721

2.8 Supplemental information

Table S1. Results of the linear mixed-effects model evaluating the effects of species, temperature, rainfall variability and competition as well as their interactions on *R:S* ratio of *C. imbricata* and *B. eriopoda*. Block was treated as a random factor. Block was treated as a random factor. *P* value was calculated by Wald chi-squared test.

Source	χ^2	df	P value
Species	10.111	1	0.001
Temperature	76.172	1	< 0.001
Rainfall	0.036	1	0.849
Competition	8.288	1	0.004
Species: temperature	4.837	1	0.028
Species: rainfall	23.136	1	< 0.001
Species: competition	23.751	1	< 0.001
Temperature: rainfall	43.986	1	< 0.001
Temperature: competition	0.003	1	0.956
Rainfall: competition	7.296	1	0.007
Species: temperature: rainfall	21.927	1	< 0.001
Species: temperature: competition	46.661	1	< 0.001
Species: rainfall: competition	18.092	1	< 0.001
Temperature: rainfall: competition	4.918	1	0.027
Species: temperature: rainfall: competition	1.107	1	0.293

Table S2. Results of the linear mixed-effects model evaluating the effects of species, temperature, rainfall variability and competition as well as their interactions on *R:S* ratio of *O. phaeacantha* and *B. curtipendula*. Block was treated as a random factor. Block was treated as a random factor. *P* value was calculated by Wald chi-squared test.

Source	χ^2	*df*	*P* value
Species	514.387	1	< 0.001
Temperature	86.650	1	< 0.001
Rainfall	14.130	1	< 0.001
Competition	2.319	1	0.128
Species: temperature	153.828	1	< 0.001
Species: rainfall	3.824	1	0.051
Species: competition	33.636	1	< 0.001
Temperature: rainfall	69.640	1	< 0.001
Temperature: competition	2.512	1	0.113
Rainfall: competition	1.064	1	0.302
Species: temperature: rainfall	31.910	1	< 0.001
Species: temperature: competition	28.441	1	< 0.001
Species: rainfall: competition	7.309	1	0.007
Temperature: rainfall: competition	11.718	1	< 0.001
Species: temperature: rainfall: competition	11.620	1	< 0.001

CHAPTER 3

Non-linear shift from grassland to shrubland in temperate barrier islands

Reference: Huang, H., Zinnert, J. C., Wood, L. K., Young, D. R., D'Odorico, P. 2018. Non-linear shift from grassland to shrubland in temperate barrier islands. Ecology. 99:1671–1681.

3.1 Abstract

Woody plant encroachment into grasslands is a major land cover change taking place in many regions of the world, including arctic, alpine and desert ecosystems. This change in plant dominance is also affecting coastal ecosystems, including barrier islands, which are known for being vulnerable to the effects of climate change. In the last century, the woody plant species *Morella cerifera* L. (Myricaceae), has encroached into grass covered swales in many of the barrier islands of Virginia along the Atlantic seaboard. The abrupt shift to shrub cover in these islands could result from positive feedbacks with the physical environment, though the underlying mechanisms remain poorly understood. We use a combination of experimental and modelling approaches to investigate the role of climate warming and the ability of *M. cerifera* to mitigate its microclimate thereby leading to the emergence of alternative stable states in barrier island vegetation. Nighttime air temperatures were significantly higher in myrtle shrublands than grasslands, particularly in the winter season. The difference in the mean of the 5% and 10% lowest minimum temperatures between shrubland and grassland calculated from two independent datasets ranged from 1.3 to 2.4°C. The model results clearly show that a small increase in near-surface temperature can induce a non-linear shift in ecosystem state from a stable state with no shrubs to an alternative stable state dominated by *M. cerifera*. This modeling framework improves our understanding and prediction of barrier island vegetation stability and resilience under climate change, and highlights the existence of important nonlinearities and hystereses that limit the reversibility of this ongoing shift in vegetation dominance.

3.2 Introduction

Vegetation cover has important influences on the near-surface atmospheric conditions, including temperature, humidity, boundary layer stability, and rainfall formation (Geiger 1965, Pielke et al. 1998, Bonan 2008, Li et al. 2016). For example, deforestation and land use change disrupt the surface energy balance thereby altering the microclimate (Avissar et al. 2002, Bonan 2008, Lawrence and Vendekar 2014, Li et al. 2015, Runyan and D'Odorico 2016). A major change in land cover taking place in many regions of the world is associated with the encroachment of woody plants into grasslands, a phenomenon that has been observed in arctic, alpine, desert, and coastal ecosystems (Archer et al. 1995, Chapin et al. 2000, Maher et al. 2005, Bader et al. 2007, Knapp et al. 2008, McKee and Rooth 2008, Ravi et al. 2009). This abrupt replacement of grasses with woody plants has significant impacts on ecosystem structure, functioning, and the provision of ecosystem services such as livestock grazing, surface soil sheltering and carbon sequestration, and therefore has been viewed as an indicator of land degradation and desertification in dryland regions (Van Auken 2000).

Shrub encroachment has been ascribed to a variety of mechanisms including overgrazing, fire suppression, atmospheric CO_2 rise, and climate change, depending on the specific ecosystem considered (D'Odorico et al. 2012). Especially in cold regions where low temperature events

limit the growth of cold-sensitive woody plants, the ongoing climate warming provides opportunities for woody plants to be released from cold-induced damage, contributing to their expansion (Tape et al. 2006). Besides the gradual impact of regional climate warming, the vegetation-microclimate feedbacks may play a role in facilitating shrub encroachment in the shorter term by improving the environmental conditions for shrub species (D'Odorico et al. 2010, 2013). The increase in woody plant cover has been found to affect the microclimate by altering surface energy fluxes (Geiger 1965, Langvall and Örlander 2001, Beltrán-Przekurat et al. 2008, D'Odorico et al. 2010). Specifically, the nocturnal long-wave radiation emitted by the ground can be absorbed by the vegetation canopy and partially reflected and re-radiated back to the ground surface, consequently reducing the radiation loss to the atmosphere and creating warmer microclimate conditions in the shrubland (He et al. 2010, 2014). Because many of the encroaching woody plants are cold intolerant (Pockman and Sperry 1997, Körner 1998, Krauss et al. 2008), this local warming effect interacting with regional climate warming can in turn promote the survival and growth of cold-sensitive woody plants by reducing the exposure to extreme low temperature events. Thus, a positive feedback between vegetation and microclimate may exist in grassland-woodland ecotones (D'Odorico et al. 2013). In many cases woody plant encroachment has led to a relatively abrupt and potentially irreversible land cover change (Van Auken 2000, D'Odorico et al. 2012), suggesting the possible occurrence of a critical transition in a bistable system with alternative stable states of grassland and shrubland. Bistable ecosystem dynamics are often induced by the positive feedbacks between vegetation and the physical environment; thus, microclimate feedbacks and climate warming likely play a crucial role in the transition to shrub dominance in many landscapes worldwide (D'Odorico et al. 2013).

Freeze-induced damage limits the latitudinal distribution of many woody plants across the globe including mangroves in coastal ecosystems (Stuart et al. 2006), *Betula nana* (dwarf birch) and other shrub species in arctic regions (Wookey et al. 2009). The cold sensitivity of woody plants compared with grasses has been ascribed to many different physiological mechanisms, including cold-induced decrease in photosynthetic rates and primary productivity, reduced growth, limited regeneration capacity, and plant frost damage (Tranquillini 1979, Grace et al. 1989, Körner 1998). In cold environments, low temperatures and short growing seasons prevent plants from maintaining a balanced or positive carbon budget as a result of limited carbon assimilation. In addition, extreme temperature events can also cause freezing-induced xylem embolisms and a loss of hydraulic conductivity (Medeiros and Pockman 2011, Buchner and Neuner 2011). Furthermore, cold stress weakens the competitiveness of woody plants with respect to grasses by inhibiting seed production and germination and therefore the reproduction capacity (Körner 1998). The cold intolerance of woody plants often sets the latitudinal limits to their distribution; however, the decreased frequency of extreme cold events due to climate warming tends to reduce the chances that shrubs experience freezing damage in the cold months, and contributes to their expansion in transition zones (Cavanaugh et al. 2014), therefore highlighting the important role of warming effect in shrub encroachment in shrub-grass ecotones.

In the last century, the woody plant species *Morella cerifera* L. (Myricaceae) has encroached into grass swales composed of both graminoids and forbs in many of the barrier islands along the Virginia segment of the Atlantic seaboard of the USA (Young 1992, Young et al. 1995). *M. cerifera* is a nitrogen fixing shrub with relatively high growth rate and resource use efficiency which largely contributes to its expansion, and plays an important role in successional processes

(Collins and Quinn 1982, Young et al. 1995). Conversion from grassland to shrubs to maritime forest is part of the typical successional pattern in coastal areas, however, recent studies have demonstrated that the majority of shrub expansion has occurred from previously established thickets compared to new colonization from a successional trajectory (Zinnert et al. 2011). Due to high shrub leaf area index, there has been little to no development of new maritime forest at the Virginia Coast Reserve (VCR), indicating a delay in succession (Brantley and Young 2007, Bissett et al. 2016). Patterns of *M. cerifera* expansion vary from island to island, with higher rates on some islands and loss of shrubs due to erosion on others. Even with these dynamics, the overall cover of *M. cerifera* has increased approximately 40% over the last 27 years (Figure 1) despite loss of island area across the VCR. This change in *M. cerifera* cover is associated with important effects on the surrounding environmental conditions such as temperature regime, water table depth, and soil nutrient levels. For example, recent research (Thompson et al. 2017) has documented an increase in soil moisture and nutrients as well as the occurrence of significantly higher winter minimum temperatures inside shrub thickets, suggesting the existence of a warmer microclimate during winter resulting from the encroachment of *M. cerifera*. These islands lie at the northern limit of the latitudinal range of *M. cerifera* (Shao and Halpin 1995) and specifically, *M. cerifera* expansion has not been affected by direct human disturbances since 1930s (Thompson 2016), therefore the ongoing encroachment of *M. cerifera* and the possible warming effect through the surface energy balance may indicate that a positive feedback between vegetation cover and microclimate could exist due to the cold intolerance of *M. cerifera*. Processes related to land use (e.g., grazing and fire suppression) have also been invoked to explain woody plant encroachment in drylands (e.g., van Auken, 2000; D'Odorico et al. 2012; Yu and D'Odorico 2014). These processes do not seem to be relevant to the case of the VCR, where no recent history of grazing or fire management exists. Therefore, the VCR provides an ideal system for investigating how climate warming and microclimate feedback may interact to serve as a mechanism of shrub expansion, without confounding effect from other drivers.

In this study we (i) provide additional experimental evidence of the modified microclimate created by the establishment of *M. cerifera*; (ii) present results from laboratory experiments demonstrating the cold sensitivity of this shrub species; and (iii) develop a process-based modelling framework showing the potential emergence of bi-stable shrub-grass dynamics and a nonlinear shift from grassland to shrubland in Virginia barrier island vegetation as a result of positive feedbacks with microclimate conditions and *M. cerifera*'s cold sensitivity.

3.3 Materials and Methods

3.3.1 Study site
This study focused on Hog Island (37° 40' N, 75° 40' W), a barrier island within the Virginia Coast Reserve Long-Term Ecological Research site (VCR LTER). The VCR includes a chain of barrier islands, and is the longest stretch of undeveloped coastline on the eastern United States. Hog Island is not affected by direct anthropogenic disturbance as it has been free of human occupation since the mid-1930s, though historic anthropogenic disturbances including grazing, lumbering and farming have been reported to occur earlier in the history of these barrier islands (Levy 1990). It is ~12 km in length and ~2 km across at the widest point. Hog Island consists of oceanfront strand and dunes, interior grass/forb dune/swale complexes with expanding shrub thickets, and tidal salt marshes on the lagoon side. The expanding species, *Morella cerfiera*, forms dense monospecific patches of tall (4-7 m) thickets that exclude all other species

(Thompson et al. 2017) (Figure 1). Expansion of *M. cerifera* into grassland dominated by *Spartina patens* (Aiton) Muhl. and *Andropogon virginicus* L. has increased significantly on Hog Island since 1949 (Young et al. 1995, Zinnert et al. 2016) and currently covers more than 45% of the island. Because of its limited exposure to direct anthropogenic disturbances and its position at the northern latitudinal limit of cold sensitive *M. cerifera*, Hog Island is an ideal system for studying the impacts of climate warming and microclimate feedbacks on shrub encroachment.
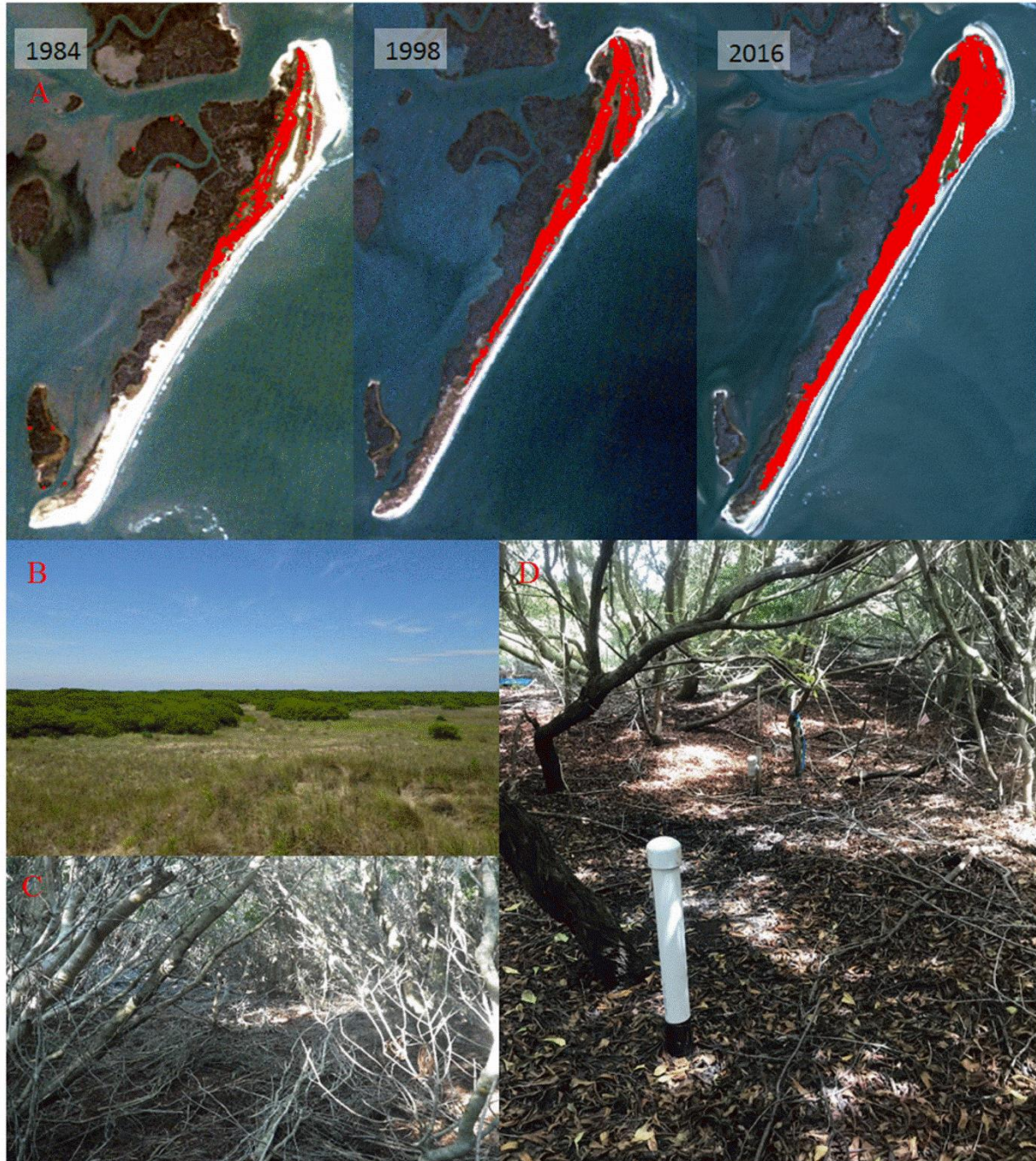

Figure 1. Shrub encroachment on Hog Island, VA. (A) Expansion of *Morella cerifera* (red) on Hog Island, VA from 1984 (74 ha), to 1998 (184 ha) to 2016 (393 ha). (B) Shrubland-grassland ecotones on Hog Island. (C) Image inside a shrub thicket. (D) Temperature measurement inside the shrub thickets. Note the absence of other species.

The mean annual temperature ranges from 11.9°C to 14.7°C, and mean annual precipitation typically varies between 1065 to 1167 mm/year (Brantley and Young 2010). The long-term climate data from a nearby NOAA meteorological station in Painter, Virginia reveal that only 4 low temperature events (< -15°C) have occurred since 1985, while 10 events were documented from the previous 30 years. There is a general warming trend in mean winter temperature from 1955 to 2017, which we argue is contributing to *M. cerifera* expansion (Figure 2).
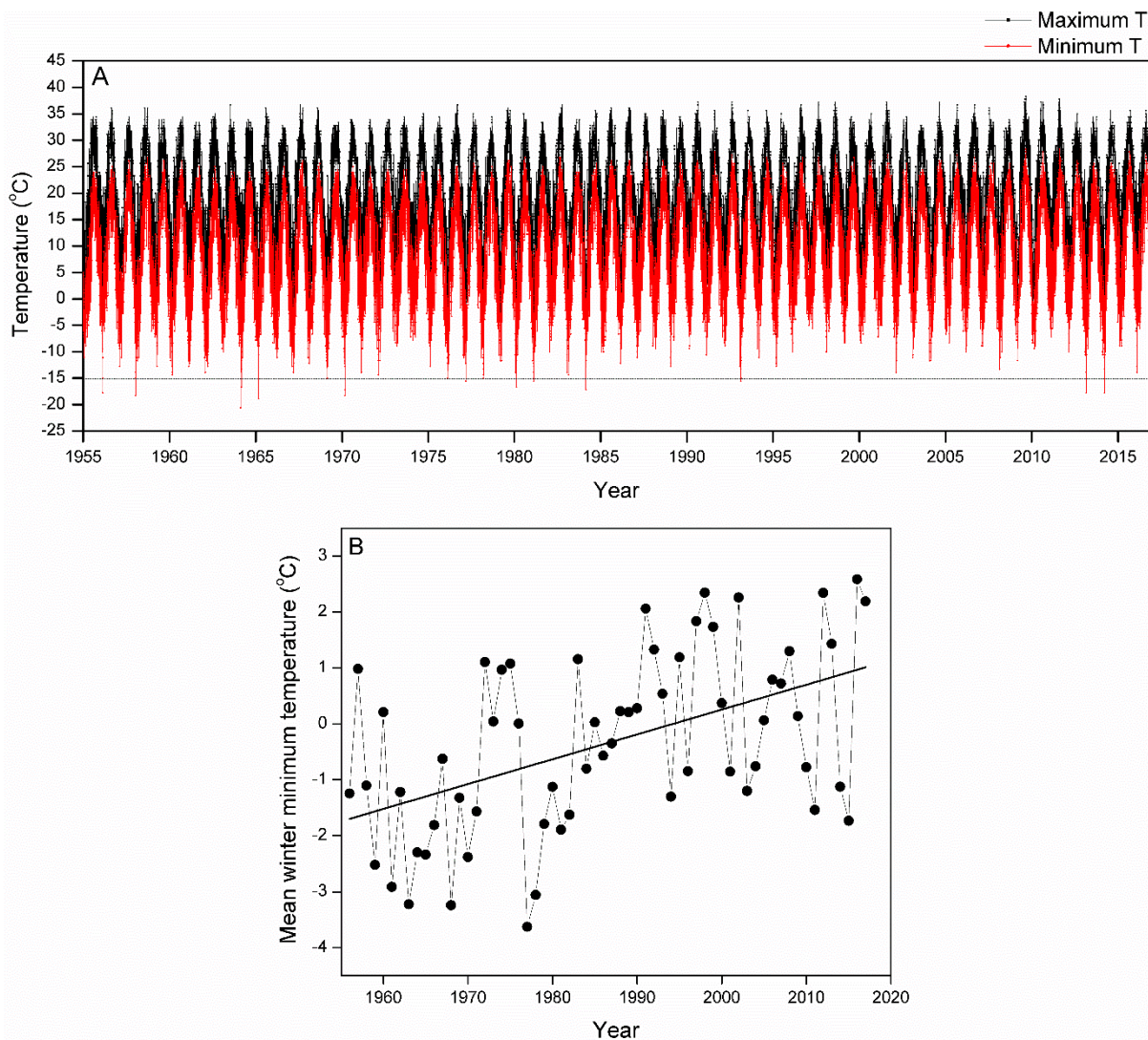
Figure 2. Trends in daily maximum and minimum temperature (A) and annual mean winter minimum temperature (B) in Painter, VA between December 1955 and September 2017. Since 1985, only 4 low temperature events (< -15°C) were observed. The annual mean winter minimum temperature also exhibited a significant increasing trend over time ($P < 0.001$) as shown by the OLS regression line.

3.3.2 Temperature data
The hourly air temperature measurements (hereafter referred to 'dataset A') were made 20 cm

51

above the ground by temperature sensors located in 5 grassland and 5 shrubland sites (HOBO U23-003, Onset Inc.) on Hog Island, VA from July 2014 to June 2015. Additionally, we acquired bihourly air temperature records ('dataset B') on Hog Island from May 2015 to March 2016 from Thompson et al. (2017). As spatial extent of *M. cerifera* thickets can be quite large, the temperatures were measured 10m inside and outside the shrub thicket edge to identify the warming effect of *M. cerifera* shrubland. The daily minimum and maximum temperatures were extracted and used to determine the warming effect of shrubland and therefore the model parameter (see below). Thompson et al. (2017) found that temperatures inside of shrub thickets are similar to those of younger, free standing shrubs.

3.3.3 Freezing experiment
Experiments were focused on shrubs as grasses are dormant during low temperature events. We assessed the effect of freezing on hydraulic conductivity of adult *Morella cerifera* shrubs at -15 and -20°C (n = 4). These were compared to shrubs grown at 7 and 25°C to serve as reference conditions for hydraulic conductivity at lower temperatures (7°C) and under ideal growth conditions (25°C). Adult shrubs (~ 1.5 m height) of local stock were purchased from a nursery and transplanted into 12 L pots. Shrubs were randomly assigned into treatments. A subset of shrubs were grown in an environmental chamber (20°C night / 25°C day, Model #E15, Conviron, Winnipeg, Manitoba, Canada) at 1000 µmol m^{-2} s^{-1} PAR for 10-hour photoperiod. The remaining shrubs were grown in low temperatures (4°C night /7°C day) in a cold room with 1000 µmol m^{-2} s^{-1} photosynthetic active radiation (PAR) and 10-hour photoperiod to mimic natural conditions preceding low temperature events. Plants were given 21 days to acclimate to growing conditions. Freezing took place with intact plants placed in a chest freezer (Model FFFC09M1RW, Frigidaire, Charlotte, NC) at 0°C. Cooling/warming proceeded at 0.5°C min^{-1} using the intrinsic rate of cooling of the freezer. Minimum temperature was maintained for 180 min at -15°C, and -20°C before warming to 0°C. 0°C was used to reduce additional damage to tissues from rapid changes in temperature.

Immediately post-freeze, 3-4 samples were excised per pot and prepared for hydraulic conductivity as described in Sperry et al. (1988). Stem segments were ~10 cm long and 5-10 mm in diameter. The hydraulic conductivity apparatus consisted of an IV-bag supplying a filtered (0.2 µm) 20 mM KCl solution via low gravitational pressure (~5 kPa) to a stem segment. Removal of in situ embolisms was prevented by a low hydraulic head. Flow rate was determined by measuring the volume of water expelled over a known amount of time and hydraulic conductivity was calculated as the mass flow rate of the solution through the stem segment divided by the pressure gradient along the segment path length (k_h, kg m s^{-1} MPa^{-1}). Stem specific conductivity (k_s, kg s^{-1} MPa^{-1} m^{-1}) was calculated from k_h divided by sapwood area.

3.3.4 Modelling framework
We modeled the change rate in *M. cerifera's* normalized density, S/S_c, as the result of a logistic growth and a mortality rate that is a temperature-dependent linear function of shrub biomass (D'Odorico et al. 2013),

$$\frac{d\left(S/S_c\right)}{dt} = \alpha \frac{S}{S_c}\left(1 - \frac{S}{S_c}\right) - \beta f(T_{min})\frac{S}{S_c}, \tag{1}$$

where S_c is the carrying capacity, which is assumed to be equal to 1, and α (year^{-1}) is the intrinsic growth rate of *M. cerifera*, and β (year^{-1}) is the maximum death rate caused by cold intolerance. The effect of temperature can be accounted for through the function, $f(T_{min})$, of minimum temperature, T_{min} as in D'Odorico et al. (2013),

$$f\left(T_{min}\right) = \begin{cases} 1; & T_{min} < T_1 \\ \dfrac{T_2 - T_{min}}{T_2 - T_1}; & T_1 \leq T_{min} \leq T_2 \\ 0; & T_{min} > T_2 \end{cases}, \tag{2}$$

where T_1 and T_2 are two critical temperatures defining the cold tolerance of *M. cerifera*. T_{min} is defined as the local minimum temperature within shrub thickets where the vegetation-microclimate feedback creates a warming effect. For bare soil with no plant cover, near surface minimum temperature equals T_b (i.e. background temperature). The encroachment and establishment of *M. cerifera* results in a local increase, $\triangle T_{max}$, in minimum temperature (Hayden 1998, He et al. 2010). This warming feedback is assumed to be expressed by a linear function of shrub cover, S i.e.

$$T_{min} = T_b + \Delta T_{max} \frac{S}{S_c}, \tag{3}$$

where ΔT_{max} represents the maximum warming effect with a full *M. cerifera* canopy.

The value of parameters α and β were determined empirically ($\alpha = 0.5$ year^{-1} and $\beta = 10$ year^{-1}) in a way that shrub encroachment (i.e., an increase in S from 0 to $0.95 \times S_c$) occurs in about 20-30 years, in agreement with studies documenting the rate of land cover change in these islands (Young et al. 2007); conversely, a full woody plant canopy can collapse into the state $S/S_c = 0$ within few years when temperature is consistently smaller than T_1.

According to previous studies, temperatures below -15°C would start to cause cold stress injury in some *Morella* species (Larcher 1995). Based on the hydraulic conductivity experiment under temperature treatments, we used equation (2) with T_1 and T_2 estimated to be equal to -20°C and -15°C, respectively. It should be noted that the overall modelling results are not sensitive to uncertainty in the determination of T_1 and T_2. The maximum increase $\triangle T_{max}$ in minimum temperature induced by the presence of a complete shrub cover was assumed to be equal to 2°C based on the results from two independent temperature datasets, which is also consistent with Thompson et al. (2017).

The stable states of these vegetation dynamics can be determined by inserting equations (2) and (3) in equation (1), setting the left-hand side of equation (1) equal to zero with T_{min} expressed as a function of S and $\triangle T_{max}$ to account for the shrub-microclimate feedback. Equilibrium points were determined by setting $\dfrac{d\left(S/S_c\right)}{dt} = 0$. After solving for S/S_c, we find that the system has three possible equilibrium states i.e. $S_{e1} = 0$, $S_{e2} = 1$, and

$$S_{e3} = \frac{T_2 - \left(T_b + \dfrac{\alpha}{\beta}(T_2 - T_1)\right)}{\left(\tau - \dfrac{\alpha}{\beta}\right)(T_2 - T_1)}, \tag{4}$$

where $\tau = \dfrac{\Delta T_{max}}{T_2 - T_1}$. Since S_{e3} can only exist between 0 and 1, based on equation (4), bistability (i.e., a dynamic with two alternative stable states separated by an unstable state) exists only when

$$T_2 - \tau(T_2 - T_1) \leq T_b \leq T_2 - \frac{\alpha}{\beta}(T_2 - T_1) \tag{5}$$

i.e. -17°C $\leq T_b \leq$ -15.25°C.

3.3.5 Statistical analyses
The difference in hourly (dataset A) and bihourly (dataset B) temperature between shrubland and grassland during nighttime and daytime was tested using Student's *t*-test ($\alpha = 0.05$). To focus on temperature differences on the coldest nights, we considered the days with the 10% and the 5% lowest minimum air temperatures and calculated their means to compare the minimum temperature difference between shrubland and grassland – and therefore estimate the parameter $\triangle T_{max}$ in the modelling framework. The Student's *t*-test ($\alpha = 0.05$) was used to determine whether the minimum temperature difference is significant at 95% confidence interval. Differences in stem specific hydraulic conductance were determined with ANOVA with subsampling. Pairwise comparisons were made using Tukey's test ($\alpha = 0.05$).

3.4 Results
The analysis shows that shrubland has a lower frequency of freezing events (records with temperature below 0°C) than grassland for both dataset A (540 times versus 622 times in total of 8172 records) and dataset B (134 times versus 159 times in total of 3571 records). In the nighttime, the shrubland was (on average) consistently and significantly warmer than the grassland both during the whole year ($P = 0.012$ and 0.004 for dataset A and B, respectively) and during the winter season ($P < 0.01$ for both datasets) (Figure 3); conversely, in the daytime, the grassland was consistently warmer than the shrubland, both during the whole year ($P < 0.0001$ for both datasets) and the winter season ($P < 0.01$ for both datsets) (Figure 4). The warming effect due to the existence of shrub cover was further confirmed by the significant increase in minimum temperatures in shrubland (Figure 5). The results from dataset A show that the mean of the 5% lowest minimum temperatures in shrubland and grassland were -6.14 ± 0.45°C and -7.43 ± 0.31°C, respectively; these two values were statistically different ($P = 0.024$). The mean of the 10% lowest minimum temperatures in shrubland and grassland were -4.09 ± 0.45°C and -5.60 ± 0.37°C, respectively; these values were also statistically different ($P = 0.012$). Similar results were found from dataset B. The mean of the 5% lowest minimum temperatures measured in the shrubland was -3.74 ± 0.60°C, statistically higher ($P = 0.003$) than the mean temperature of -6.11 ± 0.43°C in the grassland. The mean of the 10% lowest minimum temperatures in shrubland and grassland are -1.68 ± 0.53°C and -4.09 ± 0.44°C, respectively; these values were statistically different ($P = 0.001$). These results are in agreement with Thompson et al. (2017) who analyzed a segment of dataset B. The mean temperature difference between shrubland and grassland during the coldest nights was about 2°C. We also assume that the magnitude of this warming

effect is $\triangle T_{max} \approx 2°C$, based on the results shown in Figure 5.

Figure 3. Nighttime temperature comparison between shrubland and grassland in Hog Island during the whole year (A, C) and the winter season (B, D) based on dataset A (A, B) and B (C, D). Dataset A includes hourly temperature records from July 2014 to June 2015 and dataset B has bihourly temperature records from May 2015 to March 2016. In the nighttime, the shrubland is consistently warmer than the grassland, both during the whole year ($P = 0.012$ and 0.004 for dataset A and B, respectively) and the winter season ($P < 0.0001$ and $P = 0.009$ for dataset A and B, respectively).
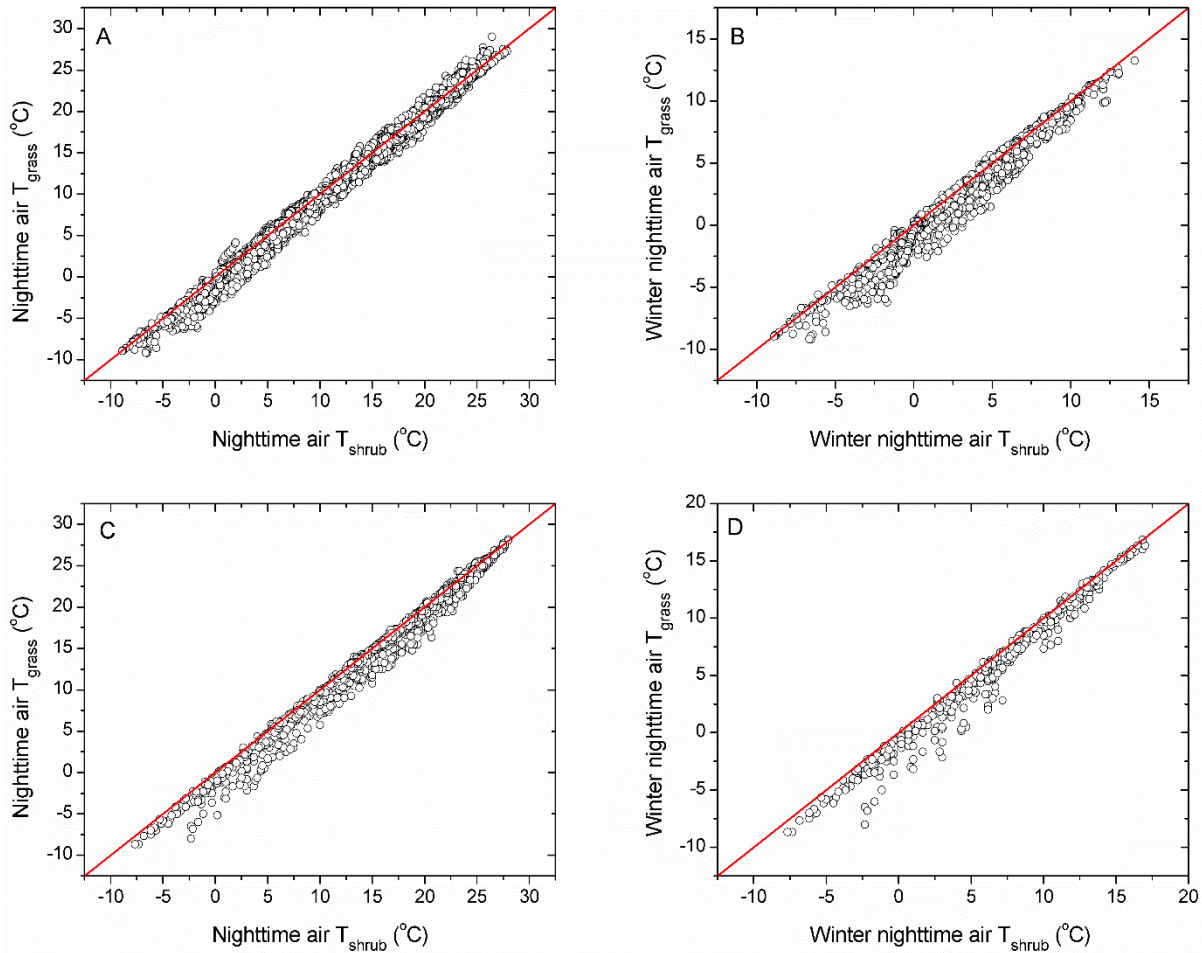
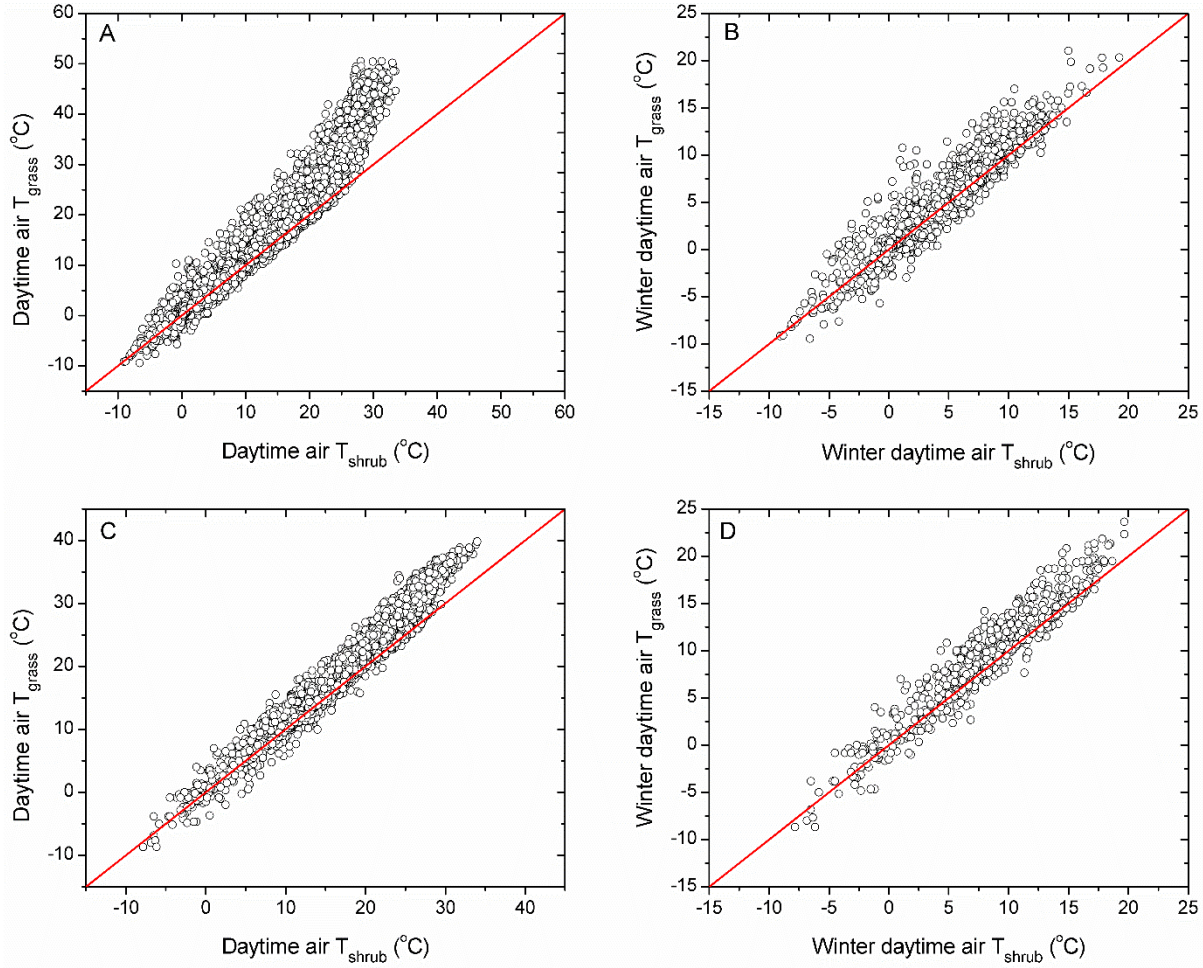**Figure 4. Daytime temperature comparison between shrubland and grassland in Hog Island during the whole year (A, C) and the winter season (B, D) based on dataset A (A, B) and B (C, D).** In the daytime, the grassland is consistently warmer than the shrubland, both during the whole year ($P < 0.0001$ for both dataset A and B) and the winter season ($P = 0.0003$ and $P = 0.0014$ for dataset A and B, respectively).
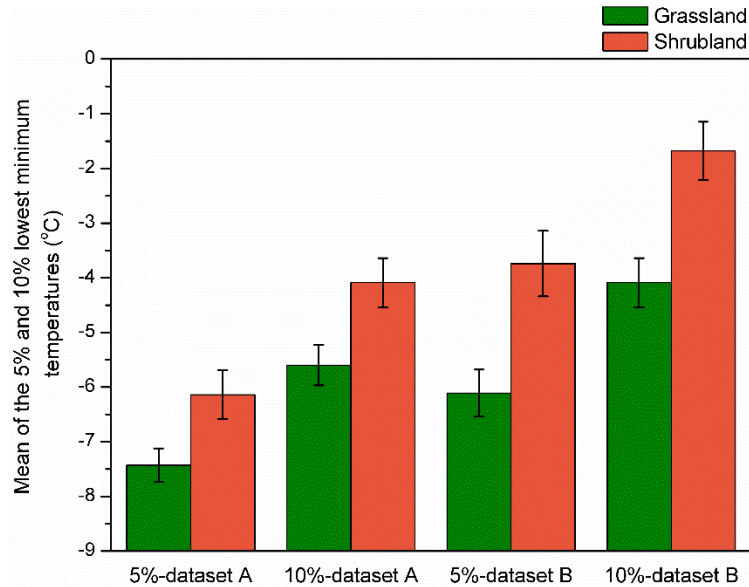
56

Figure 5. Difference in mean daily minimum temperature between shrubland and grassland in Hog Island calculated from both dataset A and B. The mean of the 5% and 10% lowest minimum temperatures were calculated respectively to determine the warming effect of shrubland and therefore estimate the parameter $\triangle T_{max}$ in our modelling framework. The Student's t test analysis ($\alpha = 0.05$) indicates a statistically significant warmer temperature in the shrubland than in the grassland ($P \leq 0.024$).

In our experimental analysis, at reference temperatures of 7°C or 25°C, stem-specific hydraulic conductance (k_s) was not statistically different, but freezing-induced cavitation significantly reduced stem hydraulic conductance at $T_2 = -15°C$ ($P < 0.0001$). k_s was reduced to ~0 at $T_1 = -20°C$ (Figure 6).
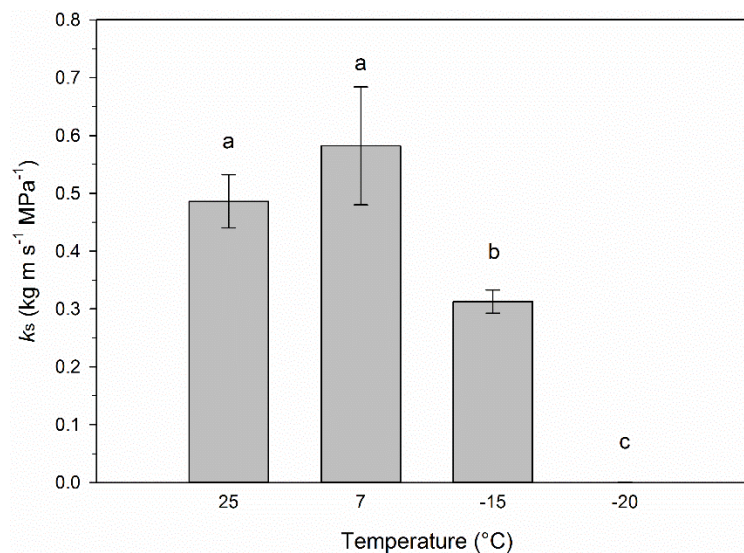

Figure 6. Mean ± 1 SE stem-specific hydraulic conductivity (k_s) for *M. cerifera* shrubs after freezing. Letters indicate differences according to post-hoc Tukey's test ($\alpha = 0.05$).

Ecosystem stability is here investigated using our modelling framework and looking at how the rate of change in S/S_c varies as a function of S/S_c (Figure 7). This analysis shows how the stable states of the system vary with different background temperature ranges (Figure 7). Specifically, we found that (i) when T_b is lower than -17°C, $f(T_{min})$ equals either 1 or $\dfrac{T_2 - T_{min}}{T_2 - T_1}$ [see equation (2)] because T_{min} cannot exceed -15°C even with the maximum warming effect (i.e. $\triangle T_{max}$). In these climate conditions the ecosystem is stable only with no woody plant cover ($S = 0$) because there are no other stable equilibrium points in the interval (0, 1); (ii) when T_b lies between -17°C and -15.25°C, the rate of change of normalized shrub density would follow

$$\frac{d(S/S_c)}{dt} = \alpha S(1 - S/S_c) - \beta(S/S_c) f(T_{min}),$$ which becomes $$\frac{d(S/S_c)}{dt} = \alpha S(1 - S/S_c)$$ when T_{min}

exceeds -15°C as a result of the warming effect of shrub cover. For example, in the case of $T_b = -16°C$, the rate of change of S/S_c will shift to the latter equation when S reaches 0.5, which is when the T_{min} increases to -15°C (Figure 7). Therefore, in this case the system has two stable equilibrium points $S_{e1} = 0$ and $S_{e2} = 1$, and an unstable equilibrium S_{e3}, which ranges between 0 and 1; (iii) when T_b is larger than -15.25°C, $f(T_{min})$ equals $\dfrac{T_2 - T_{min}}{T_2 - T_1}$ (when $T_{min} \leq -15°C$) or 0

(when $T_{min} > -15°C$). In these conditions the system has only two equilibrium points in the interval (0, 1), $S_{e1} = 0$ (unstable) and $S_{e2} = 1$ (stable), and the dynamics tends to a full shrub cover state, regardless of the initial shrub cover conditions. Therefore, because of the nonlinear response of vegetation to near surface temperature associated with this feedback, vegetation response to climate warming may exhibit a threshold behavior with an abrupt transition from the grassland stable state to full shrub cover ($S = S_c$) as T_b increases above about -15°C (Figure 8).
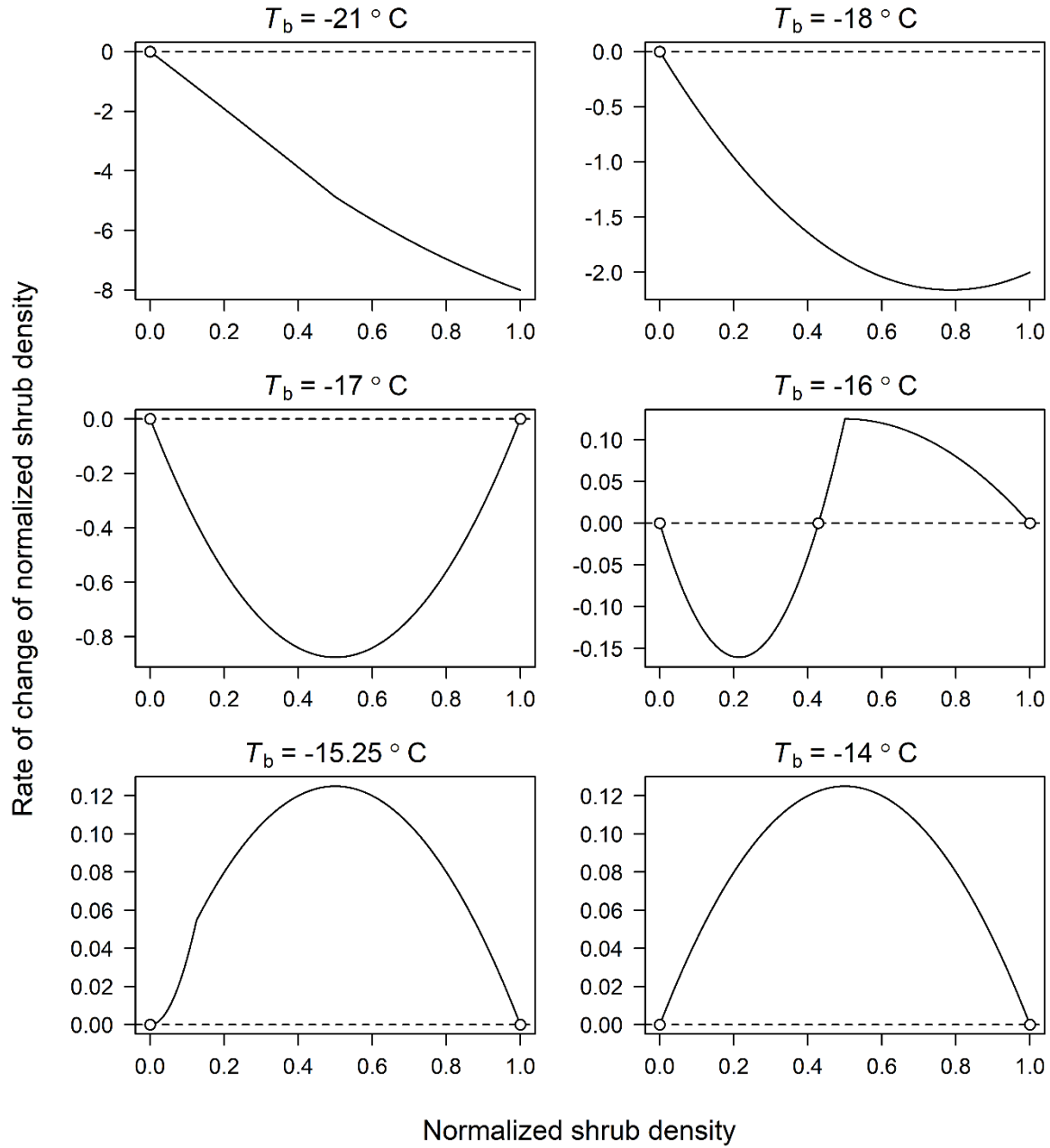
Figure 7. The rate of change of normalized shrub density ($d(S/S_c)/dt$) versus normalized shrub density (S/S_c) under different background temperature (T_b) conditions.
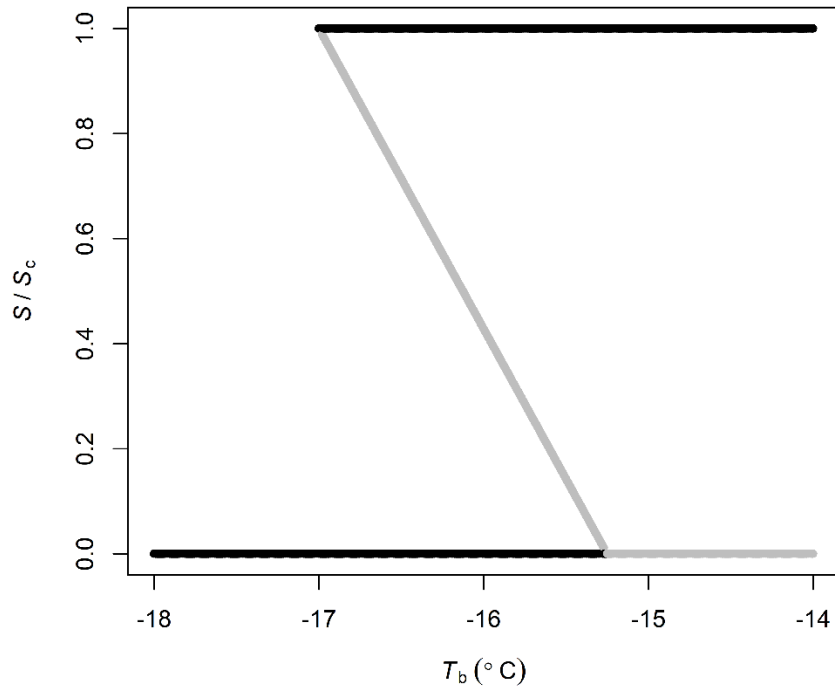
Figure 8. Bi-stable states induced by vegetation-microclimate feedback in shrubland-grassland ecotones. Stable and unstable states are indicated by dark and grey lines respectively. S/S_c is the normalized density of *M. cerifera* ranging from 0 to 1, T_b is the temperature without the presence of *M. cerifera*. When T_b reaches a threshold value (approximately -15°C), the ecosystem would shift rapidly from grassland to shrubland which is highly hysteretic.

3.5 Discussion

The modelling results clearly show that a small increase in the background minimum temperature, T_b, can cause a shift in the state of the system from one stable state with no shrub dominance to its alternative stable state with a full shrub canopy. The transition is expected to occur in a non-linear way through the positive feedback between vegetation and microclimate (Figure 8). Based on the results shown in Figure 6, we set $T_1 = -20°C$, which is a conservative estimate because there is evidence that plant mortality from irreversible xylem damage occurs already when the stem conductance is reduced by 80% (Bartlett et al. 2016). When temperature is below -15°C, *M. cerifera* would suffer from cold induced injury and lose competitiveness with grasses, thereby leading to the stabilization of the ecosystem with full grass cover.

The cold intolerance of *M. cerifera* has been widely documented in the literature (for example, Larcher 1995), is further supported by our freezing experiment (Figure 6), and is evidenced by the fact that the barrier islands in which its encroachment has been documented (i.e., Hog Island, in Virginia) are at the northern limit of *M. cerifera*'s latitudinal range. It has also been documented that in these islands the establishment of *M. cerifera* has modified the microclimate by increasing nocturnal temperatures and mitigating the exposure to extreme low temperature events and cold-induced stress, especially during extremely cold nights. Even though the mechanisms underlying this warming effect still have to be documented, studies developed in other grass-shrub transition zones have highlighted how the presence of shrub cover may alter

60

the surface energy fluxes, for example, by reducing the nocturnal longwave radiation loss (D'Odorico et al. 2013) or the diurnal ground heat flow (He et al. 2010, 2015). Likewise, these effects could explain how the shrubland of *M. cerifera* may create warmer microclimatic conditions. Field measurements on Hog Island have documented significantly higher average minimum temperatures inside the shrub thickets than in grass swales (Figures 3 and 5, Young et al. 1992, Thompson et al. 2017). The warming effect promotes further survival and growth of young seedlings especially in ecotone areas close to the "tree line" (Maher et al. 2005, Maher and Germino 2006). Moreover, warming could also indirectly benefit shrub growth by enhancing microbial activity and nutrient cycling (Thompson et al. 2017). Through this vegetation-microclimate feedback, *M. cerifera* shrubs act as 'ecosystem engineers', i.e., as organisms that create their own habitat (Jones et al. 1994), thereby promoting their own survival and growth. Due to the positive vegetation-microclimate feedback, the grassland could eventually experience an abrupt transition to another stable state with full woody plant when the minimum background temperature exceeds a threshold value as a result of climate warming.

The abrupt and discontinuous transition, both temporally and spatially, from grassland to shrubland has been observed in several ecosystems around the world (Archer et al. 1988, Chapin et al. 2000, Maher et al. 2005, Bader et al. 2007, Knapp et al. 2008, McKee and Rooth 2008, Ravi et al. 2009, D'Odorico et al. 2013). The positive feedback between vegetation and microclimate can substantially release the pressure of *M. cerifera* from cold induced injury or mortality. When a combination of regional climate warming and microclimate feedback results in an increase in minimum temperature within shrub thickets that exceeds the threshold temperature for woody plant growth, an abrupt transition is expected to take place between the two stable states of the system, namely from grass to shrub dominance. It should be noted that at the study sites an increase in shrub cover was also observed from 1949 to 1989 even though this period experienced several extreme cold events. However the rate of expansion was greater between 1974 and 1989 (Young et al. 2007). This effect may be attributed to other mechanisms such as the feedback of bird dispersal of seeds or the lagging effects of previous anthropogenic disturbances (Young et al. 1995). Records from the 1970s document that shrub thickets of *M. cerifera* were not present on most islands (McCaffrey and Dueser 1990). Climate warming has been invoked as one of the major factors causing grass replacement by shrubs (Van Auken 2000, D'Odorico 2012) and is projected to accelerate in the near future as a result of anthropogenic CO_2 emissions (Cox et al. 2000) thereby creating a more favorable environment for the encroachment of cold-sensitive shrubs into regions where the extreme cold events usually exclude their existence.

Conditions for *M. cerifera* establishment must be favorable with respect to salinity (Sande and Young 1992), elevation, and distance from the shoreline (Young et al. 2011). Sediment flux is an important consideration in this dynamic landscape, with development of a freshwater lens necessary for establishment and growth. Once established, shrubs are able to survive under periods of high saline conditions that may occur during storm overwash (Tolliver et al. 1997, Naumann et al. 2008). Enhanced leaf area index of shrubs coupled with microclimate warming likely increases evapotranspiration (Shao et al. 1995), creating a potential additional feedback with water availability in a system dependent on precipitation for recharging the freshwater lens (Aguilar et al. 2012). Despite the multiple environmental drivers that control shrub establishment, expansion across several islands has occurred at an unprecedented rate since the

1980s (Zinnert et al. 2016), even with accelerated sea-level rise (Sallenger et al. 2012) and reduction in island area.

The abrupt transition to shrubland can be highly hysteretic and potentially irreversible as evidenced by the ineffectiveness of many shrub-removal programmes (Rango et al. 2005, Bestelmeyer et al. 2009, D'Odorico et al. 2012) especially when self-sustained internal feedbacks act through their impact on ecosystem structure, functioning and resilience (Thompson et al. 2017). The ongoing shrub expansion in Hog Island (VA) would decrease plant species diversity and modify wildlife habitats (Zinnert et al. 2017). Increased carbon and nitrogen input into the system from shrub expansion (Brantley and Young 2010) alters biogeochemical cycling and may impact adjacent communities. In the short-term, shrubs provide resistance to storm events, by stabilizing sediments and reducing energy associated with storms (Claudino-Sales et al. 2008, U.S. Army Corps of Engineers 2013). Over longer timeframes, this resistance may prevent natural island migration through increasing shoreline erosion and creating a barrier to sediment overwash, thereby increasing the vulnerability of barrier islands to sea level rise (Zinnert et al. 2016, Thompson et al. 2017). As barrier islands protect lagoons and marshes with many economically and ecologically important species, the transition from grassland to shrubland has far reaching consequences on multiple ecosystems. Our simplified modelling framework provides a general theoretical mechanism for the emergence of bi-stable vegetation dynamics in shrubland-grassland ecotones and facilitates our understanding and prediction of how the stability of these ecosystems may nonlinearly change under future climate change scenarios.

3.6 References

Aguilar, C., J. C. Zinnert, M. J. Polo, and D. R. Young. 2012. NDVI as an indicator for changes in water availability to woody vegetation. Ecological Indicators 23:290–300.

Archer, S., C. Scifres, C. R. Bassham, and R. Maggio. 1988. Autogenic succession in a subtropical savanna: conversion of grassland to thorn woodland. Ecological Monographs 58:111–127.

Archer, S., D. S. Schimel, and E. A. Holland. 1995. Mechanisms of shrubland expansion: land use, climate, or carbon dioxide. Climate Change 29:91–99.

Avissar, R., P. L. Silva-Dias, M. A. F. Silva-Dias, and C. Nobre. 2002. The Large-Scale Biosphere-Atmosphere Experiment in Amazonia (LBA): insights and future research needs. Journal of Geophysical Research 107:8086.

Bader, M., M. Rietkerk, and A. Bregt. 2007. Vegetation structure and temperature regimes of tropical alpine treelines. Arctic, Antarctic, and Alpine Research 39:353–364.

Bartlett, M. K., T. Klein, S. Jansen, B. Choat, and L. Sack, 2016. The correlations and sequence of plant, stomatal, hydraulic, and wilting responses to drought. Proceedings of the National Academy of Sciences of the United States of America 113:13098–13103.

Beltrán-Przekurat, A., Sr. R. A. Pielke, D. P. C. Peters, K. A. Snyder, and A. Rango. 2008. Modeling the effects of historical vegetation change on near-surface atmosphere in the northern Chihuahuan Desert. Journal of Arid Environments 72:1897–1910.

Bestelmeyer, B. T., A. J. Tugel, G. L. Peacock, D. G. Robinett, P. L. Shaver, J. R. Brown, J. E. Herrick, H. Sanchez, and K. M. Havstad. 2009. State-and-transition models for heterogeneous landscapes: a strategy for development and application. Rangeland Ecology & Management 62:1–15.

Bissett, S. N., J. C. Zinnert, and D. R. Young. 2016. Woody expansion facilitates liana expansion and affects physical structure in temperate coastal communities. Ecosphere 7:e01383.

Bonan, G. B. 2008. Forests and climate change: forcings, feedbacks, and the climate benefits of forests. Science 320:1444–1449.

Brantley, S. T., and D. R. Young. 2007. Leaf-area index and light attenuation in rapidly expanding shrub thickets. Ecology 88:524–530.

Brantley, S. T., and D. R. Young. 2010. Linking light attenuation, sunflecks and canopy architecture in mesic shrub thicket. Plant Ecology 206:225–326.

Buchner, O., and G. Neuner. 2011. Winter frost resistance of *Pinus cembra* measured *in situ* at the alpine timberline as affected by temperature conditions. Tree Physiology 31:1217–1227.

Cavanaugh, K.C., J. R. Kellner, A.J. Forde, D.S. Gruner, J.D. Parker, W. Rodriguez, and I. C. Feller. 2014. Poleward expansion of mangroves is a threshold response to decreased frequency of extreme cold events. Proceedings of the National Academy of Sciences USA 111:723–727.

Chapin, F. S., A. D. McGuire, J. Randerson, R. Pielke, D. Baldocchi, S. E. Hobbie, N. Roulet, W. Eugster, E. Kasischke, E. B. Rastetter, S. A. Zimov, and S. W. Running. 2000. Arctic and boreal ecosystems of western North America as components of the climate system. Global Change Biology 6:211–223.

Claudino-Sales, V., P. Wang, and M. H. Horwitz. 2008. Factors controlling the survival of coastal dunes during multiple hurricane impacts in 2004 and 2005: Santa Rosa barrier island, Florida. Geomorphology 95:295–315.

Collins, B. S., and J. A. Quinn. 1982. Displacement of *Andropogon scoparius* on the New Jersey Piedmont by the successional shrub *Myrica pensylvanica*. American Journal of Botany 69:680–689.

Cox, P. M., R. A. Betts, C. D. Jones, S. A. Spall, and I. J. Totterdell. 2000. Acceleration of global warming due to carbon-cycle feedbacks in a coupled climate model. Nature 408:184–187.

D'Odorico, P., Fuentes, J. D., Pockman,W. T., Collins, S. L., He, Y., Medeiros, J. S., De Wekker, S. and Litvak, M. E. 2010. Positive feedback between microclimate and shrub encroachment in the northern Chihuahuan desert. Ecosphere 1:1–11.

D'Odorico, P., G. S. Okin, and B. T. Bestelmeyer. 2012. A synthetic review of feedbacks and drivers of shrub encroachment in arid grasslands. Ecohydrology 5:520–530.

D'Odorico, P., Y. He, S. Collins, S. F. De Wekker, V. Engel, and J. D. Fuentes. 2013. Vegetation–microclimate feedbacks in woodland–grassland ecotones. Global Ecology and Biogeography 22:364–379.

Geiger, R. 1965. The climate near the ground, 4th edn. Harvard University Press, Cambridge, MA.

Grace, J., S. J. Allen, and C. Wilson. 1989. Climate and the meristem temperatures of plant communities near the tree-line. Oecologia 79:198–204.

Hayden, B. P. 1998. Ecosystem feedbacks on climate at the landscape scale. Philosophical Transactions of the Royal Society B: Biological Sciences 353:5–18.

He, Y., P. D'Odorico, S. F. J. De Wekker, J. D. Fuentes, and M. Litvak. 2010. On the impact of shrub encroachment on microclimate conditions in the northern Chihuahuan desert. Journal of Geophysical Research 115:D21120.

He, Y., P. D'Odorico, and S. F. J. De Wekker. 2014. The relative importance of climate change and shrub encroachment on nocturnal warming in the Southwestern United States.

International Journal of Climatology 35:475–480.

He, Y., P. D'Odorico, and S. F. J. De Wekker. 2015. The role of vegetation-microclimate feedback in promoting shrub encroachment in the northern Chihuahuan desert, Global Change Biology 21:2141–2154

Jones, C. G., J. H. Lawton, and M. Shachak. 1994. Organisms as ecosystem engineers. Oikos 69:373–386.

Knapp, A. K., J. M. Briggs, S. L. Collins, S. R. Archer, M. S. Bret-Harte, B. E. Ewers, D. P. Peters, D. R. Young, G. R. Shaver, E. Pendall, and M. B. Cleary. 2008. Shrub encroachment in North American grasslands: shifts in growth form dominance rapidly alters control of ecosystem carbon inputs. Global Change Biology 14:615–623.

Körner, C. 1998. A re-assessment of high elevation treeline positions and their explanation. Oecologia 115:445–459.

Krauss, K. W., C. E. Lovelock, K. L. McKee, L. López-Hoffman, S. M. L. Ewe, and W. P. Sousa. 2008. Environmental drivers in mangrove establishment and early development: a review. Aquatic Botany 89:105–127.

Langvall, O., and G. Örlander. 2001. Effects of pine shelterwoods on microclimate and frost damage to Norway spruce seedlings. Canadian Journal of Forest Research 31:155–164.

Larcher, W. 1995. Physiological Plant Ecology, 3rd edn. Springer-Verlag, Berlin.

Lawrence, D., and K. Vandecar. 2014. Effects of tropical deforestation on climate and agriculture, Nature Climate Change 5:27–36.

Levy, G. F. 1990. Vegetation dynamics on the Virginia barrier islands. Virginia Journal of Science 41:300–306.

Li, Y., M. Zhao, S. Motesharrei, Q. Mu, E. Kalnay, and S. Li. 2015. Local cooling and warming effects of forests based on satellite observations. Nature Communications 6:6603.

Li, Y., M. Zhao, D. J. Mildrexler, S. Motesharrei, Q. Mu, E. Kalnay, F. Zhao, S. Li, and K. Wang. 2016. Potential and Actual Impacts of Deforestation and Afforestation on Land Surface Temperature. Journal of Geophysical Research: Atmospheres 121:14,372–14,386.

Maher, E. L., and M. J. Germino. 2006. Microsite variation among conifer species during seedling establishment at alpine-treeline. Ecoscience 13:334–341.

Maher, E. L., M. J. Germino, and N. J. Hasselquist. 2005. Interactive effects of tree and herb cover on survivorship, physiology, and microclimate of conifer seedlings at the alpine tree-line ecotone. Canadian Journal of Forest Research 35:567–574.

McCaffrey, C. A., and R. D. Dueser. 1990. Plant associations and the Virginia barrier islands. Virginia Journal of Science 41:282–299.

McKee, K. L., and J. E. Rooth. 2008. Where temperate meets tropical: multi-factorial effects of elevated CO_2, nitrogen enrichment, and competition on a mangrove-salt marsh community. Global Change Biology 14:971–984.

Medeiros, J. S., and W. T. Pockman. 2011. Drought increases freezing tolerance of both leaves and xylem of *Larrea tridentata*. Plant, Cell and Environment 34:43–51.

Naumann, J. C., D. R. Young, and J. E. Anderson. 2008. Leaf fluorescence, reflectance, and physiological response of freshwater and saltwater flooding in the evergreen shrub, *Myrica cerifera*. Environmental and Experimental Botany 63:402–409.

Pielke, R. A., R. Avissar, M. Raupach, A. J. Dolman, X. Zeng, and A. S. Denning. 1998. Interactions between the atmosphere and terrestrial ecosystems: influence on weather and climate. Global Change Biology 4:461–475.

Pockman, W. T., and J. S. Sperry. 1997. Freezing-induced xylem cavitation and the northern

limit of *Larrea tridentata*. Oecologia 109:19–27.

Rango, A., L. Huenneke, M. Buonopane, J. E. Herrick, and K. M. Havstad. 2005. Using historic data to assess effectiveness of shrub removal in southern New Mexico. Journal of Arid Environments 62:75–91.

Ravi, S., P. D'Odorico, L. Wang, C. S. White, G. S. Okin, S. A. Macko, and S. L. Collins. 2009. Post-fire resource redistribution in desert grasslands: a possible negative feedback on land degradation. Ecosystems 12:434–444.

Runyan, C. W., and P. D'Odorico. 2016. Global Deforestation, Cambridge University Press, New York.

Sallenger, A. H., K. S. Doran, and P. A. Howd. 2012. Hotspot of accelerated sea-level rise on the Atlantic coast of North America. Nature Climate Change 2:884–888.

Sande, E., and D. R. Young. 1992. Effect of sodium chloride on growth and nitrogenase activity in seedlings of *Myrica cerifera* L. New Phytologist 120:345–350.

Shao, G., H. H. Shugart, and D. R. Young. 1995. Simulation of transpiration sensitivity to environmental changes for shrub (*Myrica cerifera*) thickets on a Virginia barrier island. Ecological Modeling 78:235–248.

Shao, G., and P. N. Halpin. 1995. Climatic controls of eastern North American coastal tree and shrub distributions. Journal of Biogeography 22:1083–1089.

Sperry, J. S., J. R. Donnelly, and M. T. Tyree. 1988. A method for measuring hydraulic conductivity and embolism in xylem. Plant, Cell and Environment 11:35–40.

Stuart, S. A., B. Choat, K. C. Martin, N. M. Holbrook, and M. C. Ball. 2007. The role of freezing in setting the latitudinal limits of mangrove forests. New Phytologist 173:576–583.

Tape, K., M. Sturm, and C. Racine. 2006. The evidence for shrub expansion in Northern Alaska and the Pan-Arctic. Global Change Biology 12:686–702.

Thompson, J. A., J. C. Zinnert, and D. R. Young. 2017. Immediate effects of microclimate modification enhance native shrub encroachment. Ecosphere 8:e01687.

Thompson, J. A. 2016. Mechanisms of Native Shrub Encroachment on a Virginia Barrier Island. Thesis. Virginia Commonwealth University, Richmond, Virginia, USA.

Tolliver, K. S., D. W. Martin, and D. R. Young. 1997. Freshwater and saltwater flooding response for woody species common to barrier island swales. Wetlands 17:10–18.

Tranquillini, W. 1979. Physiological ecology of the alpine timberline: tree existence at high altitudes with special reference to the European Alps. Springer, Berlin.

U.S. Army Corps of Engineers. 2013. Coastal Risk Reduction and Resilience. U.S. Army Corps of Engineers Civil Works Directorate, Washington, DC.

Van Auken, O. 2000. Shrub invasions of North American semiarid grasslands. Annual Review of Ecology and Systematics 31:197–215.

Wookey, P. A., R. Aerts, R. D. Bardgett, F. Baptist, K. A. Brathen, J. H. C. Cornelissen, L. Gough, I. P. Hartley, D. W. Hopkins, S. Lavorel, and G. R. Shaver. 2009. Ecosystem feedbacks and cascade processes: understanding their role in the responses of Arctic and alpine ecosystems to environmental change. Global Change Biology 15:1153–1172.

Young, D. R. 1992. Photosynthetic characteristics and potential moisture stress for the actinorhizal shrub, *Myrica cerifera*, on a Virginia barrier island. American Journal of Botany 79:2–7.

Young, D. R., E. Sande, and G. A. Peters. 1992. Spatial relationships of Frankia and *Myrica cerifera* on a Virginia, USA barrier island. Symbiosis 3:209–220.

Young, D. R., G. Shao, and J. H. Porter. 1995. Spatial and temporal growth dynamics of barrier

island shrub thickets. American Journal of Botany 82:638–645.

Young, D. R., J. H. Porter, C. M. Bachmann, G. Shao, R. A. Fusina, J. H. Bowles, D. Korwan, and T. F. Donato. 2007. Cross-scale patterns in shrub thicket dynamics in the Virginia barrier complex. Ecosystems 10:854–863.

Young, D. R., S. T. Brantley, J. C. Zinnert, and J. K. Vick. 2011. Landscape position and habitat polygons in a dynamic coastal environment. Ecosphere 2:71.

Yu, K. L., and P. D'Odorico. 2014. An ecohydrological framework for grass displacement by woody plants in savannas. Journal of Geophysical Research: Biogeosciences 119:192–206.

Zinnert, J. C., S. A. Shiflett, J. K. Vick, and D. R. Young. 2011. Woody vegetative cover dynamics in response to climate change on an Atlantic coast barrier island: remote sensing approach. Geocarto International 26:595–612.

Zinnert, J. C., S. A. Shifflet, S. Via, S. Bissett, B. Dows, P. Manley, and D. R. Young. 2016. Spatial–temporal dynamics in barrier island upland vegetation: the overlooked coastal landscape. Ecosystems 19:685–697.

Zinnert, J. C., J. A. Stallins, S. T. Brantley, and D. R. Young. 2017. Crossing scales: complexity of barrier island processes for predicting future change. Bioscience 67:39–52.

CHAPTER 4

Critical transition to woody plant dominance through microclimate feedbacks in North American coastal ecosystems

Reference: Huang, H., Anderegg, L. D. L., Dawson, T. E., Mote, S., D'Odorico, P. 2020. Critical transition to woody plant dominance in North American coastal ecosystems. Ecology. 101:e03107.

4.1 Abstract
Climate warming is facilitating the expansion of many cold-sensitive woody species in woodland-grassland ecotones worldwide. Recent research has demonstrated that this range expansion can be further enhanced by positive vegetation-microclimate feedbacks whereby woody canopies induce local nocturnal warming, which reduces freeze-induced damage and favors the establishment of woody plants. However, this local positive feedback can be counteracted by biotic drivers such as browsing and the associated consumption of shrub biomass. The joint effects of large-scale climate warming and local-scale microclimate feedbacks on woody vegetation dynamics in these ecotones remain poorly understood. Here, we used a combination of experimental and modelling approaches to investigate the effects of woody cover on microclimate and the consequent implications on ecological stability in North American coastal ecosystems. We found greater browsing pressure and significant warming (~2°C) beneath shrub canopies compared to adjacent grasslands, which reduces shrub seedlings' exposure to cold damage. Cold sensitivity is evidenced by the significant decline in xylem hydraulic conductivity in shrub seedlings when temperatures dropped below -2°C. Despite the negative browsing-vegetation feedback, a small increase in minimum temperature can induce critical transitions from grass to woody plant dominance. Our framework also predicts the threshold temperature of -7°C for mangrove–salt marsh ecotones on the Atlantic coast of Florida. Above this reference temperature a critical transition may occur from salt marsh to mangrove vegetation, in agreement with empirical studies. Thus, the interaction between ongoing global warming trends and microclimate feedbacks may significantly alter woody vegetation dynamics and ecological stability in coastal ecosystems where woody plant expansion is primarily constrained by extreme low temperature events.

4.2 Introduction
The relatively rapid encroachment of woody plants into non-woody systems is resulting in major shifts in plant distribution and abundance around the globe (Archer et al. 1995, Maher et al. 2006, Knapp et al. 2008, McKee and Rooth 2008, Ravi et al. 2009, Myers-Smith et al. 2011, Fan et al. 2019). This relatively abrupt change in plant community composition has significant impacts on ecosystem structure, functioning, and services such as carbon and nitrogen cycling, ecosystem productivity, and soil stabilization (Schlesinger et al. 1999, Huenneke et al. 2002, Li et al. 2007). The widespread increase in woody plant dominance in ecosystems ranging from tundra to temperate grasslands to tropical savannahs has been attributed to a number of exogenous and endogenous factors such as overgrazing, fire suppression, increased atmospheric CO_2 concentrations, nitrogen deposition, land abandonment, and climate change (Van Auken 2000, Sankaran et al. 2005, Ward 2005, Gehrig-Fasel et al. 2007, D'Odorico et al. 2012, Huang et al. 2018). Previous studies have suggested that climate warming is driving the range shift of many species across the globe (Chen et al. 2011) and contributes to the expansion of woody

plants in ecological transition zones where the latitudinal distribution of trees and shrubs is restricted by cold stress (D'Odorico et al. 2010, 2013). Indeed, many woody species are more cold-intolerant than grasses because of the negative effect of extreme low temperatures on their reproduction, photosynthesis, and xylem conductivity (e.g., D'Odorico et al. 2013). For instance, cold spells that do not affect senesced grasses limit the capacity of woody plants to maintain a positive carbon balance and cause significant physiological damage to newly developed tissues (Tranquillini 1979). Moreover, extreme low-temperature events can cause xylem embolisms in woody plants (Pockman and Sperry 1997) and lead to the loss of hydraulic conductivity and potential plant mortality (Buchner and Neuner 2011, Medeiros and Pockman 2011), although plants may adapt to freezing stress, for example, by decreasing vessel diameters (Medeiros and Pockman 2014). Woody seedlings and juveniles are particularly susceptible to environmental stress, including cold-induced damage, with a bottleneck effect that limits the poleward expansion of woody plant populations in woodland-grassland ecotones (Harper 1977). Global or regional warming, however, reduces the probability of freezing events during the winter season and potentially enables woody plants to survive and establish in these ecotones where their distributions are primarily controlled by extreme cold events (D'Odorico et al. 2013).

In addition to large-scale climate warming, woody encroachment in many cold regions can be favored by a positive feedback between vegetation and microclimate, whereby woody plants modify the surface energy balance with the effect of increasing the minimum (i.e., nocturnal) temperatures (D'Odorico et al. 2010, 2013). In some ecotones such as in the Chihuahuan desert or on Virginia barrier islands, woody cover can reduce radiative cooling by absorbing a fraction of nocturnal long-wave radiation emitted by the ground surface and reflecting it back to the surface, thereby creating warmer nocturnal microclimate conditions under woody canopies (He et al. 2010, Huang et al. 2018). Therefore, vegetation-microclimate feedbacks may substantially favor the survival and establishment of woody plant seedlings at boundaries of their latitudinal range where further expansion is constrained by cold stress.

Positive feedbacks may induce nonlinear behaviors in ecosystem dynamics, including bifurcations, alternative stable states, and critical transitions (May 1977, Scheffer et al. 2001). Previous studies have explained woody plant encroachment as a shift between alternative stable states in ecosystem dynamics (Andreries et al. 2002, Bestelmeyer et al. 2009). Such transitions are often difficult to anticipate (Ratajczak et al. 2018) and irreversible, as evidenced by the failure of many bush control programs (Rango et al. 2005, Bestelmeyer et al. 2009). In bistable ecosystems, gradual variations in external drivers may not lead to noticeable changes until a critical (i.e., bifurcation) point is reached. At that point a grassland undergoes a critical transition to the stable woodland state. We argue that the combined effects of (endogenous) vegetation-microclimate feedbacks and (exogenous) climate warming are likely driving the rapid expansion of woody plants into open grassland in ecotones where woody plant growth is limited by extreme low temperature events.

Empirical evidence confirms the occurrence of vegetation-microclimate feedbacks associated with nocturnal warming beneath woody canopies. This effect has been found to facilitate woody plant encroachment in a variety of ecosystems such as alpine meadows and arid grasslands (D'Odorico et al. 2013). The expansion of woody plants in coastal ecosystems, however, remains understudied despite its important impacts on carbon sequestration, biodiversity, and ecological

resilience (D'Odorico et al. 2013, Guo et al. 2017, Huang et al. 2018). The establishment of cold-sensitive woody plants at coastal ecotones may benefit from the establishment of warmer microclimate conditions that reduce exposure to freeze-induced mortality (Thompson et al. 2017, Huang et al. 2018), which has also been observed in mangrove-salt marsh ecotones in the Atlantic coast of Florida, USA (Devaney et al. 2017). The latitudinal distribution of mangroves in these ecotones is primarily limited by extreme cold events (Stuart et al. 2007, Cavanaugh et al. 2014). The local warming effect of mangrove canopies indicates that the widely observed mangrove expansion may also be facilitated by vegetation-microclimate feedbacks.

The effect of local warming or other positive feedbacks can be counteracted by biotic factors such as browsing, although the effect of browsing on woody plant dynamics may depend on the specific ecosystem and plant functional types (Vowles et al. 2017). Browsers can negatively affect woody plant growth and establishment directly by consuming woody vegetation, thus contributing to negative feedbacks. For example, it has been observed in coastal mangrove ecosystems that mangrove crabs tend to preferentially target seedlings growing under woody canopies and reduce mangrove seedling growth (Devaney et al. 2017). Therefore, the overall woody vegetation dynamics and their susceptibility to state change will depend on the relative strength of positive and negative feedbacks associated with microclimate and herbivory, respectively. To date, these complex dynamics remain poorly understood in coastal plant communities because field measurements and process-based models that can be used to investigate the combined effects of these abiotic and biotic drivers on vegetation dynamics are still lacking.

In this study, we focus on two California coastal sage scrub (CSS) species, *Artemisia californica* and *Rhus integrifolia*. *R. integrifolia* has increased its cover substantially in southern California from 1931 to 2000 (Taylor 2004). *A. californica* has also been increasing in abundance in some coastal regions of California even though the fire regime has remained relatively unaltered over the last five centuries (Taylor 2004). The decrease in overall extent of the CSS community in which *A. californica* occurs, however, has been documented in California as a result of land use change (Pratt and Mooney 2013). Both species are drought-tolerant but cold-sensitive, and their latitudinal ranges are primarily limited by cold spells (Moreno and Oechel 2012). Climate warming has been considered as one of the major drivers of the northward expansion of CSS species (Taylor 2004, Riordan and Rundel 2014). Long-term climate data suggest the occurrence of significant warming trends in nocturnal winter conditions at field sites close to the northern limits of these two shrub species (both $P < 0.047$, Figure 1). We use a combination of experimental and modelling approaches to assess the microclimate warming effects induced by woody canopies, identify the cold tolerance thresholds of these two shrub species, and quantitatively investigate the coupled effects of regional climate change, vegetation-microclimate feedbacks and herbivory on ecosystem stability and resilience in coastal plant communities. We also apply our model to investigate the stability of mangrove-salt marsh ecotones on the Atlantic coast of Florida as mangroves (*Rhizophora mangle*, *Avicennia germinans*, and *Laguncularia racemosa*) are expanding their distribution as a result of global warming (Cavanaugh et al. 2014).
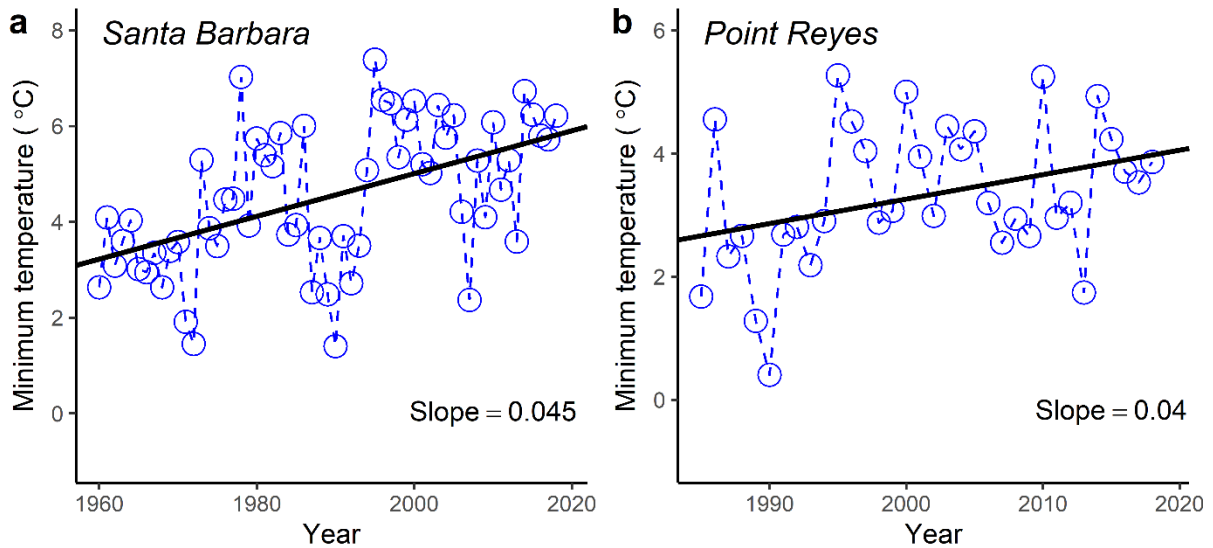
Figure 1. Long term trend in the 30% coldest winter minimum temperatures in Santa Barbara, California from 1960 to 2018 (a) and Point Reyes from 1985 to 2018 (b). The fitted OLS regression lines indicate the significant warming trends at both sites (both $P < 0.047$).

4.3 Materials and Methods

4.3.1 Study system

R. integrifolia is distributed along coastal California from Baja California (Mexico) to Santa Barbara (California, USA) (The Jepson Herbarium at the University of California at Berkeley, http://ucjeps.berkeley.edu). The current geographic distribution of *A. californica* ranges from Northern Baja (Mexico) to Mendocino County (California, USA) (Pratt and Mooney 2013). The study sites are located in Arroyo Hondo Preserve (34°47' N 120°14' W) and Point Reyes National Seashore (37°55' N, 122°44' W), which are close to the northern limits of the observed range of *R. integrifolia* and *A. californica*, respectively. The Arroyo Hondo Preserve (AHP, Figure 2a) is located along the Pacific coast in Santa Barbara County, California, USA. The mean annual temperature (MAT) is 12°C and the mean annual precipitation (MAP) is 413 mm with nearly 80% falling within the winter growing season (Beighley et al. 2005). The plant community is a mosaic of grassland dominated by e.g. *Bromus* sp. and woodland vegetation. The Point Reyes National Seashore (PRNS, Figure 2b) is a peninsula located in Marin County, California, USA. The MAT is 10°C and MAP is 735 mm. The dominant species in the study site include many grass species such as *Vulpia bromoides* and shrub species including *A. californica*.

4.3.2 Climate warming and microclimate effects

We used long-term climate data for locations in the proximity of the Arroyo Hondo Preserve (i.e., meteorological records from Santa Barbara, NOAA National Climatic Data Center) and Point Reyes (i.e., at Point Reyes Station, based on PRISM Climate Group data [2019]) to analyze the general trend in minimum temperatures in southern and northern California, respectively. To assess the effect of woody cover on microclimate, we monitored the paired local temperatures from November 2018 to March 2019 in shrub thickets and adjacent open grassland. Specifically, four locations were randomly selected at each study site in the proximity to the shrub-grass ecotone. At each location, one temperature sensor (HOBO® U23-003 by Onset, Bourne,

Massachusetts, USA) was deployed 20 cm above the ground level under the shrub canopy and one deployed at the same height in adjacent open canopy areas 3 m from the shrub patch to record the half-hourly air temperature. All sensors were previously tested in the lab to verify the consistency of temperature measurements among sensors.

Figure 2. The two field sites in this study: Arroyo Hondo Preserve (a) and Point Reyes field station (b). The seedlings were transplanted both beneath shrub canopies (c) and in adjacent grassland (d) at Arroyo Hondo to investigate the microclimate impacts on seedling growth.

4.3.3 Seedling transplant experiment

We conducted a seedling transplant experiment in shrub and grass patches at AHP to investigate the extent to which the presence of a shrub canopy affects the survival and growth of shrub seedlings as a result of microclimate modifications and browsing (Figure 2c, d). Seedling transplants at PRNS are prohibited by National Park Service. Two microsites, one under the shrub canopy and one in the adjacent open canopy area were randomly selected at each of the four ecotones instrumented with temperature sensors. Four to five-month old *R. integrifolia* seedlings ($n = 80$) of similar size were purchased on November 15, 2018 from a nearby nursery (Santa Barbara Natives Inc.) where climate conditions are similar to the field site. Ten seedlings were transplanted in each microsite and watered to avoid initial water stress. The seedling height was recorded for each shrub seedling immediately after the transplantation. On December 28, we tracked the height and the existence of freeze damage for each of the surviving seedlings in each plot. The existence of black spotting or foliar necrosis on shrub leaves was considered as a sign of freeze-induced injury. The aboveground biomass of every seedling was harvested on March

15, 2019 after determining the final seedling height and whether seedlings suffered from freeze damage. Plant samples were then dried at 65°C for 72 h to measure aboveground dry biomass.

4.3.4 Freezing experiment

We conducted a freezing experiment to assess the physiological response of *A. californica* and *R. integrifolia* to low temperature treatments and evaluate how that response is affected by acclimation to asymmetric climate warming for 3 months prior to freezing. The term 'asymmetric warming' is here used to refer to a warming treatment in which the temperature is increased with respect to control (i.e., no acclimation) conditions more at night than during the day. We only investigated the cold sensitivity of shrub species because in the two study sites the dominant grass species are more tolerant to cold stress than shrubs. For example, *Stipa pulchra*, a grass species that coexists with *R. integrifolia* in AHP, also appears abundantly in northern California where it may survive extreme cold events with temperatures as low as -15°C. Seedlings of *A. californica* ($n = 48$) and *R. integrifolia* ($n = 48$) were purchased from a nursery and 24 seedlings of each species were randomly placed into each of the two growth chambers for a three-month acclimation period. Each chamber had different temperature conditions, based on the average of winter temperatures at AHP and Point Reyes Station: one chamber with 18°C/5°C daytime/nighttime temperatures to reflect the current climate scenario and one with 20°C/9°C to simulate future asymmetric warming scenario. The light intensity was set to 800 umol m^{-2} s^{-1} photosynthetic active radiation (PAR) from 7 am to 7 pm. Plants were watered based on the mean growing season precipitation at AHP (330 mm) and PYNS (402 mm), respectively. After acclimation, the volumetric soil water content was measured in pots of both species and temperature treatments with five replicates using a soil moisture sensor (Waterscout SMEC300, Spectrum Technologies Inc., Plainfield, IL, USA). Plant individuals ($n = 4$ per each species from each chamber) were then assigned to one of five freezing temperature treatments (-2°C, -4°C, -6°C, -8°C and -10°C) and maintained for 3 h in a low-temperature 815 Precision Incubator (Thermo Scientific, Waltham, MA). Immediately after the freezing treatment, shrubs were gradually warmed to 5°C at rates of ~0.12°C min^{-1} and maintained at that temperature for 1 h. The remaining shrubs served as the control group without freezing treatment and were maintained under 5°C for 4 h before measurement. Plants were removed from the incubator and three branch samples were cut from each shrub individual and defoliated using a razor blade under distilled water to avoid cavitation. The xylem hydraulic conductivity was then measured immediately using a hydraulic conductivity apparatus (Sperry et al. 1988, Kolb et al. 1996). The branch sample was attached to the tubing system filled with 20 mmol/L KCl solution and then enclosed within a vacuum canister. The vacuum pressure drove the solution through the xylem from the beaker on an analytical balance (Acculab ALC-80.4; Sartorius Corp., Bohemia, NY, USA) and the mass flow rate was recorded. The hydraulic conductivity (k_h, kg m s^{-1} MPa^{-1}) was calculated as the slope of the change in mass flow rate through the stem segment over the change in vacuum pressure gradient. The xylem specific hydraulic conductivity (k_s, kg m^{-1} s^{-1} MPa^{-1}) was determined by dividing k_h by the branch cross-sectional area with pith area excluded.

4.3.5 Modelling framework

We developed a minimal process-based modelling framework to investigate how climate warming, vegetation-microclimate feedbacks and browsing can lead to the emergence of alternative stable states in coastal ecosystems. The change rate in normalized woody plant cover (S_n) can be modelled as the result of a logistic growth and mortality from freezing stress and

browsing (D'Odorico et al. 2013, Huang et al. 2018)

$$\frac{d(S_n)}{dt} = \alpha S_n(1-S_n) - \beta f(T_{min})S_n - c\frac{(S_n)^2}{(S_n)^2+1},$$ (1)

where $S_n = S/S_c$, S is the woody plant cover per unit area, and S_c is the carrying capacity of woody plant cover, α (time^{-1}) is the intrinsic increase rate of woody cover, β (time^{-1}) is the maximum mortality rate of woody plants resulting from cold sensitivity, and c is the maximum browsing pressure. To account for the stronger browsing-induced disturbance observed under the canopies of *R. integrifolia*, the browsing pressure is expressed as the product of c by a nonlinear term (Noy-Meir 1975, May 1977). We assume that *A. californica* shrubs may also be browsed by herbivores (Genin and Badan-Dangon 1991), even though the volatile chemicals produced by their leaves may decrease their attractiveness to herbivores. The negative impact of extreme low temperatures on woody plant growth is modelled by the function $f(T_{min})$ characterizing the shrub response to T_{min}, the minimum near surface temperatures within woody plant thickets (Figure 3)

$$f(T_{min}) = \frac{1}{2} - \frac{1}{2}\tanh\left(\frac{T_{min}-\overline{T}}{k(T_1-T_2)}\right),$$ (2)

where T_1 and T_2 are two critical temperature values defining the species-specific cold sensitivity of woody plants, $\overline{T} = (T_1+T_2)/2$, and k is a parameter determining the rate of convergence of $f(T_{min})$ from 0 to 1. T_1 is the temperature when woody plants start to experience a reduction in the xylem's hydraulic conductivity and T_2 is the temperature when a nearly complete loss of xylem hydraulic conductivity occurs. The existence of woody cover can create a warming effect leading to an increase in T_{min} compared with local background minimum temperature (T_b) without woody cover (Hayden 1998, He et al. 2010). The magnitude of this local warming effect depends on woody plant cover S_n and can be expressed as (D'Odorico et al. 2013, Huang et al. 2018)

$$T_{min} = T_b + \Delta T_{max}S_n,$$ (3)

where $\triangle T_{max}$ denotes the maximum warming effect when S reaches its carrying capacity (i.e., $S_n = 1$).
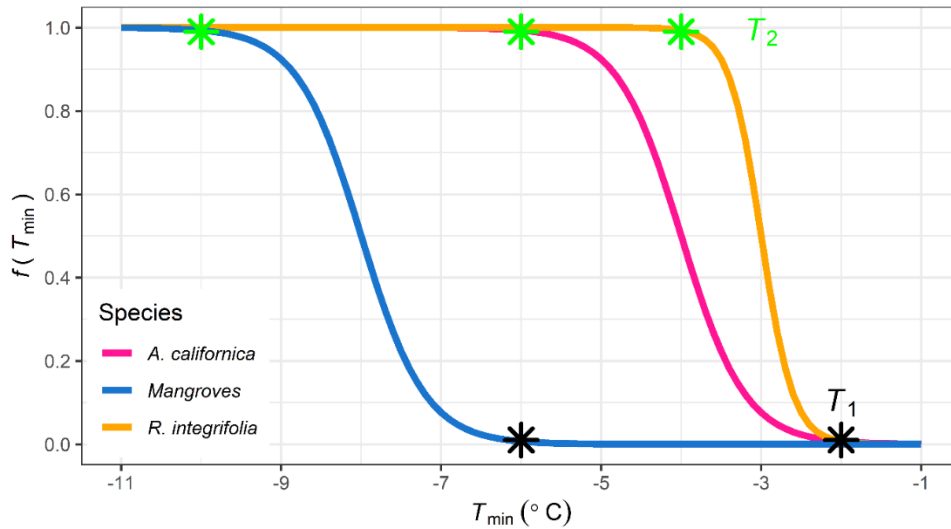

Figure 3. The mortality rate of woody plants as a function of the minimum temperature within shrub thickets (T_{min}). T_1 and T_2 are two critical temperatures defining the species-

73

specific cold sensitivity of woody plants. See Eq. 2 and its description for the details. The values of T_1 and T_2 were estimated based on the results of freezing experiments.

We set $\alpha = 0.5$ year^{-1} and $\beta = 10$ year^{-1} according to previous work (Huang et al. 2018) to reflect the fact that the establishment of a full shrub thicket typically takes two to three decades while the collapse in shrub density from a full cover state due to cold-induced shrub mortality can occur within a few years when temperature consistently reaches values lower than T_2. We should note that the model results were qualitatively not sensitive to different parametrizations of α and β. We set $T_1 = -2°C$ and $T_2 = -6°C$ for *A. californica* and $T_1 = -2°C$ and $T_2 = -4°C$ for *R. integrifolia* respectively, based on results from the freezing experiment. We extracted the 20% coldest nights to determine the maximum warming effect that shrub canopy can induce (i.e., $\triangle T_{max}$). According to the temperature data, $\triangle T_{max}$ was 1.75°C for *A. californica* and 2.15°C for *R. integrifolia*. We simulated scenarios with different c values (0, 0.5, 1, and 5) to examine to what extent ecosystem stability is sensitive to the strength of browsing pressure. The equilibrium states of woody vegetation dynamics were identified by (i) first inserting Eqs. 2 and 3 into Eq. 1 and (ii) setting $\dfrac{dS_n}{dt} = 0$ under varying conditions of T_b and c.

Mangroves such as *Rhizophora mangle* (red mangrove), *Avicennia germinans* (black mangrove), and *Laguncularia racemosa* (white mangrove) have been encroaching into the adjacent salt marsh areas along the Atlantic coast of Florida, USA (Cavanaugh et al. 2014). The increase in minimum temperatures has been suggested to be the major driver of the expansion of these cold-intolerant woody species (Osland et al. 2017). This phenomenon can be further sustained and entrenched by the microclimate warming effects associated with the establishment of mangrove canopies (D'Odorico et al. 2013). Here we apply the modelling framework to investigate whether and to what extent the vegetation-microclimate feedbacks can lead to the emergence of bistability and critical transitions in mangrove-salt marsh ecotones. In the case of mangroves, we set $T_1 = -6°C$, $T_2 = -10°C$ and $\triangle T_{max} = 3.24°C$ based on empirical data from the literature (Cavanaugh et al. 2014, Devaney et al. 2017). The main variables and parameters in the modelling framework were summarized in Table 1.

Table 1. Summary of main variables and parameters in the modelling framework.

	Symbol	Default value
Variables		
Woody plant cover	S	
Minimum temperature within woody thickets	T_{min}	
Background minimum temperature without woody cover	T_b	
Maximum herbivory pressure	c	
Parameters		
Intrinsic increase rate of woody cover	α	0.5 year^{-1}
Maximum woody plant mortality rate due to cold sensitivity	β	10 year^{-1}
Carrying capacity of woody plant cover	S_c	1

Parameter determining the rate of convergence of $f(T_{min})$ from 0 to 1	k	0.2
Critical temperature at which woody plant mortality starts to occur	T_1	-2°C (*A. californica*) -2°C (*R. integrifolia*) -6°C (mangroves)
Critical temperature resulting in complete mortality of woody plants	T_2	-6°C (*A. californica*) -4°C (*R. integrifolia*) -10°C (mangroves)
Maximum warming effect of woody canopy	$\triangle T_{max}$	1.75°C (*A. californica*) 2.15°C (*R. integrifolia*) 3.24°C (mangroves)

4.3.6 Statistical analyses

The nighttime (from 8 pm to 6 am) temperatures were extracted to calculate the nightly mean temperature in shrub thickets and in adjacent open canopy areas. The difference in mean temperatures between shrubland and grassland was tested using the Student's *t*-test ($\alpha = 0.05$). The relationship between the nighttime temperature difference between shrubland and adjacent grassland and the minimum temperature in grasslands was fitted by standardized major axis (SMA) regression using lmodel2 function in lmodel2 package (Legendre 2014) given that both variables may contain measurement errors. The effects of freezing treatments and warming acclimation as well as their interactions on xylem specific hydraulic conductivity were analyzed using the linear mixed-effects models through lmer function in lme4 package (Bates et al. 2015) and pairwise comparisons were conducted using Tukey's HSD test through TukeyHSD function in stats package ($\alpha = 0.05$). The Student's *t*-test ($\alpha = 0.05$) was used to detect the significance of the difference in soil moisture of pots in control and warming treatments. The mean seedling height and above-ground biomass of individual seedlings growing under shrub canopies and in grassland areas were calculated for each of the eight plots (microsites) and then compared using the Student's *t*-test ($\alpha = 0.05$) to avoid pseudo-replication. The difference in the proportion of damaged seedlings was determined using generalized linear model (GLM) regression through glm function in in stats package. All the analyses were conducted in R (R Core Team 2018).

4.4 Results

4.4.1 Microclimate warming effects of woody cover

We found empirical evidence of reduced freezing stress underneath the shrub canopies of both *A. californica* and *R. integrifolia*. At both the Arroyo Hondo site near the northern range edge of *R. integrifolia* and the Point Reyes site near the northern boundary of *A. californica*, grasslands experienced multiple freeze events (nine freezing nights at Arroyo Hondo and six at Point Reyes) while the understory of shrub thickets experienced none (Figure 4a, d). Both minimum and mean nightly temperatures were significantly higher within the shrub thickets than in adjacent grassland areas throughout the winter season at both sites (Tukey HSD test, all $P < 0.001$). Notably, during the coldest nights when shrubs are most vulnerable to freeze damage (nights with 20% lowest minimum temperatures), the minimum temperature was on average 2.15°C and 1.75°C higher within shrub thickets than in adjacent grassland areas at Arroyo Hondo and Point Reyes, respectively (Tukey HSD test, both $P < 0.001$, Figure 4b, e), suggesting the occurrence of an ecologically important microclimate modification by shrub cover. Furthermore, a stronger shrub-induced warming occurred during colder nights at both field sites (Figure 4c, f).
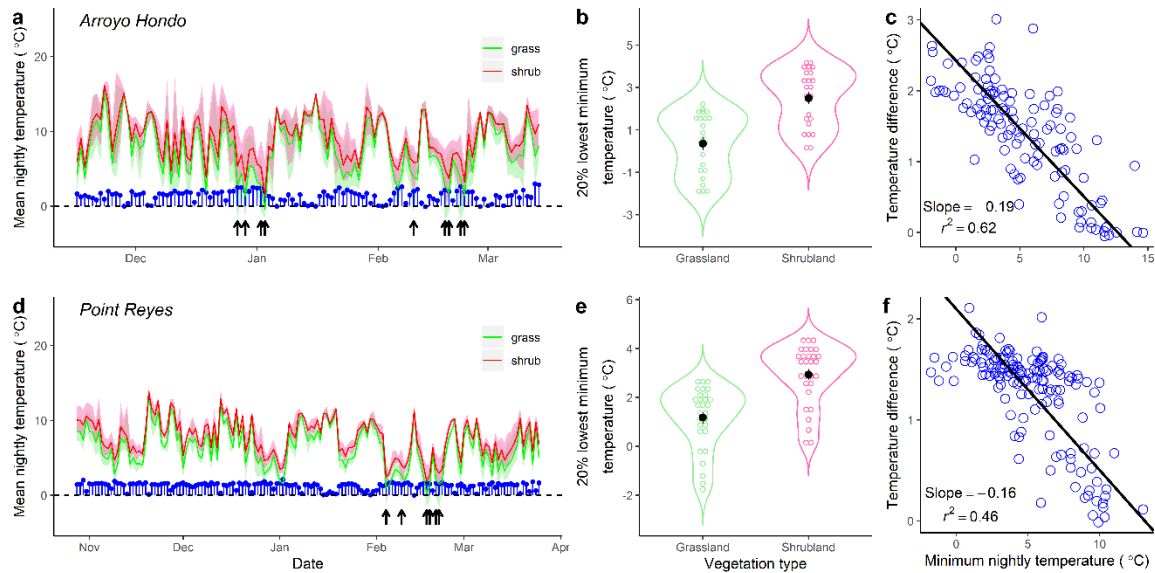
Figure 4. Local temperature difference between shrubland and grassland during cold season. (a) and (d), mean (line), maximum and minimum (shaded) nightly temperatures within shrub thickets (T_{shrub}, pink) and in open grassland (T_{grass}, green) at Arroyo Hondo Preserve and Point Reyes field station, respectively. Blue points represent the nightly temperature difference ($T_{\text{shrub}} - T_{\text{grass}}$) and black arrows indicate the freezing events documented in grassland. (b) and (e), violin plots showing the 20% lowest minimum nightly temperatures between two microsites at the two field sites, respectively. Black points represent the mean value and error bars indicate one standard error. (c) and (f), the relationship between nightly temperature difference ($T_{\text{shrub}} - T_{\text{grass}}$) and minimum nightly temperature in grassland at the two field sites, respectively.

4.4.2 Seedling growth underneath shrub canopy versus in open grassland
A seedling transplant experiment underneath versus outside of shrub canopies confirmed the importance of shrub microclimate warming. A significant lower percentage of transplanted *R. integrifolia* seedlings suffered from freeze damage (see Methods) under shrub canopies (27.5%) than in adjacent grassland areas (65%, GLM, deviance = 11.60, $P < 0.001$, Figure 5a). However, seedlings beneath shrubs had significantly lower mean aboveground biomass (0.78 g) and height (2.71 cm) at the end of the growing season than seedlings in grassland (9.87 g and 31.16 cm respectively, Tukey HSD test, both $P < 0.001$, Figure 5b, c). The reduced seedling biomass under shrub canopies is likely due to the consumption of above-ground biomass by herbivores such as dusky-footed woodrats (*Neotoma fuscipes*) and lagomorphs which are known to be present in Arroyo Hondo Preserve. Indeed, consistent physical damage to the seedlings (loss of foliage and chewed stems) was widely observed in seedlings transplanted under shrub canopies compared to seedlings transplanted in the open grassland (Huang, pers. obs.).
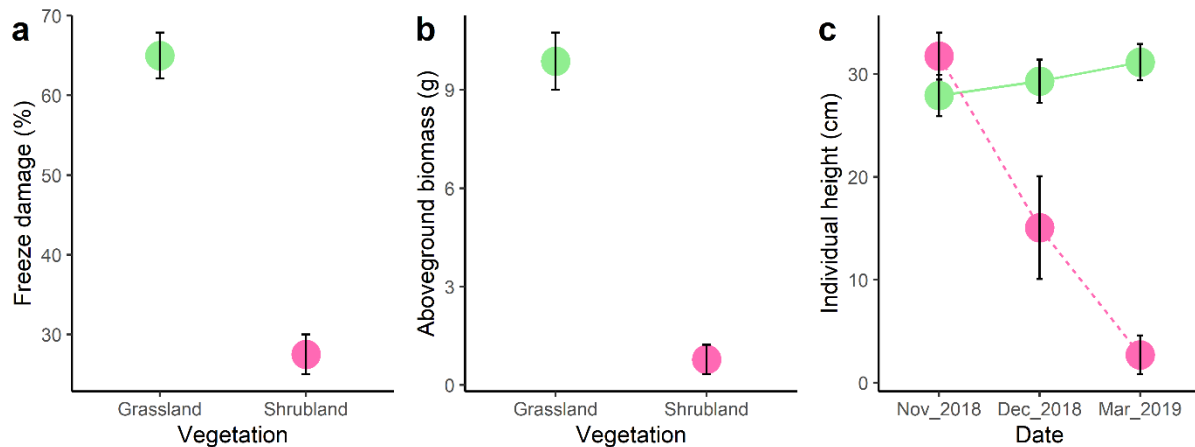
76

Figure 5. Seedling growth of *R. integrifolia* during winter growing season under shrub canopy versus in open grassland. (a), the percentage of transplant seedlings experiencing freeze-induced damage. (b), the mean individual aboveground biomass of transplanted seedlings. (c), the changes in mean individual height of transplanted seedlings underneath shrub canopy (pink) and in open grassland (green) across the winter season. Error bars indicate one standard error of the mean.

4.4.3 Hydraulic vulnerability of shrub seedlings to freezing temperatures

The xylem specific hydraulic conductivity (k_s) of both shrub species showed a decrease with increasing freezing stress (Figure 6). Under the current climate scenario, *A. californica* and *R. integrifolia* lost 51.6% and 53.8% of k_s, respectively, when freezing temperature dropped from 5°C to -2°C and 86.3% and 96.2% of k_s, respectively, when air temperatures dropped from 5°C to -10°C (Tukey HSD test, all $P < 0.001$). Likewise, shrubs acclimated under warmer conditions exhibited similar declining trends in k_s with decreasing freezing temperatures. For example, the k_s of *A. californica* and *R. integrifolia* decreased by 48.3% (78.1%) and 35.1% (95.2%), respectively, when temperature cooled from 5°C to -2°C (-10°C) (Tukey HSD test, all $P < 0.018$). Interestingly, warm-acclimated plants of both species had lower k_s when above freezing, but converged on equally low k_s values as unacclimated plants once frozen. The linear mixed-effects model results indicated that the freezing treatment, warming acclimation and their interactions all had significant effects on k_s of both species (all $P < 0.018$, Table 2).

Table 2. Results of the linear mixed-effects model evaluating the effects of freezing treatment, warming acclimation and their interactions on the xylem-specific hydraulic conductivity of *A. californica* and *R. integrifolia*.

Source	χ^2	df	*P* value
A. californica			
Freezing treatment	678.42	5	< 0.001
Acclimation	22.77	1	< 0.001
Freezing treatment × Acclimation	37.10	5	< 0.001
R. integrifolia			

77

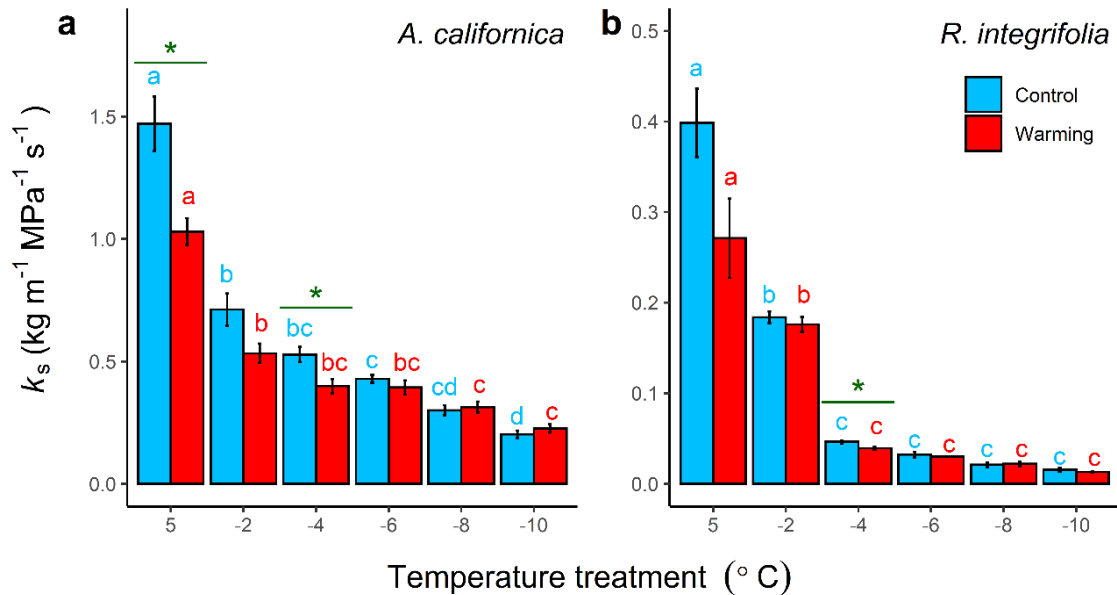|			
Freezing treatment	1159.72	5	< 0.001
Acclimation	12.37	1	< 0.001
Freezing treatment × Acclimation	44.77	5	< 0.001

Figure 6. Xylem-specific hydraulic conductivity (k_s) of *A. californica* (a) and *R. integrifolia* (b) in response to freezing temperatures. Shrub seedlings were grown under both control (18°C/5°C daytime/nighttime temperatures) and warming conditions (20°C/9°C) for three months before freezing treatments and measurements. Error bars indicate one standard error of the mean. Different letters indicate significant differences ($P < 0.05$) among temperature treatments in control and warmed groups, respectively. Asterisk indicates a significant difference ($P < 0.05$) between control and warmed groups under a given freezing temperature treatment.

4.4.4 Abiotic and biotic controls of ecosystem stability

The modelling results show that woody vegetation dynamics may be bistable within a range of minimum background temperatures (i.e., temperature in the absence of woody canopies, T_b) (Figure 7). For example, the system is stable only with no woody cover when the browsing pressure $c = 0$ and T_b is lower than roughly -3.5°C for *A. californica*, -4°C for *R. integrifolia* and -9°C for mangroves; while the system has only one stable state with woody cover when T_b exceeds a critical threshold (about -3°C for *A. californica*, -2.5°C for *R. integrifolia* and -7°C for mangroves). When T_b falls between the above two critical temperatures, the system is bistable such that it can be stable both with grass cover and colder nocturnal microclimate and with woody cover and warmer nights. As T_b increases as a result of climate warming, the system may shift in a relatively discontinuous way to the woody stable state. The bistable dynamics are also dependent on browsing pressure (c) on woody plants, which affects the size of the basin of attraction, hence the resilience or the capacity of the system to withstand disturbances without

changing the basin of attraction (Holling 1973, Scheffer et al. 2001). Figure 7 shows that, as expected, both the woody cover and its resilience decreased with increasing browsing pressure (c), indicating that the system is less prone to woody plant encroachment.
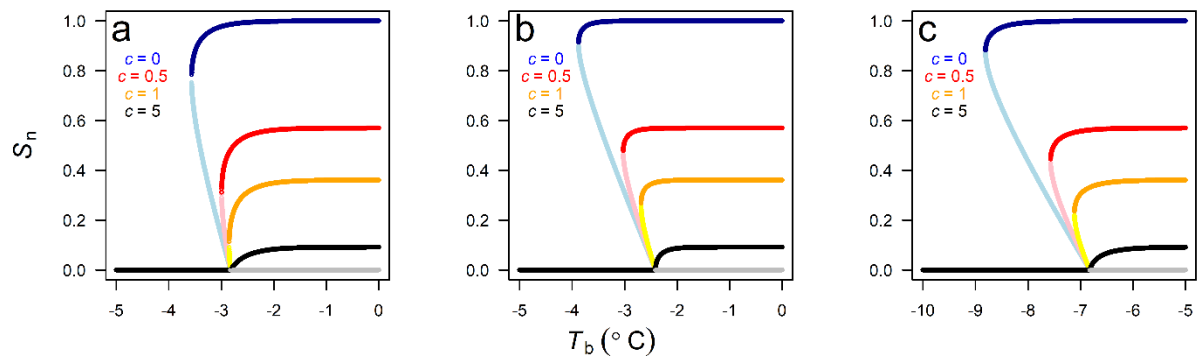

Figure 7. Bistability of woody vegetation dynamics induced by vegetation-microclimate feedbacks. (a) *A. californica* at Point Reyes field station; (b) *R. integrifolia* at Arroyo Hondo Preserve; and (c) mangroves (*Laguncularia racemose*, *Rhizophora mangle* and *Avicennia germinans*) on the Atlantic coast of Florida. This figure shows how sensitive the normalized woody plant density (S_n) is to background temperature (T_b) under different browsing pressures denoted by c. For example, around the temperature transition zone of about -7°C, a small increase in T_b can lead to transition from salt marsh to a stable mangrove cover. Stable states are indicated by horizontal blue, red, orange and black lines while unstable states are indicated by vertical light blue, pink, yellow and grey lines.

4.5 Discussion

The existence of vegetation canopy cover can significantly alter local-scale biophysical processes such as heat transfer and radiative cooling, and further affect microclimate conditions including near-surface temperature and humidity (Geiger 1965, Bonan 2008, Li et al. 2015). Our study shows the occurrence of a significant local warming effect induced by the presence of woody cover. The local temperature in the coldest nights (20% lowest quintile) was nearly 2°C higher in shrub thickets than in adjacent grassland areas both in *R. integrifolia*-grass ecotones in southern California and in *A. californica*-grass ecotones in northern California. Previous studies have found a similar warming effect of ~3°C in mangrove patches that are expanding along the Atlantic coast of Florida (Devaney et al. 2017), and ~2°C in shrub canopies that have spread on the barrier islands of Virginia (Huang et al. 2018), indicating that this microclimate feedback may exist in many coastal woodland-grassland ecotones where freezing stress occurs and limits woody encroachment. The degree of this warming effect may primarily depend on elements of canopy structure such as canopy density or leaf area index because the presence of the woody canopy reduces the rate of radiative cooling at night (He et al. 2010), although other factors such as the background environmental conditions such as temperature and wind speed can also be important. This microclimate warming can play a crucial role in maintaining shrub physiological functions when minimum temperatures are near the freezing point (Figure 6). For example, it significantly reduced the probability of freeze-induced damage in shrub seedlings growing beneath woody canopies with respect to those in open grassland areas. Therefore, the local vegetation-microclimate feedback can act as a more immediate mechanism for woody plant encroachment in many ecotones. Moreover, it can lead to the emergence of important non-linear behaviors as shown by the model simulations.

Both *A. californica* and *R. integrifolia* experienced a significant decline (51.6% and 53.8%, respectively in control/no acclimation treatment, and 48.3% and 35.1% under warming acclimation) in xylem hydraulic conductivity when temperature decreased from 5°C to -2°C, suggesting that these species exhibit a strong cold sensitivity. The warming acclimation significantly increased shrubs' vulnerability to hydraulic failure by significantly reducing the hydraulic conductivity (with respect to non-acclimated individuals) at higher freezing temperatures but no significant differences in hydraulic conductivity were found between warm-acclimated and non-acclimated shrubs under more extreme freezing stress (Figure 6). In contrast to previous work showing that drought may increase cold tolerance of woody plants (Medeiros and Pockman 2011), we found a warming-induced decline in hydraulic conductivity, which can be explained as the effect of water stress (e.g., from drought-induced cavitation). The significant interactive effects of warming and freezing treatment were confirmed by the linear mixed-effects model analysis (Table 2). The occurrence of drought stress under warming is evidenced by the significantly lower soil moisture found in warm-acclimated pots than in the control group for both *A. californica* (5.1% versus 7.7%, respectively, $t = 4.15$, $P = 0.001$) and *R. integrifolia* (9.0% versus 12.6%, respectively, $t = 5.00$, $P < 0.001$).

The significantly reduced biomass and consistent physical damage under woody canopies are primarily attributed to browsing rather than other factors such as shading and resource competition (i.e., seedlings appeared damaged rather than merely suppressed), although these factors can also alter seedling growth dynamics. The effect of shading on seedling growth highly depends on the shade tolerance of the specific woody species. For example, the shading effect of mangrove canopies may contribute to the mortality of white mangrove seedlings, but it is not likely to affect the growth of red and black mangrove seedlings due to their higher shade tolerance (Devaney et al. 2017). In the Arroyo Hondo Preserve the browsing-induced loss in shrub seedling biomass may come from small mammals such as dusky-footed woodrats and lagomorphs that probably prefer to forage within shrub thickets to avoid predators. The higher woody seedling biomass consumption by herbivores in woodland compared to grassland was also observed at mangrove-salt marsh ecotones on the Atlantic coast of Florida (Devaney et al. 2017). Therefore, the positive vegetation-microclimate feedback may be counteracted by browsing. In addition, woody plant encroachment and critical transitions from grassland to woodland are less likely to occur if the browsing pressure is extremely intense ($c = 5$, Figure 7) which directly causes a substantial reduction in woody biomass. Therefore, woody vegetation dynamics are controlled by complex interactions between abiotic factors (e.g., microclimate) and biotic drivers (e.g., browsing) (Figure 8). We should note that in the modeling framework we have assumed that woody plants have competitive advantages over grasses and the only factor limiting woody plant expansion in these ecotones is cold stress. Therefore, a loss of grass biomass from grazing would have minimal effects on woody cover change. However, the presence or absence of grasses is known to affect shrubs through the dynamics of fire (Holdo et al. 2009), which is not explicitly accounted for in this study partially because (i) this indirect effect of grass biomass on woody vegetation dynamics is site-specific and relatively difficult to quantify; and (ii) some woody species such as *R. integrifolia* are relatively fire resistant and can resprout after fire events.
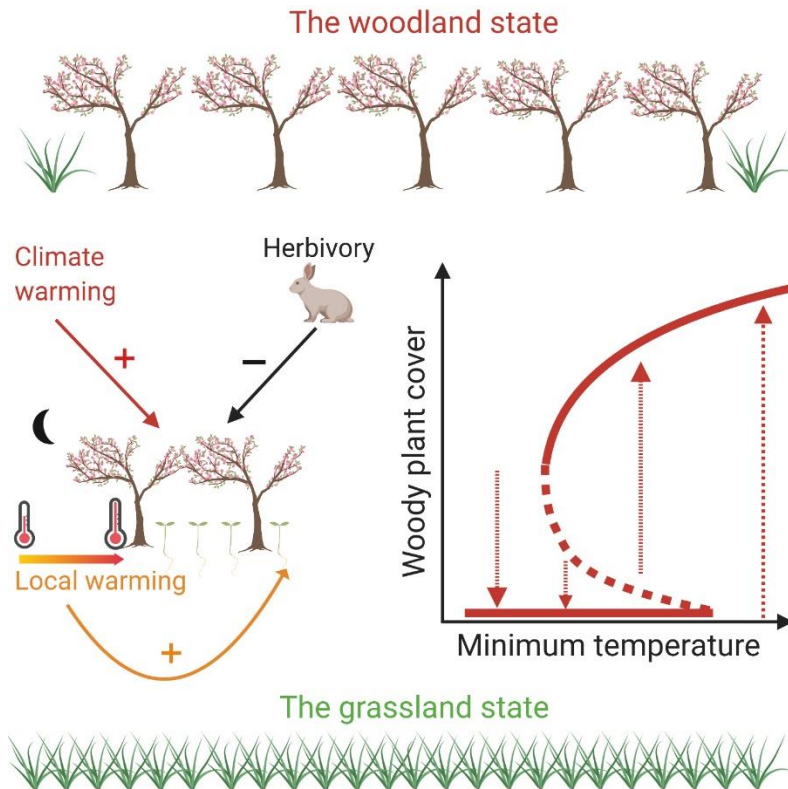
Figure 8. Woody plant encroachment affected by exogenous drivers (climate warming and browsing) and the positive vegetation-microclimate feedbacks.

Mangroves in coastal ecosystems along the Atlantic coast of Florida can increase the nocturnal minimum temperatures by about 3°C on coldest nights (Devaney et al. 2017). Moreover, biogeographical studies have shown that the mangrove cover declined by nearly 25% when minimum temperature drops below -6°C while there was almost no mangrove cover when the minimum temperature reaches -10°C (Cavanaugh et al. 2014). Our modelling analysis shows that the vegetation can shift from the stable salt marsh state to another stable state with full mangrove cover when minimum temperature exceeds -7°C (Figure 7c), although browsing may reduce the resilience of mangrove vegetation. For instance, previous work has documented the severe damage of crab (*A. pisonii*) herbivory to mangrove leaves (Devaney et al. 2017). Our model prediction shows a remarkable agreement with empirical observations that North American mangroves may establish in areas where the minimum temperature exceeds -7.1°C (Osland et al. 2017). This nonlinear transition may also occur in many other mangrove-salt marsh ecotones worldwide including those existing in South America, Southeast Africa, Eastern Asia and New Zealand, where the latitudinal limits of mangrove distribution is primarily controlled by minimum temperatures (Osland et al. 2017). Our analysis of vegetation dynamics at these ecotones suggests that the widely observed poleward expansion of mangroves is likely to continue under global warming with local non-linear changes or tipping points in response to increasing temperatures and has important impacts on the structure, functioning, and resilience of coastal ecosystems (Cavanaugh et al. 2014, Guo et al. 2017).

Vegetation-microclimate feedbacks have been proposed as an important mechanism sustaining woody plant encroachment in many woodland-grassland ecotones worldwide, including the

displacement of alpine meadow by forests and shrub encroachment into arid grasslands (D'Odorico et al. 2013). Our study suggests that woody plant encroachment and vegetation type transitions in some coastal ecosystems can also be enhanced by the mitigation of local temperature regimes through positive feedbacks between woody canopy and the physical environment, although biotic factors such as browsing may counteract the effect of this local warming feedback. Climate warming, which is expected to continue (with increasing magnitude) in the next several decades (IPCC 2014), will likely facilitate the expansion of woody plants in cold-limiting regions. This non-linear and often highly irreversible transition in vegetation type has significant influences on ecological and hydrological processes across scales and further impacts ecosystem functioning and services in ways both positive and negative for human society. For example, woody plant encroachment may potentially enhance carbon and nutrient storage and can increase vegetation biomass and productivity, which increases the wave attenuation capacity of coastal ecosystems (Kelleway et al. 2017). Specifically, the existence of mangroves can lead to greater sediment accretion and organic matter accumulation thereby increasing surface elevations and the system's resilience in response to sea level rise and storm disturbances (Saintilan et al. 2014). However, in some cases shrub encroachment in coastal zones may also cause shoreline erosion in the long term by blocking sediment transport in barrier islands (Zinnert et al. 2016, 2017). Furthermore, woody plant expansion can result in a substantial loss in plant diversity (Ratajczak et al. 2012), create a more unsuitable habitat for fauna adapted to open canopy areas, and lead to the loss of the associated ecosystem services (Kelleway et al. 2017). Therefore, depending on the specific system, this transition in plant dominance can be viewed either as a positive or a negative change (Eldridge et al. 2011). Ecosystem bistability often involves hysteresis such that the ecosystem's reversal to the original state requires additional changes in external forcing, which adds significantly to the difficulties of ecological restoration and environmental management (Scheffer and Carpenter 2003).

Our findings suggest that climate warming may induce a non-linear shift in some coastal ecosystems from a stable state without woody cover to a stable state with woody plant dominance through vegetation-microclimate feedbacks. Interestingly, our results show that seedlings growing under shrub canopies experienced significantly less freeze damage but were at a higher risk of browsing damage. Our model identifies a threshold nocturnal temperature i.e., -2.5°C and -3°C for shrubland-grassland ecotones in southern and northern California as well as -7°C for mangrove-salt marsh ecotones along the Atlantic coast of Florida above which a critical transition to woodland may occur. Therefore, this study highlights how the complex interactions of large-scale drivers (i.e., climate warming) and local abiotic and biotic feedbacks may induce critical transitions to a state with woody plant dominance, although other variables such as soil nutrients, water availability, fire management, and land use change may also regulate woody vegetation dynamics in these ecosystems. Such a transition may be widespread, involving different woody plant species across a variety of coastal regions where the latitudinal limits of woody plants are majorly constrained by cold stress.

4.6 References

Anderies, J. M., M. A. Janssen, and B. H. Walker. 2002. Grazing, management, resilience and the dynamics of a fire-driven rangeland system. Ecosystems 5:23–44.

Archer, S., D. S. Schimel, and E. A. Holland. 1995. Mechanisms of shrubland expansion: land use, climate, or carbon dioxide. Climatic Change 29:91–99.

Bates, D., M. Mächler, B. M. Bolker, and S. C. Walker. 2015. Fitting linear mixed-effects models using lme4. Journal of Statistical Software 67:1–48.

Beighley, R. E., T. Dunne, and J. M. Melack. 2005. Understanding and modeling basin hydrology: Interpreting the hydrogeological signature. Hydrological Processes 19:1333–1353.

Bestelmeyer, B. T., A. J. Tugel, G. L. Peacock, D. G. Robinett, P. L. Shaver, J. R. Brown, J. E. Herrick, H. Sanchez, and K. M. Havstad. 2009. State-and-transition models for heterogeneous landscapes: a strategy for development and application. Rangeland Ecology and Management 62:1–15.

Bonan, G. B. 2008. Forests and climate change: forcings, feedbacks, and the climate benefits of forests. Science 320:1444–1449.

Buchner, O., and G. Neuner. 2011. Winter frost resistance of *Pinus cembra* measured in situ at the alpine timberline as affected by temperature conditions. Tree Physiology 31:1217–1227.

Cavanaugh, K. C., J. R. Kellner, A. J. Forde, D. S. Gruner, J. D. Parker, W. Rodriguez, and I. C. Feller. 2014. Poleward expansion of mangroves is a threshold response to decreased frequency of extreme cold events. Proceedings of the National Academy of Sciences 111:723–727.

Chen, I.-C., J. K. Hill, R. Ohlemuller, D. B. Roy, and C. D. Thomas. 2011. Rapid range shifts of species associated with high levels of climate warming. Science 333:1024–1026.

Devaney, J. L., M. Lehmann, I. C. Feller, and J. D. Parker. 2017. Mangrove microclimates alter seedling dynamics at the range edge. Ecology 98:2513–2520.

D'Odorico, P., J. D. Fuentes, W. T. Pockman, S. L. Collins, Y. He, J. S. Medeiros, S. De Wekker, and M. E. Litvak. 2010. Positive feedback between microclimate and shrub encroachment in the northern Chihuahuan desert. Ecosphere 1:1–11.

D'Odorico, P., G. S. Okin, and B. T. Bestelmeyer. 2012. A synthetic review of feedbacks and drivers of shrub encroachment in arid grasslands. Ecohydrology 5:520–530.

D'Odorico, P., Y. He, S. Collins, S. F. De Wekker, V. Engel, and J. D. Fuentes. 2013. Vegetation–microclimate feedbacks in woodland–grassland ecotones. Global Ecology and Biogeography 22:364–379.

Eldridge, D. J., M. A. Bowker, F. T. Maestre, E. Roger, J. R. Reynolds, and W. G. Whitford. 2011. Impacts of shrub encroachment on ecosystem structure and functioning: towards a global synthesis. Ecology Letters 14:709–722.

Fan, Y., X. Y. Li, H. Huang, X. C. Wu, K. L. Yu, J. Q. Wei, C. C. Zhang, P. Wang, X. Hu, and P. D'Odorico. 2019. Does phenology play a role in the feedbacks underlying shrub encroachment? Science of the Total Environment 657:1064–1073.

Gehrig-Fasel, J., A. Guisan, and N. E. Zimmermann. 2007. Tree line shifts in the Swiss Alps: Climate change or land abandonment? Journal of Vegetation Science 18:571–582.

Geiger, R. 1965. The climate near the ground. Fourth edition. Harvard University Press, Cambridge, Massachusetts, USA.

Genin, D., and A. Badan-Dangon. 1991. Goat herbivory and plant phenology in a Mediterranean shrubland of northern Baja California. Journal of Arid Environment 21:113–121.

Guo, H., C. Weaver, S. Charles, A. Whitt, S. Dastidar, P. D'Odorico, J. D. Fuentes, J. S. Kominoski, A. R. Armitage, and S. C. Pennings. 2016. Coastal regime shifts: rapid responses of coastal wetlands to changes in mangrove cover. Ecology 98:762–772.

Harper, J. L. 1977. Population Biology of Plants. Academic Press, London, UK.

Hayden, B. P. 1998. Ecosystem feedbacks on climate at the landscape scale. Philosophical Transactions of the Royal Society B: Biological Sciences 353:5–18.

He, Y., P. D'Odorico, S. F. J. De Wekker, J. D. Fuentes, and M. Litvak. 2010. On the impact of shrub encroachment on microclimate conditions in the northern Chihuahuan desert. Journal of Geophysical Research 115:D21120.

Holdo, R. M., R. D. Holt, and J. M. Fryxell. 2009. Grazers, browsers, and fire influence the extent and spatial pattern of tree cover in the Serengeti. Ecological Applications 19:95–109.

Holling, C. S. 1973. Resilience and stability of ecological systems. Annual Review of Ecology, Evolution, and Systematics 4:1–23.

Huang, H., J. C. Zinnert, L. K. Wood, D. R. Young, and P. D'Odorico. 2018. Non-linear shift from grassland to shrubland in temperate barrier islands. Ecology 99:1671–1681.

Huenneke, L. F., J. P. Anderson, M. Remmenga, and W. H. Schlesinger. 2002. Desertification alters patterns of aboveground net primary production in Chihuahuan ecosystems. Global Change Biology 8:247–264.

IPCC. 2014. Climate change 2014: Synthesis report. Contribution of working groups I, II, and III to the fifth assessment report of the Intergovernmental Panel on Climate Change. Geneva, Switzerland.

Kelleway, J. J., K. Cavanaugh, K. Rogers, I. C. Feller, E. Ens, C. Doughty, and N. Saintilan. 2017. Review of the ecosystem service implications of mangrove encroachment into salt marshes. Global Change Biology 23:3967–3983.

Knapp, A. K., J. M. Briggs, S. L. Collins, S. R. Archer, M. S. Bret-Harte, B. E. Ewers, D. P. Peters, D. R. Young, G. R. Shaver, E. Pendall, and M. B. Cleary. 2008. Shrub encroachment in North American grasslands: shifts in growth form dominance alters control of ecosystem carbon inputs. Global Change Biology 14:615–623.

Kolb, K. J., J. S. Sperry, and B. B. Lamont. 1996. A method for measuring xylem hydraulic conductance and embolism in entire root and shoot systems. Journal of Experimental Botany 47:1805–1810.

Legendre, P. 2014. lmodel2: Model II Regression. R package version 1.7-3.

Li, J., G. S. Okin, L. J. Hartman, and H. E. Epstein. 2007. Quantitative assessment of wind erosion and soil nutrient loss in desert grasslands of southern New Mexico, USA. Biogeochemistry 85:317–332.

Li, Y., M. Zhao, S. Motesharrei, Q. Mu, E. Kalnay, and S. Li. 2015. Local cooling and warming effects of forests based on satellite observations. Nature Communications 6:6603.

Maher, E. L., and M. J. Germino. 2006. Microsite variation among conifer species during seedling establishment at alpine treeline. Ecoscience 13:334–341.

May, R. M. 1977. Thresholds and breakpoints in ecosystems with a multiplicity of stable states. Nature 269:471–477.

Medeiros, J. S., and W. T. Pockman. 2014. Freezing regime and trade-offs with water transport efficiency generate variation in xylem structure across diploid populations of *Larrea* sp. (Zygophyllaceae). American Journal of Botany 101:598–607.

Medeiros, J. S., and W. T. Pockman. 2011. Drought increases freezing tolerance of both leaves and xylem of *Larrea tridentata*. Plant, Cell and Environment 34:43–51.

McKee, K. L., and J. E. Rooth. 2008. Where temperate meets tropical: multi-factorial effects of elevated CO_2, nitrogen enrichment, and competition on a mangrove-salt marsh

community. Global Change Biology 14:971–984.

Moreno, J. M., and W. C. Oechel. 2012. Global change and Mediterranean-type ecosystems. Springer-Verlag, New York, New York, USA.

Myers-Smith, I. H., et al. 2011. Shrub expansion in tundra ecosystems: dynamics, impacts and research priorities. Environmental Research Letters 6:45509.

Noy-Meir, I. 1975. Stability of grazing systems: an application of predator-prey graphs. Journal of Ecology 63:459–481.

Osland, M. J., L. C. Feher, K. T. Griffith, K. C. Cavanaugh, N. M. Enwright, R. H. Day, C. L. Stagg, K. W. Krauss, R. J. Howard, and J. B. Grace. 2016. Climatic controls on the global distribution, abundance, and species richness of mangrove forests. Ecological Monographs 87:341–359.

Pockman, W. T., and J. S. Sperry. 1997. Freezing-induced xylem cavitation and the northern limit of *Larrea tridentata*. Oecologia 109:19–27.

Pratt, J. D., and K. A. Mooney. 2013. Clinal adaptation and adaptive plasticity in *Artemisia californica*: implications for the response of a foundation species to predicted climate change. Global Change Biology 19:2454–2466.

PRISM Climate Group. 2019. http://prism.oregonstate.edu. Oregon State University.

R Development Core Team. 2018. R: a language and environment for statistical computing. R Core Team, Vienna, Austria.

Rango, A., L. Huenneke, M. Buonopane, J. E. Herrick, and K. M. Havstad. 2005. Using historic data to assess effectiveness of shrub removal in southern New Mexico. Journal of Arid Environments 62:75–91.

Ratajczak, Z., J. B. Nippert, and S. L. Collins. 2012. Woody encroachment decreases diversity across North American grasslands and savannas. Ecology 93:697–703.

Ratajczak, Z., S. Carpenter, A. Ives, C. Kucharik, T. Ramiadantsoa, M. Stegner, J. Williams, J. Zhang, and M. Turner. 2018. Abrupt change in ecological systems: inference and diagnosis. Trends in Ecology and Evolution 33:513–526.

Ravi, S., P. D'Odorico, L. Wang, C. S. White, G. S. Okin, S. A. Macko, and S. L. Collins. 2009. Post-fire resource redistribution in desert grasslands: a possible negative feedback on land degradation. Ecosystems 12:434–444.

Riordan, E. C., and P. W. Rundel. 2014. Land use compounds habitat losses under projected climate change in a threatened California ecosystem. PLoS ONE 9:e86487.

Saintilan, N., N. C. Wilson, K. Rogers, A. Rajkaran, and K. W. Krauss. 2014. Mangrove expansion and salt marsh decline at mangrove poleward limits. Global Change Biology 20:147–157.

Sankaran, M., N. P. Hanan, R. J. Scholes, J. Ratnam, D. J. Augustine, B. S. Cade, J. Gignoux, S. I. Higgins, X. Le Roux, and F. Ludwig. 2005. Determinants of woody cover in African savannas. Nature 438:846–849.

Scheffer, M., S. Carpenter, J. Foley, C. Folke, and B. Walker. 2001. Catastrophic shifts in ecosystems. Nature 413:591–596.

Scheffer, M., and S. R. Carpenter. 2003. Catastrophic regime shifts in ecosystems: linking theory to observation. Trends in Ecology and Evolution 18:648–656.

Schlesinger, W. H., A. D. Abrahams, A. J. Parsons, and J. Wainwright. 1999. Nutrient losses in runoff from grassland and shrubland habitats in Southern New Mexico: I. rainfall simulation experiments. Biogeochemistry 45:21–34.

Sperry, J. S., J. R. Donnelly, and M. T. Tyree. 1988. A method for measuring hydraulic

conductivity and embolism in xylem. Plant, Cell and Environment 11:35–40.

Stuart, S. A., B. Choat, K. C. Martin, N. M. Holbrook, and M. C. Ball. 2007. The role of freezing in setting the latitudinal limits of mangrove forests. New Phytologist 173:576–583.

Taylor, R. S. 2004. A natural history of coastal sage scrub in southern California: Regional floristic patterns and relations to physical geography, how it changes over time, and how well reserves represent its biodiversity. PhD Dissertation. University of California, Santa Barbara.

Thompson, J. A., J. C. Zinnert, and D. R. Young. 2017. Immediate effects of microclimate modification enhance native shrub encroachment. Ecosphere 8:e01687.

Tranquillini, W. 1979. Physiological ecology of the alpine timberline: tree existence at high altitudes with special reference to the European Alps. Springer, Berlin, Germany.

Van Auken, O. 2000. Shrub invasions of North American semiarid grasslands. Annual Review of Ecology and Systematics 31:197–215.

Vowles, T., B. Gunnarsson, U. Molau, T. Hickler, L. Klemedtsson, and R. G. Björk. 2017. Expansion of deciduous tall shrubs but not evergreen dwarf shrubs inhibited by reindeer in Scandes mountain range. Journal of Ecology 105:1547–1561.

Ward, D. 2005. Do we understand the causes of bush encroachment in African savannas? African Journal of Range and Forage Science 22:101–105.

Zinnert, J. C., S. A. Shifflet, S. Via, S. Bissett, B. Dows, P. Manley, and D. R. Young. 2016. Spatial–temporal dynamics in barrier island upland vegetation: the overlooked coastal landscape. Ecosystems 19:685–697.

Zinnert, J. C., J. A. Stallins, S. T. Brantley, and D. R. Young. 2017. Crossing scales: complexity of Barrier Island processes for predicting future change. BioScience 67:39–52.

CHAPTER 5

Critical phenomena in the spatio-temporal patterns of woody vegetation encroachment in coastal ecosystems

5.1 Abstract

Ecosystems may undergo critical transitions from one stable state to another in response to gradual changes in external drivers such as climate conditions and disturbance regime. Ecosystem state changes can be relatively abrupt, non-linear, and difficult to anticipate in real-world situations. Recent work has shown that climate warming may cause an abrupt grassland-to-shrubland transition in ecotones through vegetation-microclimate feedbacks whereby woody plants reduce nocturnal cooling and their own exposure to freezing stress. It is unclear how such a transition is associated with signs of critical phenomena in the spatio-temporal patterns of woody vegetation and whether such patterns can serve as leading indicators of critical transitions in coastal vegetation dynamics. Here, we combine high-resolution imagery from 1972 to 2013 with a stochastic cellular automata model to investigate the spatial patterns of woody patches on Hog Island (Virginia, USA) and shed light on the underlying mechanisms. We show that the size distribution of woody patches follows a power law in the years preceding woody plant expansion (after 1990). The model results confirm that the patch size distribution follows a power law when the background minimum temperature is between -16°C and -15.5°C. The observed critical phenomena are primarily driven by vegetation-microclimate feedbacks and serve as early warning signals of critical transitions associated with temperature-controlled woody plant encroachment in this island.

5.2 Introduction

The poleward expansion of cold-sensitive woody species into adjacent grasslands has been observed in a variety of ecosystems worldwide, ranging from arctic tundras to desert and coastal grasslands (Archer et al. 1995, Maher and Germino 2006, Knapp et al. 2008, McKee and Rooth 2008, Huang et al. 2018, 2020). This widespread shift in vegetation dominance has profound impacts on carbon sequestration, ecosystem productivity, and resilience (Huenneke et al. 2002, Li et al. 2007, D'Odorico et al. 2012). Woody plant encroachment may result from a number of factors, including climate warming, increasing atmospheric CO_2, nitrogen deposition, and land use change (Van Auken 2000, Sankaran et al. 2005, Gehrig-Fasel et al. 2007, D'Odorico et al. 2012). In regions where freezing stress has historically limited the expansion of woody plants, global or regional warming may reduce the frequency of extreme cold events and the associated freeze-induced mortality of woody plants (Cavanaugh et al. 2014, Huang et al. 2018, 2020). This phenomenon can be enhanced by local-scale vegetation-microclimate feedbacks, which can also play an important role in driving the range shifts of many cold-sensitive woody species by altering the near surface energy balance, thereby reducing cold stress exposure (D'Odorico et al. 2013, He et al. 2014, Huang et al. 2018). Specifically, woody canopies can absorb part of the nighttime long-wave radiation from the ground surface and then reflect or reradiate it back to the ground, thus reducing radiative cooling and creating a warmer microclimate compared to

87

adjacent open canopy areas and grasslands (He et al. 2010, D'Odorico et al. 2013). Because of this positive feedback, an abrupt shift from one stable state with grass cover to another with woody plant dominance may occur in cold-stressed ecotones when the minimum temperature increases above a critical threshold (D'Odorico et al. 2013, Huang et al. 2020). Thus, important non-linearities may emerge in vegetation dynamics, including bifurcations and critical transitions. It is still unclear, however, how the spatial structure of vegetation changes in the course of such transitions and whether at the verge of a shift to the woodland state vegetation patterns exhibit the emergence of critical phenomena (scaling relations and power law distributions) typical of systems approaching critical points (Sugihara and May 1990, Rodriguez-Iturbe and Rinaldo 1997, Majumder et al. 2019, Staver et al. 2019). For example, previous work has shown that the vegetation patches in some arid ecosystems including savannas may follow a power law distribution when the system is at the verge of a critical transition (Scanlon et al. 2007, Scheffer et al. 2009).

Here we focus on the case of barrier islands along the eastern shore of Virginia, USA, where the woody species, *Morella cerifera* L., has encroached into adjacent grasslands over the last century (Zinnert et al. 2016). A nearly 40% increase in *M. cerifera* cover was observed across these islands. For instance, on Hog Island (Virginia) the shrub cover has reached about 50% (Figure 1) (Zinnert et al. 2016, Huang et al. 2018). Recent work has documented the occurrence of a positive feedback between the establishment of *M. cerifera* shrubs and microclimate (Thompson et al. 2017, Wood et al. 2020). As a result of this feedback temporal dynamics of *M. cerifera* may undergo critical transitions from a stable state with grass cover to another state dominated by *M. cerifera* shrubs (Huang et al. 2018). Critical transitions have been extensively documented in a variety of ecosystems across the globe (May 1977, Scheffer et al. 2001). These non-linear ecosystem behaviors are often highly irreversible and difficult to anticipate in real-world systems (Ives and Carpenter 2007, Scheffer et al. 2009, Ratajczak et al. 2018). Here we use the case *M. cerifera* on Hog Island to investigate the spatiotemporal dynamics of shrub encroachment and document how, as they approach the critical point, these dynamics exhibit critical phenomena evidenced by scaling laws and power law distributions in the spatial patterns of vegetation. We use a combination of high-resolution imagery data from 1972 to 2013 and a process-based modelling framework to examine the size (area) distribution of woody patches and its dependence on background climate conditions. Specifically, we tested (i) whether the spatial patterning can be described by a power law in some specific years; (ii) the extent to which these empirical patterns can be explained by our physical understanding of the underlying processes through a mechanistic model of vegetation dynamics capturing the complexity of the system; and (iii) whether the spatial patterns of woody vegetation change over time.
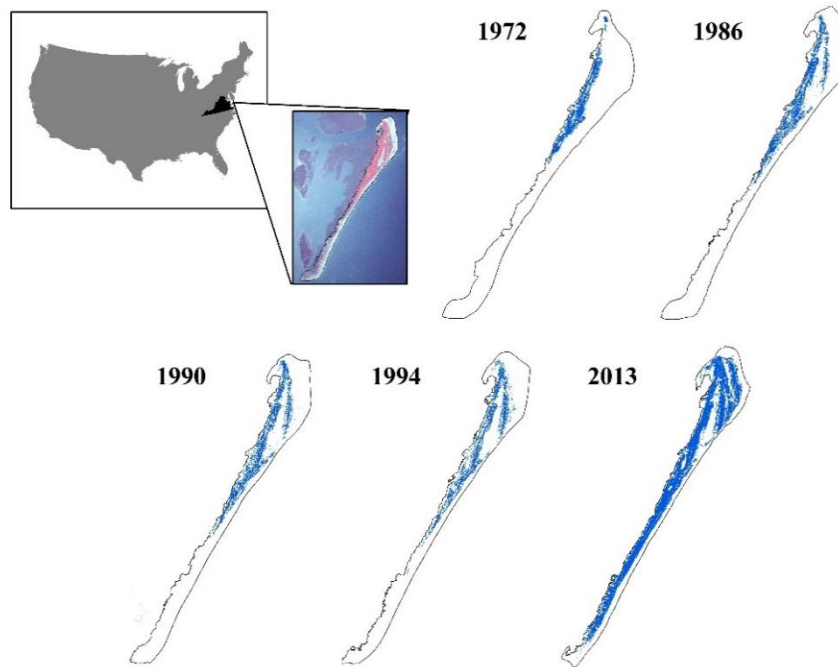
Figure 1. Changes in shrub cover on Hog Island, Virginia, USA from 1972 to 2013. The blue pixels indicate shrub patches and the upland outline (excluding marsh) is denoted each year in black. The image inset is color infrared imagery from 5 Jul 1986.

5.3 Materials and Methods

5.3.1 Satellite data processing and fragmentation analysis

To investigate the spatial patterns of *M. cerifera* on Hog Island, VA, detailed maps of evergreen shrub cover were created using georectified aerial photography and hyperspectral imagery. Cloud-free aerial photography was obtained from USGS Earth Explorer for the following dates: 2 Dec 1972 (color infrared), 5 Jul 1986 (color infrared), 5 Jul 1990 (color infrared), and 20 Mar 1994 (RGB). In 2013, hyperspectral imagery was available for Hog Island, VA (48 band hyperspectral) (USACE-TEC 2013). A seamless mosaic was performed on the multiple images which made up the 1972 scene and imagery resolution ranged from $0.41 - 1$ m^2. Regions of interest (ROI) were selected in each year for shrub cover using the bands available in each image (ENVI 5.5.3, LH3 Harris Geospatial) based on geo-rectified aerial photography, field surveyed woody thickets of known age using a Trimble Geo-XT GPS unit (Young et al. 2007), and woody thicket sampling locations of known age (Young et al. 1995). Shrub thicket homogeneity and high leaf cover, and the evergreen leaf habit relative to the otherwise sparse grassland cover and diversity in the system creates distinct boundaries that are ideal for interpretation of shrub cover (Young et al. 2007). After ROIs were selected, supervised classifications were performed using the maximum likelihood method. Accuracy assessments were performed for each classification (Table S1).

The resulting shrub cover was exported to ArcGIS 10.7 (ESRI) and then exported to the program FRAGSTATS 4.2 for spatial pattern analysis (McGarigal et al. 2012). We calculated the size (area, m^2) of each shrub patch identified in satellite images. We then fitted a power law to the inverse cumulative distribution of shrub patch sizes, defined as $P(A \geq a)$, the probability of a

cluster area A being greater than or equal to a given value a (Kéfi et al. 2007, Clauset et al. 2009).

5.3.2 Cellular automata model

We developed a stochastic cellular automata model to account for the effects of positive vegetation-microclimate feedbacks on the spatiotemporal dynamics of *M. cerifera* and explain the emergence of power laws in shrub patch size distribution. The model simulations were performed on a lattice composed of 300×50 cells to mimic the shape of Hog Island which has a length of ~12 km and a maximum width of ~2 km. We considered two vegetation states, namely, shrubs (S) or grasses (G); each cell in the lattice had either S or G cover. We define p_S (p_G) as the fraction of shrub (grass) cells in the whole lattice, and $q_{S|G}$ ($q_{G|S}$) the fraction of shrub (grass) cells in the von Neumann neighborhood of a grass (shrub) cell (the four nearest neighbors that share one edge with the focal cell).

We follow Kefi et al. (2007) and model the transition probability of a G cell to a S cell (i.e. from grassland to shrubland) as follows

$$w_{G \to S} = \alpha \left[\delta p_S + (1-\delta) q_{S|G} \right] (1 - p_S),$$

(1)

where α is the intrinsic growth rate of *M. cerifera* shrubs, δ is the fraction of shrub growth contributed globally by the presence of other shrubs in the domain and $1-\delta$ is the fraction of shrub growth facilitated locally by the presence of shrubs in the von Neumann neighborhood. The term $(1 - p_S)$ describes how the growth and establishment of shrub seedlings is constrained by limiting resources such as soil water and nutrients, light and physical space.

The cold-induced mortality probability of shrubs in a S cell (i.e. transition from shrub to grass cover) depends on T_{min}, the minimum temperatures within shrub thickets, and is expressed as

$$w_{S \to G} = \beta f(T_{min}),$$

(2)

where β is the maximum mortality probability caused by freeze damage. $f(T_{min})$ is a hyperbolic tangent function describing how shrub mortality increases from 0 to the maximum with decreasing T_{min} (Huang et al. 2020)

$$f(T_{min}) = \frac{1}{2} - \frac{1}{2} \tanh(T_{min} - \bar{T}),$$

(3)

where $\bar{T}$ is the average of two critical temperatures (T_1 and T_2) characterizing the cold intolerance of *M. cerifera* shrubs. Specifically, T_1 is the temperature when shrubs start to experience freeze-induced damage and T_2 is the temperature when shrubs suffer a nearly complete loss of xylem hydraulic conductivity. The local warming effect, which is induced by the woody canopies through altering near surface energy budget, results in a higher T_{min} compared to the background minimum temperature (T_b) in adjacent open grassland (Hayden 1998, He et al. 2010). The magnitude of this local warming effect is dependent on shrub density in the nearest neighborhood ($q_{S|S}$ or $1-q_{G|S}$) and can be modeled through a linear function as

$$T_{min} = T_b + \Delta T_{max} (1 - q_{G|S}),$$

(4)

where $\triangle T_{max}$ is the maximum local warming effect.

We performed model simulations for different values of T_b. For each of the given T_b scenarios, we ran 10 realizations. For each realization, we ran the model until the patch cover reached a

relatively stable state which is defined as the condition in which the change in the fractional cover of shrub patches between two consecutive time steps is smaller than 0.001. After the stable state was reached, the number and size of shrub patches were calculated. The mean patch size distributions for each T_b scenario were determined by averaging the values of all realizations. The initial values of p_S and $q_{G|S}$ were set to 0.5 for each simulation. The values of parameters were obtained from experimental data or estimated empirically based on shrub growth characteristics to reflect field conditions as in Huang et al. (2018). Therefore, $T_1 = -15°C$, $T_2 = -20°C$, $\triangle T_{max} = 2°C$. The parameters α and β were set at 0.05 and 1, respectively, keeping the same α/β ratio as in the corresponding parameters in Huang et al. (2018). We assigned a much greater value to β compared to α to indicate that a full shrub canopy can collapse within a relatively shorter time frame (a few years) when high freeze stress occurs, compared to the time (several decades) required for shrub patch establishment. We used $\delta = 0.3$ to reflect that shrub seedling establishment is more dependent on shrub density in the neighborhood. We should note that the modelling results are qualitatively insensitive to δ.

To further investigate the possible stable states of woodland–grassland systems under different background temperature conditions, we used mean field analysis (Kéfi et al. 2007). The mean field analysis assumes that there is no spatial structure such that the global vegetation densities (p_S or p_G) are equal to the local vegetation densities ($q_{S|G}$ or $q_{G|S}$). This simplification allows us to derive a single equation for woody plant growth

$$\frac{dS}{dt} = p_G w_{G \to S} - p_S w_{S \to G} = (1 - p_S)\alpha p_S (1 - p_S) - p_S \beta f (T_{min}). \tag{5}$$

The stable equilibrium points were determined at different T_b temperatures by setting $\frac{dS}{dt} = 0$ in

Eqn (5) and solving for it.

5.4 Results
The long-term historical climate data from a nearby NOAA meteorological station in Painter, Virginia shows that the annual minimum temperature significantly increased from 1972 to 2013 on Virginia barrier islands (Figure 2; slope = 0.12, $P < 0.001$). This long-term climate warming is consistent with the observed expansion of the cold sensitive *M. cerifera* shrub across Hog Island over this period (Figure 1).
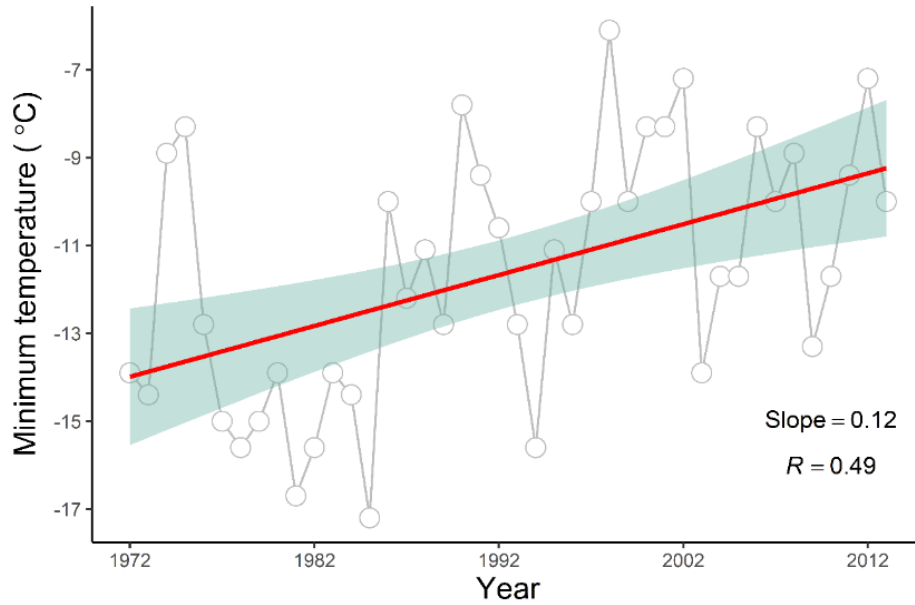
Figure 2. Long term changes in annual lowest minimum temperature in Painter station, Virginia from 1972 to 2013. The shaded area represents the 95% confidence interval range.

The results from imagery data show that the size distribution of shrub patches on Hog Island varied from 1972 to 2013. Around the years 1986 and 1990, the shrub patch size distribution followed a power law, $P[A \geq a] \sim a^{-\lambda}$ ($\lambda = 0.73$ and 0.76, $R^2 > 0.99$; Figure 3 B, C), while both in the previous and in the subsequent years it deviated from a power law (Figure 3 A, D, and E). As expected, the number of larger patches and their size increased between 1972 and 2013 in the course of the encroachment process. In the years between 1986 and 1990 the spatial patterns of vegetation exhibited signs of critical phenomena, as evidenced by the emergence of power law distribution of shrub patch size and the associated fractal properties. The year 1990 preceded the relatively rapid expansion of *M. cerifera* across the island. The emergence of critical phenomena (i.e., power law distributions) suggests that the shift in species dominance may be associated with a phase transition.
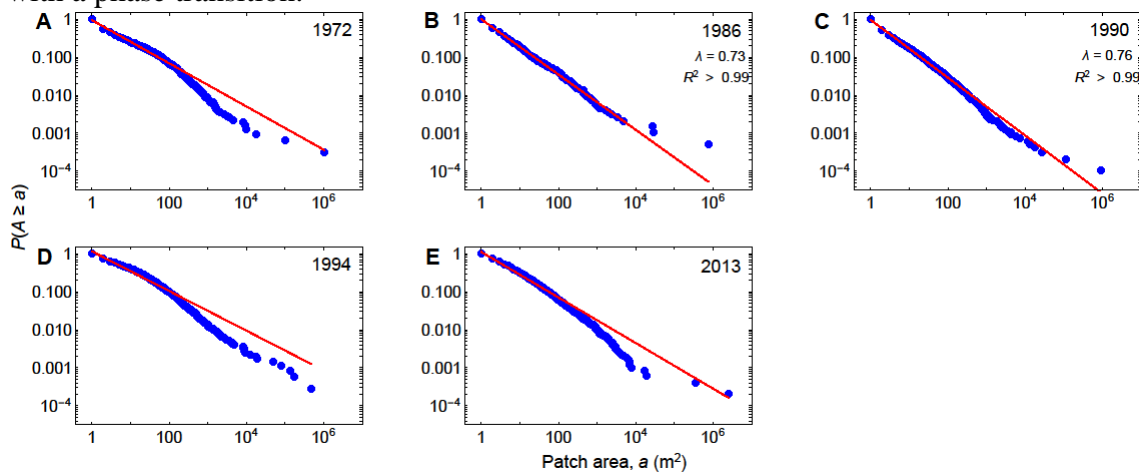

Figure 3. The observed size distribution of woody patches on Hog Island based on imagery data in 1972 (A), 1986 (B), 1990 (C), 1994 (D) and 2013 (E). The size distribution follows a power law in 1986 and 1990.

92

Previous work has investigated the dynamics of shrub expansion in the time domain and shown how positive feedbacks between shrubs and microclimate may induce critical transitions (D'Odorico et al. 2013). The occurrence of such feedbacks is supported by empirical evidence of nocturnal warming in the presence of *M. cerifera* and the cold sensitivity of this species, which undergoes a significant decline in xylem conductivity as the temperature drops below -15°C (Huang et al. 2018). Interestingly, the last five decades have seen a consistent warming trend in the Eastern shore of Virginia, which has reduced *M. cerifera*'s exposure to cold ($T < $ -15°C) events (Figure 2). To explain the processes underlying these critical phenomena and the occurrence of a phase transition in the spatiotemporal dynamics of woody plant encroachment, we developed a stochastic cellular automata model that accounts for the vegetation-microclimate feedbacks, expressing the local facilitation by adjacent woody canopies on the transition rate of grasses to shrubs. We used this model to examine whether the observed power law in patch size distribution may emerge from positive vegetation-microclimate feedbacks (see *Methods and Materials* for details). Differently from previous efforts (Scanlon et al. 2007), the model was parameterized using experimental data from field and laboratory measurements (Huang et al. 2018) to provide realistic representations of the driving processes.

The modeling results show that the patch-size distribution changed depending on the minimum background temperature (T_b). The distribution deviated from a power law and was closer to an exponential distribution when T_b was lower than -16.5°C (Figure 4A, B). At these temperatures *M. cerifera* shrubs are likely to experience freeze-induced mortality via losses of xylem hydraulic conductivity (Huang et al. 2018). Therefore, at these low temperatures most shrub patches were relatively small while the formation of large patches was prevented by freezing stress, as indicated by the exponential distribution. In contrast, we found that the size distribution can be overall described by a power law when T_b is in the -15.5─-16.0°C range. The best fit to a power law was found with T_b = -15.84°C (Figure 4C). At this temperature the warmer microclimate conditions that occur beneath woody canopies as the result of vegetation-microclimate feedbacks significantly reduce the cold-induced mortality of *M. cerifera* shrubs thereby triggering critical transitions from grassland to shrubland (Huang et al. 2018). Interestingly, power law distributions are detected in shrub patches only when the system is undergoing a critical state change. In fact, as T_b increased above -15.3°C, the patch size distribution deviated from a power law (Figure 4D). This finding indicates that critical phenomena occur only at the verge of the transition, consistent with the theory of critical point physics. The existence of this sharp transition is explained by the fact that only a slight increase in minimum temperatures is needed to release shrubs from cold stress thereby allowing woody patches to continue to grow even without the warming effect of vegetation-microclimate feedbacks. This leads to an increased proportion of large patches, as shown in Figure 4D.
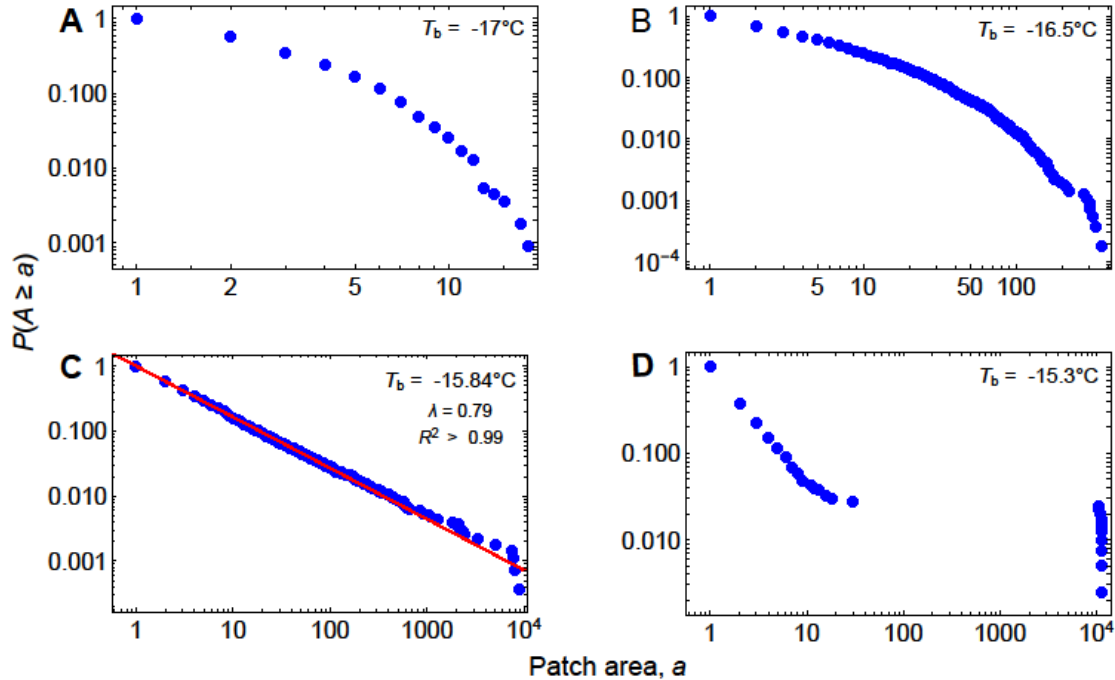
Figure 4. Cellular automata model results showing the size distribution of woody patches under different background minimum temperature (T_b) conditions: -17°C (A), -16.5°C (B), -15.84°C (C), and -15.3°C (D). The size distribution follows a power law when T_b = -15.84°C.

Overall, the spatial patterns of shrub patches obtained from the cellular automata model are consistent with the empirical observations from satellite data. For example, the shrub patches on Hog Island exhibited a power law distribution in 1986 and 1990 and deviated from a power law both before and after, suggesting that the emergence of these fractal properties is evidence of critical phenomena at the critical point. The -15.8°C temperature at which the model predicts a power law distribution of shrub patches corresponds to the limit for cold stress tolerance detected by physiological measurements in *M. cerifera* (Huang et al. 2018). In particular, the scaling exponent λ estimated from the model (0.79) is very similar to that calculated from the 1986 and 1990 imagery data (0.73 and 0.76, respectively).

To investigate the role played by the positive shrub-microclimate feedback in the emergence of critical behavior, we ran some simulations without accounting for the local warming effect in the neighborhood of shrub canopies (i.e. $\triangle T_{max} = 0$). Interestingly, we found that the size distribution deviated from a power law at the original critical temperature -15.84°C but followed a power law at a higher temperature -14.84°C (Figure 5). In addition, the spatial patterns of shrub patches were relatively insensitive to the extent to which shrub growth was driven by global or local controls (i.e., insensitive to the parameter δ). Thus, such a power law distribution is not induced by local interactions of positive feedbacks with abiotic environment but is simply the result of a percolation effect because the power law distribution is found only when the shrub density is close to 0.59, which corresponds to the percolation threshold for a square lattice (Stauffer and Aharony 1985, Taubert et al. 2018). According to percolation theory, random uncorrelated dispersal with density of 0.59 should lead to power law distribution in patch size.

These findings corroborate our proposition that the observed power law of vegetation patterning in 1986 and 1990 is driven by the local-scale vegetation-microclimate feedbacks.
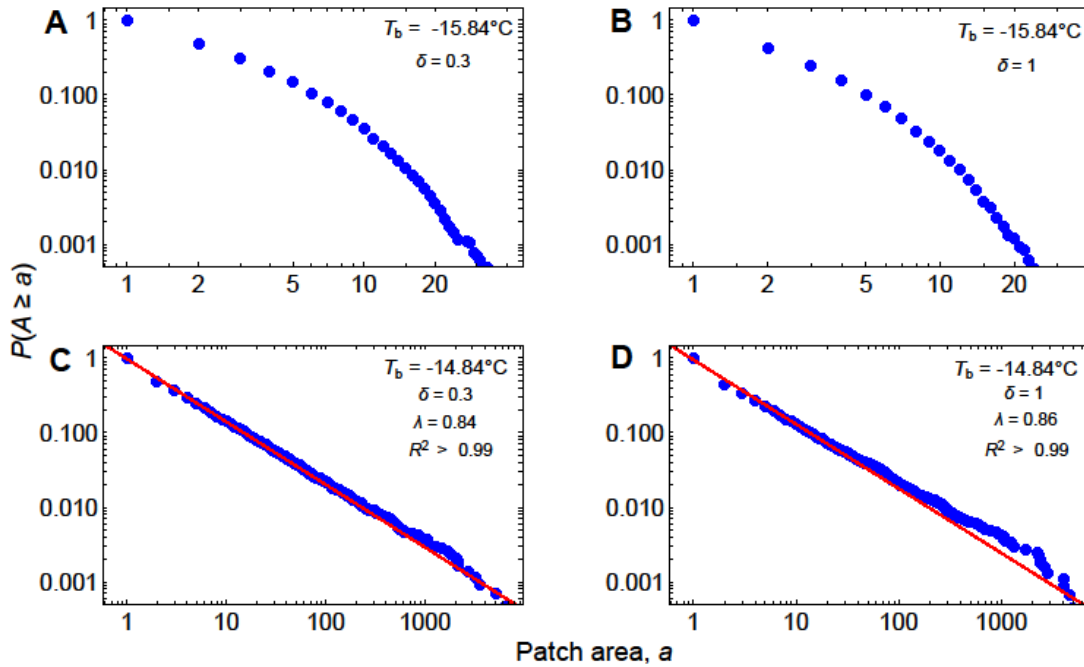

Figure 5. The size distribution of woody patches under two background minimum temperature (T_b) conditions -15.84 (*A*, *B*) and -14.84 (*C*, *D*) when there are no positive vegetation-microclimate feedbacks ($\triangle T_{max} = 0°C$). We used $\delta = 0.3$ (*A*, *C*) and 1 (*B*, *D*) respectively and the results are relatively insensitive to changes in δ.

5.5 Discussion

Previous efforts have demonstrated how positive vegetation-microclimate feedbacks are able to induce a non-linear transition from grassland to shrubland in the temporal dynamics of vegetation (Huang et al. 2018, 2020). In the case of the spatiotemporal dynamics of shrub encroachment, a mean field analysis of our model's dynamics shows how these feedbacks may induce a bifurcation in the equilibrium states of woodland-grassland systems as a function of the background temperature conditions (Figure 6). Although the mean field analysis does not take the spatial structure into account, it shows the non-linear behavior emerging in response to large-scale climate warming and local microclimate feedbacks. Specifically, the system exhibits a critical transition from a stable grassland state to a stable state dominated by shrub vegetation when background temperature reaches -16°C, in agreement with the -15.84°C threshold for power law behavior in the patch size distribution in the vegetation patterns generated by the cellular automata model (Figure 4C). Notice that simulations with the cellular automata model showed the emergence of power-law scaling in cluster size distribution when the steady-state shrub density was approximately 0.5, which is similar to the shrub density at the bifurcation point where the critical transition occurs (Figure 6).
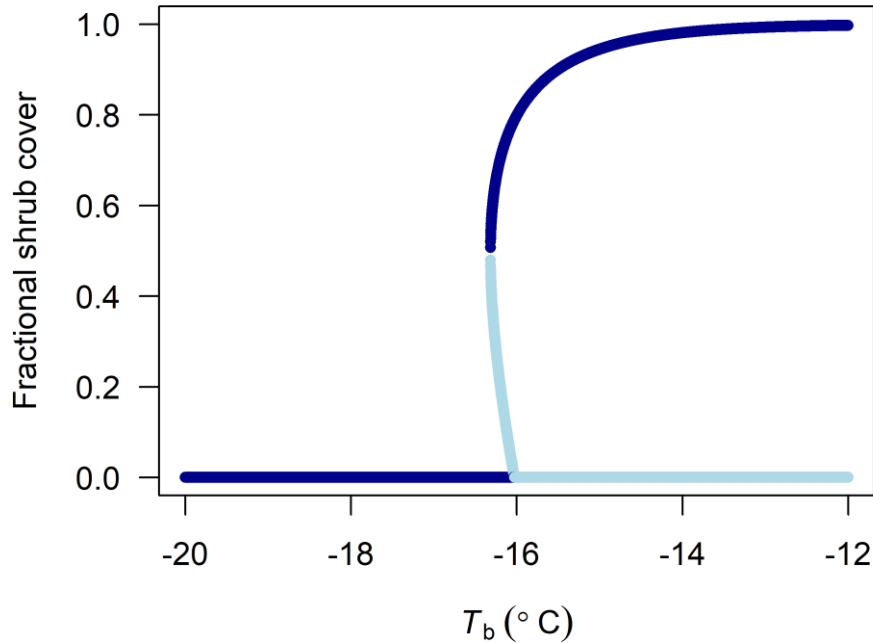
Figure 6. Bifurcation in the dynamics of woody vegetation on Hog Island based on mean field analysis of the cellular automata model. Stable and unstable states are indicated by blue and light blue lines, respectively. When T_b reaches nearly -16°C, the system may undergo a critical transition from grassland to shrubland.

Our empirical and modeling results suggest that power law size distribution of woody patches emerges when the ecosystem approaches a critical transition from a grassland to a woody plant-dominated state. This power law patterning arises from the local positive feedback between woody plants and microclimate where woody canopies create a local nocturnal warming effect (D'Odorico et al. 2013, Huang et al. 2018). Previous studies have found evidence of power law scaling in tree patch size distributions in arid ecosystems such as savannas where water is the major limiting factor (Kéfi et al. 2007, Scanlon et al. 2007, Berdugo et al. 2017). It is still unclear whether critical phenomena can also emerge in temperature-controlled shifts in plant community composition. Our study demonstrates that this characteristic spatial patterning of vegetation patchiness may be ubiquitous and can be used as a precursor of woody plant encroachment in coastal landscapes where shrub expansion is primarily limited by extreme low temperatures. We considered the case of woody vegetation encroachment on a Virginia barrier island, where the expansion of *M. cerifera*, which was historically limited by its cold sensitivity, has been recently enabled by warming trends (Figure 1). We note that the model aims to mimic the spatial patterning of shrub patches observed on Hog Island only qualitatively. Thus, the modelling results are not expected to match the empirical patterns exactly because (1) the observed shrub cover may not be at a steady state; (2) there might be other processes involved in the spatial patterning of shrub patches such as wind damage and storm surge, which are not taken into account in the model; and (3) the lattice size used to run the cellular automata model was limited by the computational cost of the simulations.

Critical transitions are widespread phenomena in natural systems and are often difficult to diagnose. They often entail relatively abrupt and potentially irreversible changes in ecosystem

structure and services (Scheffer et al. 2001, 2009). Therefore, the characteristic distribution of vegetation clusters may serve as a robust indicator of a phase transition in plant dominance, which can be used to detect ecosystem response to regional and global environmental change. The local positive feedback between vegetation and microclimate appears to play a crucial role in driving large-scale shifts in species composition, vegetation spatial patterning, and ecosystem state changes.

5.6 References

Archer, S., D. S. Schimel, and E. A. Holland. 1995. Mechanisms of shrubland expansion: land use, climate, or carbon dioxide. Climatic Change 29:91–99.

Berdugo, M., S. Kéfi, S. Soliveres, and F. T. Maestre. 2017. Plant spatial patterns identify alternative ecosystem multifunctionality states in global drylands. Nature Ecology and Evolution 1:3.

Cavanaugh, K. C., J. R. Kellner, A. J. Forde, D. S. Gruner, J. D. Parker, W. Rodriguez, and I. C. Feller. 2014. Poleward expansion of mangroves is a threshold response to decreased frequency of extreme cold events. Proceedings of the National Academy of Sciences 111:723–727.

Clauset, A., C. R. Shalizi, and M. E. J. Newman. 2009. Power-law distributions in empirical data. SIAM Review 51:661–703.

D'Odorico, P., G. S. Okin, and B. T. Bestelmeyer. 2012. A synthetic review of feedbacks and drivers of shrub encroachment in arid grasslands. Ecohydrology 5:520–530.

D'Odorico, P., Y. He, S. Collins, S. F. De Wekker, V. Engel, and J. D. Fuentes. 2013. Vegetation–microclimate feedbacks in woodland–grassland ecotones. Global Ecology and Biogeography 22:364–379.

Gehrig-Fasel, J., A. Guisan, and N. E. Zimmermann. 2007. Tree line shifts in the Swiss Alps: Climate change or land abandonment? Journal of Vegetation Science 18:571–582.

Hayden, B. P. 1998. Ecosystem feedbacks on climate at the landscape scale. Philosophical Transactions of the Royal Society B: Biological Sciences 353:5–18.

He, Y., P. D'Odorico, S. F. J. De Wekker, J. D. Fuentes, and M. Litvak. 2010. On the impact of shrub encroachment on microclimate conditions in the northern Chihuahuan desert. Journal of Geophysical Research 115:D21120.

He, Y., P. D'Odorico, and S. De Wekker. 2014. The relative importance of climate change and shrub encroachment on nocturnal warming in the Southwestern United States. International Journal of Climatology 35:475–480.

Huang, H., J. C. Zinnert, L. K. Wood, D. R. Young, and P. D'Odorico. 2018. Non-linear shift from grassland to shrubland in temperate barrier islands. Ecology 99:1671–1681.

Huang, H., L. D. L. Anderegg, T. E. Dawson, S. Mote, and P. D'Odorico. 2020. Critical transition to woody plant dominance through microclimate feedbacks in North American coastal ecosystems. Ecology 101:e03107.

Huenneke, L. F., J. P. Anderson, M. Remmenga, and W. H. Schlesinger. 2002. Desertification alters patterns of aboveground net primary production in Chihuahuan ecosystems. Global Change Biology 8:247–264.

Ives, A. R., and S. R. Carpenter. Stability and diversity of ecosystems. 2007. Science 317:58–62.

Maher, E. L., and M. J. Germino. 2006. Microsite variation among conifer species during seedling establishment at alpine treeline. Ecoscience 13:334–341.

Kéfi, S., M. Rietkerk, M. van Baalen, and M. Loreau. 2007. Local facilitation, bistability and transitions in arid ecosystems. Theoretical Population Biology 71:367–379.

Knapp, A. K., J. M. Briggs, S. L. Collins, S. R. Archer, M. S. Bret-Harte, B. E. Ewers, D. P. Peters, D. R. Young, G. R. Shaver, E. Pendall, and M. B. Cleary. 2008. Shrub encroachment in North American grasslands: shifts in growth form dominance alters control of ecosystem carbon inputs. Global Change Biology 14:615–623.

Li, J., G. S. Okin, L. J. Hartman, and H. E. Epstein. 2007. Quantitative assessment of wind erosion and soil nutrient loss in desert grasslands of southern New Mexico, USA. Biogeochemistry 85:317–332.

Majumder, S., K. Tamma, S. Ramaswamy, and V. Guttal. 2019. Inferring critical thresholds of ecosystem transitions from spatial data. Ecology 100:e02722.

May, R. M. 1977. Thresholds and breakpoints in ecosystems with a multiplicity of stable states. Nature 269:471–477.

McGarigal, K., S. A. Cushman, and E. Ene. 2012. FRAGSTATS v4: Spatial pattern analysis program for categorical and continuous maps. University of Massachusetts at Amherst, MA. Retrieved from http://www.umass.edu/landeco/research/fragstats/fragstats.html

McKee, K. L., and J. E. Rooth. 2008. Where temperate meets tropical: multi-factorial effects of elevated CO_2, nitrogen enrichment, and competition on a mangrove-salt marsh community. Global Change Biology 14:971–984.

Newman, M. 2005. Power laws, Pareto distributions and Zipf's law. Contemporary Physics 46:323–351.

Ratajczak, Z., S. Carpenter, A. Ives, C. Kucharik, T. Ramiadantsoa, M. Stegner, J. Williams, J. Zhang, and M. Turner. 2018. Abrupt change in ecological systems: inference and diagnosis. Trends in Ecology and Evolution 33:513–526.

Rodriguez-Iturbe, I., and A, Rinaldo. 1997. *Fractal River Basins: Chance and Self-Organization*. Cambridge University Press, New York.

Sankaran, M., N. P. Hanan, R. J. Scholes, J. Ratnam, D. J. Augustine, B. S. Cade, J. Gignoux, S. I. Higgins, X. Le Roux, and F. Ludwig. 2005. Determinants of woody cover in African savannas. Nature 438:846–849.

Scanlon, T. M., K. K. Caylor, S. A. Levin, and I. Rodriguez-Iturbe. 2007. Positive feedbacks promote power-law clustering of Kalahari vegetation. Nature 449:209–212.

Scheffer, M., J. Bascompte, W. A. Brock, V. Brovkin, S. R.Carpenter, V. Dakos, H. Held, E. H. van Nes, M. Rietkerk,and G. Sugihara. 2009. Early-warning signals for critical transitions. Nature 461:53–59.

Scheffer, M., S. Carpenter, J. Foley, C. Folke, and B. Walker. 2001. Catastrophic shifts in ecosystems. Nature 413:591–596.

Stauffer, D., and A. Aharony. 1985. *Introduction to Percolation Theory*. Taylor and Francis, London.

Staver, A. C., G. P. Asner, I. Rodriguez-Iturbe, S. A. Levin, and I. Smit. 2019. Spatial patterning among savanna trees in high resolution, spatially extensive data. Proceedings of the National Academy of Sciences 116:10685.

Sugihara, G., and R. M. May. 1990. Applications of fractals in ecology. Trends in Ecology and Evolution 5:79–86.

Taubert, F., et al. 2018. Global patterns of tropical forest fragmentation. Nature 554:519–522.

Thompson, J. A., J. C. Zinnert, and D. R. Young. 2017. Immediate effects of microclimate modification enhance native shrub encroachment. Ecosphere 8:e01687.

USACE-TEC, JALBTCX Hyperspectral imagery for Hog Island, VA, 2013. Virginia Coast Reserve Long-Term Ecological Research Project Data Publication knb-lter-vcr.229.7. doi:10.6073/pasta/6a5cc305e93c2baf9283facee688c504.

Van Auken, O. 2000. Shrub invasions of North American semiarid grasslands. Annual Review of Ecology and Systematics 31:197–215.

Wood, L. K., S. Hays, and J. C. Zinnert. 2020. Decreased temperature variance associated with biotic composition enhances coastal shrub encroachment. Scientific Reports 10:8210.

Young, D. R., G. Shao, and J. H. Porter. 1995. Spatial and temporal growth dynamics of barrier island shrub thickets. American Journal of Botany 82:638–645.

Young, D. R., J. H. Porter, C. M. Bachmann, G. Shao, R. A. Fusina, J. H. Bowles, D. Korwan, and T. F. Donato. 2007. Cross-scale patterns in shrub thicket dynamics in the Virginia barrier complex. Ecosystems 10:854–863.

Zinnert, J. C., S. A. Shifflet, S. Via, S. Bissett, B. Dows, P. Manley, and D. R. Young. 2016. Spatial–temporal dynamics in barrier island upland vegetation: the overlooked coastal landscape. Ecosystems 19:685–697.

CONCLUSIONS

In this dissertation, I investigated how climate change and microclimate feedbacks may drive transitions in plant community composition and species range shifts in North American desert and coastal ecosystems. In chapters 1 and 2, I conducted greenhouse and growth chamber experiments to investigate the effects of asymmetric warming and increasing rainfall variability on two CAM-grass communities in North American desert ecosystems. I found that C4 grasses may outcompete CAM plants due to increased deep soil water availability under increased rainfall variability. However, grass species experienced mortality under asymmetric warming regardless rainfall treatments, suggesting that the competitive advantage is likely to shift from grasses to CAM plants under global warming. In chapter 3, I used a combination of experimental and modelling approach to investigate the cold intolerance of woody species *M. cerifera* and the emergence of alternative stable states induced by vegetation-microclimate feedbacks in Virginia barrier island vegetation. Results show that a small increase in near-surface temperature can induce a non-linear shift in ecosystem state from a stable state with grass cover to an alternative stable state dominated by woody cover. In chapter 4, I combined field and lab experiments and field observations with a novel mathematical model to examine how environmental drivers and microclimate feedbacks may lead to abrupt shifts in woody vegetation dynamics in North American coastal ecosystems. Results show that a critical transition from grass cover to woody plant cover occurs when the average background temperature exceeds a critical threshold, although browsing may reduce the resilience of woody vegetation. In Chapter 5, I integrated high-resolution imagery data with a novel stochastic cellular automata model to investigate the spatial patterning of woody patches on Hog Island (Virginia) and the underlying mechanisms driving these patterns. I found that the size distribution of woody patches follows a power law in some specific years, which arises from the local positive feedback between woody vegetation and microclimate and can be considered as an early warning signal of critical transitions from grassland to woodland in coastal ecosystems where woody plant expansion is primarily constrained by cold stress.

My dissertation research highlights how climate drivers and microclimate feedbacks may drive significant shifts in plant community composition in North American desert and coastal ecosystems, which have profound impacts on ecosystem structure, functioning and services. The detected ecosystem bistability and hysteresis in coastal ecotones imply that additional efforts might be required for ecological management and restoration in these ecosystems.